

ผลของตัวเร่งปฏิกิริยามัล โลซีนที่ถูกยึดเกาะบนซิลิกา-อะลูมินาชนิด ไบโมดอลสำหรับ
โคโพลิเมอร์ไรเซชันของเอทิลีนกับแอลฟา โอลิฟิน



สถาบันวิทยบริการ จุฬาลงกรณ์มหาวิทยาลัย

วิทยานิพนธ์นี้เป็นส่วนหนึ่งของการศึกษาคตามหลักสูตรปริญญาวิศวกรรมศาสตรมหาบัณฑิต


สาขาวิชาวิศวกรรมเคมี ภาควิชาวิศวกรรมเคมี

คณะวิศวกรรมศาสตร์ จุฬาลงกรณ์มหาวิทยาลัย

ปีการศึกษา 2550

ลิขสิทธิ์ของจุฬาลงกรณ์มหาวิทยาลัย

EFFECT OF BIMODAL SILICA-ALUMINA-SUPPORTED METALLOCENE
CATALYST FOR ETHYLENE/ α -OLEFIN COPOLYMERIZATION



Mr. Pongsathorn Wongwaiwattanakul

สถาบันวิทยบริการ
จุฬาลงกรณ์มหาวิทยาลัย

A Thesis Submitted in Partial Fulfillment of the Requirements
for the Degree of Master of Engineering Program in Chemical Engineering

Department of Chemical Engineering

Faculty of Engineering

Chulalongkorn University

Academic Year 2007

Copyright of Chulalongkorn University

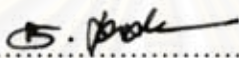
Thesis Title EFFECT OF BIMODAL SILICA-ALUMINA-SUPPORTED
METALLOCENE CATALYST FOR ETHYLENE/ α -OLEFIN
COPOLYMERIZATION

By Mr. Pongsathorn Wongwaiwattanakul

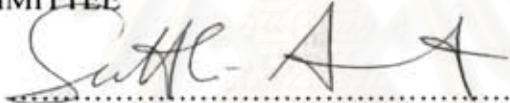
Field of Study Chemical Engineering

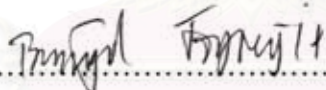
Thesis Advisor Assistant Professor Bunjerd Jongsomjit, Ph.D.

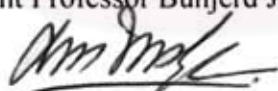
Accepted by the Faculty of Engineering, Chulalongkorn University in
Partial Fulfillment of the Requirements for the Master's Degree


..... Dean of the Faculty of Engineering
(Associate Professor Boonsom Lerdhirungwong, Dr.Ing.)

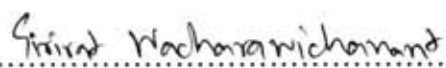
THESIS COMMITTEE


..... Chairman
(Associate Professor Suttichai Assabumrungrat, Ph.D.)


..... Thesis Advisor
(Assistant Professor Bunjerd Jongsomjit, Ph.D.)


..... Member
(Associate Professor ML. Supakanok Thongyai, Ph.D.)


..... Member
(Anongnat Somwangthanaroj, Ph.D.)


..... External Member
(Assistant Professor Sirirat Wacharawichanant, D.Eng.)

พงศธร ว่องไววัฒนกุล : ผลของตัวเร่งปฏิกิริยาเมทัล โลซีนที่ถูกยึดเกาะบนซิลิกา-อะลูมินาชนิดไบ โมดอลสำหรับ โค โพลิเมอร์ไรเซชันของเอทิลีนกับแอลฟาโอเลฟิน (EFFECT OF BIMODAL SILICA-ALUMINA-SUPPORTED METALLOCENE CATALYST FOR ETHYLENE/ α -OLEFIN COPOLYMERIZATION) อ. ที่ปรึกษา : ผศ. ดร. บรรเจิด จงสมจิตร, 108 หน้า

ตัวเร่งปฏิกิริยาเมทัล โลซีนเป็นที่สนใจในอุตสาหกรรมพอลิโอเลฟินมากขึ้นจึงมีการศึกษาและปรับปรุงเพื่อเพิ่มประสิทธิภาพ ของตัวเร่งปฏิกิริยาเมทัล โลซีน ในระบบตัวเร่งปฏิกิริยาเมทัล โลซีนแบบเอกพันธ์มีข้อเสียอย่างชัดเจนอยู่สองข้อคือ ไม่สามารถควบคุมโครงสร้างของพอลิเมอร์ และเกิดปัญหาการสูญเสียพอลิเมอร์ที่สังเคราะห์ได้เนื่องจากการติดอยู่ข้างถังปฏิกรณ์ ซึ่งข้อเสียเหล่านี้สามารถแก้ไขได้โดยการนำสารประกอบเมทัล โลซีนมายึดติดบนตัวรองรับ งานวิจัยนี้จะมุ่งเน้นการพัฒนาและปรับปรุงตัวเร่งปฏิกิริยาเรซิมิก-เอทิลีนบีสอินดีนนิลเซอร์โคเนียม ไคคลอไรด์ [*rac*-Et(Ind)₂ZrCl₂] ซึ่งยึดติดกับตัวรองรับที่มีซิลิกาเป็นองค์ประกอบและมีโครงสร้างของรูพรุนต่างกันคือรูพรุนแบบยูนิ โมดอลทั้งรูพรุนขนาดใหญ่และรูพรุนขนาดเล็ก รวมถึงรูพรุนแบบไบ โมดอล การศึกษาจะแบ่งออกเป็น 2 ส่วน ในส่วนแรกจะทำการศึกษาผลของตัวเร่งปฏิกิริยาเซอร์โค โนซีนบนตัวรองรับที่มีโครงสร้างของรูพรุนต่างกันในการเตรียมปฏิกิริยา โคพอลิเมอร์ไรเซชันของเอทิลีนกับหนึ่งออกทีน โดยมีตัวเร่งปฏิกิริยาร่วมคือคราย โมดิฟายเมทิลอะลูมินอกเซนแห่ง (dMMAO) ปริมาณอะลูมินาในครายโมดิฟายเมทิลอะลูมินอกเซนแห่งบนตัวรองรับที่มากที่สุดถูกวัด โดยการวิเคราะห์ EDX และแรงกระทำที่มีระหว่างตัวรองรับกับตัวเร่งปฏิกิริยาร่วมซึ่งมีค่าน้อย ถูกวิเคราะห์โดย TGA ส่งผลให้ค่าความว่องไวในการเกิดพอลิเมอร์ของซิลิการูพรุนใหญ่เพิ่มขึ้นอย่างเห็นได้ชัด ในส่วนที่สองจะทำการศึกษาผลของโค โม โนเมอร์ที่ใช้ในการเตรียมปฏิกิริยาโคพอลิเมอร์ไรเซชันของเอทิลีนกับแอลฟาโอเลฟินนั่นก็คือ 1-เฮกซีนและ 1-เดกซีน ซึ่งพบว่าแอลฟาโอเลฟินส่งผลต่อค่าความว่องไวในแต่ละระบบแตกต่างกัน โคพอลิเมอร์ที่ได้ทั้งหมดจะนำมาวิเคราะห์ เพื่อวัดคุณสมบัติและ โครงสร้างย่อยของพอลิเมอร์ด้วยเครื่อง DSC และเครื่อง ¹³C NMR

ภาควิชา.....วิศวกรรมเคมี..... ลายมือชื่อนิสิต.....
 สาขาวิชา.....วิศวกรรมเคมี..... ลายมือชื่ออาจารย์ที่ปรึกษา.....
 ปีการศึกษา.....2550.....

##4970446721: MAJOR CHEMICAL ENGINEERING

KEY WORD: SUPPORTED METALLOCENE CATALYST/BIMODAL/SILICA/
ALUMINA/ COPOLYMERIZATION OF ETHYLENE/ ZIRCONOCENE

PONGSATHORN WONGWAIWATTANAKUL: EFFECT OF BIMODAL
SILICA-ALUMINA-SUPPORTED METALLOCENE CATALYST FOR
ETHYLENE/ α -OLEFIN COPOLYMERIZATION. THESIS ADVISOR:
ASST. PROF. BUNJERD JONGSOMJIT, Ph.D., 108 pp.

Nowadays, metallocene catalyst becomes to be more interesting in an olefin polymerization. Therefore, it has led to extensive efforts to utilize metallocene catalysts efficiently. The homogeneous metallocene catalysts have two major disadvantages; (i) the lack of morphology control and (ii) reactor fouling. Supporting metallocene catalysts onto inorganic supports as supported metallocene catalysts can solve these problems. This research proposed the development and improvement of metallocene catalyst, such as the *rac*-Et(Ind)₂ZrCl₂/dMMAO system, by using silica-based supports with different pore structures such as unimodal pore (large pore and small pore) and bimodal pore. These studies were divided into two parts. In the first part, impact of different supported zirconocene/dMMAO on the catalytic activities during copolymerization of ethylene/1-octene was investigated. The largest amount of [Al]_{dMMAO} on the support as confirmed by the EDX measurement and the fewer interaction between dMMAO and the support as proven by the TGA analysis apparently resulted in dramatically increased polymerization activity for the large pore silica gel [SiO₂ (LP)]. In the second part, the impact of α -olefins (1-hexene, 1-octene and 1-decene) employed under the corresponding condition as mentioned in the first part was further investigated. It was found that different α -olefins can alter the polymerization activities upon different supports used. All the obtained polymers were characterized by DSC and ¹³C NMR to determine the polymer properties and polymer microstructure.

Department.....Chemical Engineering... Student's signature *Pongsathorn Wongwaiwattanakul*

Field of study...Chemical Engineering... Advisor's signature *Bunjerd Jongsomjit*

Academic year.....2007.....

ACKNOWLEDGEMENTS

The author would like to express my greatest gratitude and appreciation to Assistant Professor Dr. Bunjerd Jongsomjit, my advisor, for his invaluable suggestions, encouragement during my study and useful discussions throughout this research. His advice is always worthwhile and without him this work could not be possible.

I wish to thank Associate Professor Dr. Suttichai Assabumrungrat, as the chairman, Associate Professor Dr. ML. Supakanok Thongyai, Dr. Anongnat Somwangthanaroj and Assistant Professor Dr. Sirirat Wacharawichanant as the members of the thesis committee for their valuable guidance and revision throughout my thesis.

Sincere thanks are given to the graduate school and department of chemical engineering at Chulalongkorn University for the financial support of this work. And many thanks are given to PTT Chemical Public Company Limited for ethylene gas supply and MEKTEC Manufacturing Corporation (Thailand) Limited for DSC and NMR measurements.

Many thanks for kind suggestions and useful help to Miss Chanintorn Ketloy Miss Sirinlak Bunchongturakarn, Miss Supaluk Jiamwijitkul, Mr.Chanathip Desharun and many friends in the Center of Excellence on Catalysis and Catalytic Reaction Engineering, Department of Chemical Engineering, Faculty of Engineering, Chulalongkorn University for friendship and their assistance especially the members of Z&M group. To the many others, not specifically named, who have provided me with support and encouragement, please be assured that I think of you.

Finally, I would like to express my highest gratitude to my family and Miss Orapin Chokpaisan who are always beside me and support throughout this study.

CONTENTS

| | Page |
|--|------|
| ABSTRACT (IN THAI) | iv |
| ABSTRACT (IN ENGLISH) | v |
| ACKNOWLEDGMENTS | vi |
| CONTENTS | vii |
| LIST OF TABLES | xi |
| LIST OF FIGURES | xii |
| CHAPTER I INTRODUCTION | 1 |
| CHAPTER II LITERATURE REVIEWS | 5 |
| 2.1 Polymerization of olefins | 5 |
| 2.2 Mechanisms of homogeneous, catalytic olefin polymerization | 7 |
| 2.2.1 Chain transfer - molecular weight and molecular weight Distribution | 8 |
| 2.3 Background on Polyolefin Catalysts | 11 |
| 2.3.1 Catalyst Structure | 11 |
| 2.3.2 Polymerization mechanism | 14 |
| 2.3.3 Cocatalysts | 17 |
| 2.3.4 Catalyst Activity | 20 |
| 2.3.5 Copolymerization | 21 |
| 2.4 Metallocene Catalysts | 25 |
| 2.4.1 Olefin Polymerization with Metallocene Catalysts | 25 |
| 2.4.2 Catalyst Systems for Olefin Polymerization..... | 26 |
| 2.5 Heterogenous Systems..... | 28 |
| 2.5.1 Catalyst Chemistry..... | 28 |
| 2.5.2 Supporting Methods..... | 29 |
| 2.5.2.1 Direct Supporting of Inert Material..... | 30 |
| 2.5.2.2 Supporting Catalyst on Material Treated with Alkylaluminum..... | 32 |
| 2.5.2.3 Chemically Anchoring catalyst on Support..... | 34 |
| 2.5.2.4 Supporting on other Supports..... | 36 |

| | | |
|--------------------|---|----|
| CHAPTER III | EXPERIMENTAL | 39 |
| 3.1 | Objective of the Thesis | 39 |
| 3.2 | Scope of the Thesis | 39 |
| 3.3 | Research Methodology | 39 |
| 3.4 | Experimental | 41 |
| 3.4.1 | Chemicals | 41 |
| 3.4.2 | Equipments | 42 |
| 3.4.2.1 | Cooling System | 42 |
| 3.4.2.2 | Inert Gas Supply | 42 |
| 3.4.2.3 | Magnetic Stirrer and Heater | 43 |
| 3.4.2.4 | Reactor | 43 |
| 3.4.2.5 | Schlenk Line | 43 |
| 3.4.2.6 | Schlenk Tube | 44 |
| 3.4.2.7 | Vacuum Pump | 44 |
| 3.4.2.8 | Polymerization line | 45 |
| 3.4.3 | Supporting Procedure | 45 |
| 3.4.3.1 | Preparation of alumina-silica bimodal pore supports | 45 |
| 3.4.3.2 | Preparation of dried-MMAO (dMMAO) | 45 |
| 3.4.3.3 | Preparation of supported dMMAO (catalyst precursor) | 46 |
| 3.4.4 | Ethylene/ α -olefin Polymerization Procedures | 46 |
| 3.4.5 | Characterization of supports and catalyst precursor | 47 |
| 3.4.5.1 | N ₂ physisorption | 47 |
| 3.4.5.2 | X-ray diffraction (XRD) | 47 |
| 3.4.5.3 | Raman spectroscopy | 47 |
| 3.4.5.4 | Scanning Electron Microscope (SEM) and Energy dispersive x-ray spectroscopy (EDX) | 47 |
| 3.4.5.5 | Thermogravimetric analysis (TGA) | 47 |
| 3.4.6 | Characterization Method of Polymer | 48 |

| | Page |
|--|-----------|
| 3.4.6.1 Differential Scanning Calorimetry (DSC)..... | 48 |
| 3.4.6.2 ¹³ C Nuclear Magnetic Rasonance (¹³ C NMR)..... | 48 |
| CHAPTER IV RESULTS AND DISCUSSIONS..... | 49 |
| 4.1 Characterization of supports and supported dMMAO..... | 49 |
| 4.1.1 Characterization of supports with N ₂ physisorption..... | 49 |
| 4.1.2 Characterization of supports with X-ray diffraction (XRD)..... | 51 |
| 4.1.3 Characterization of supports with Raman spectroscopy..... | 51 |
| 4.1.4 Characterization of supports and supported dMMAO with Scanning electron microscope (SEM) and energy dispersive X-ray spectroscopy (EDX)..... | 52 |
| 4.1.5 Characterization of supports and supported dMMAO with Thermogravimetric analysis (TGA)..... | 55 |
| 4.2 Characteristics and catalytic properties of ethylene/1-octene copolymerization..... | 56 |
| 4.2.1 The effect of various supports on the catalytic activity | 57 |
| 4.2.2 The effect of various supports on the melting temperatures of copolymers..... | 58 |
| 4.2.3 The effect of various supports on the incorporation of copolymers | 59 |
| 4.3 Effect of various supports with different comonomers..... | 60 |
| 4.3.1 The effect of various supports with different comonomers on the catalytic activity..... | 60 |
| 4.3.2 The effect of various supports on the melting temperatures of copolymers with different comonomers..... | 62 |
| 4.3.3 The effect of various supports on incorporation of copolymers the with different comonomers | 63 |
| CHAPTER V CONCLUSIONS & RECOMMENDATIONS | 65 |
| 5.1 Conclusions..... | 65 |
| 5.2 Recommendations | 65 |
| REFERENCES..... | 66 |

| | |
|-------------------------|-----|
| APPENDICES | 77 |
| APPENDIX A | 78 |
| APPENDIX B | 85 |
| APPENDIX C | 92 |
| APPENDIX D | 100 |
| APPENDIX E | 106 |
| VITA | 108 |



สถาบันวิทยบริการ
จุฬาลงกรณ์มหาวิทยาลัย

LIST OF TABLES

| Table | Page |
|---|------|
| 2.1 Representative examples of metallocenes..... | 12 |
| 4.1 BET surface area and average pore diameter of different SiO ₂ -based support..... | 50 |
| 4.2 The content of [Al] _{dMMAO} on different SiO ₂ -based supports..... | 53 |
| 4.3 Copolymerization activities | 57 |
| 4.4 Melting temperatures % crystallinity of copolymers obtained different SiO ₂ -based supports..... | 59 |
| 4.5 ¹³ C NMR analysis of ethylene/1-octene copolymer..... | 60 |
| 4.6 Catalytic activities of different SiO ₂ -based -supported dMMAO with zirconocene catalyst during ethylene/ α -olefin copolymerization..... | 61 |
| 4.7 Melting temperatures, % crystallinity of copolymers obtained from different SiO ₂ -based supports with different comonomer..... | 62 |
| 4.8 ¹³ C NMR analysis of ethylene/ α -olefins copolymer..... | 64 |
| D-1 Reactivity ratios of ethylene and α -olefin monomers..... | 104 |

LIST OF FIGURES

| Figure | Page |
|--------|--|
| 2.1 | Examples of polyethenes: LDPE, HDPE and LLDPE (copolymer of ethene and 1-hexene).....6 |
| 2.2 | Common polymer tacticities.....6 |
| 2.3 | Scheme of migratory insertion mechanism, in which the metal-bound alkyl group migrates to the alkene.....8 |
| 2.4 | Scheme of termination reactions by β -H, β -CH ₃ and H-transfer to monomer.....10 |
| 2.5 | Scheme of chain transfer to aluminum.....10 |
| 2.6 | Molecular structure of metallocene.....11 |
| 2.7 | Some of zirconocene catalyst structure.....12 |
| 2.8 | Scheme of the different metallocene complex Figure structure.....13 |
| 2.9 | Cossee mechanism for Ziegler-Natta olefin polymerization.....14 |
| 2.10 | The propagation step according to the trigger mechanism.....15 |
| 2.11 | Propagation mechanism in polymerization.....15 |
| 2.12 | Chain transfer via β -H elimination.....16 |
| 2.13 | Chain transfer via β -CH ₃ elimination.....16 |
| 2.14 | Chain transfer to aluminum.....17 |
| 2.15 | Chain transfer to monomer.....17 |
| 2.16 | Chain transfer to hydrogen.....17 |
| 2.17 | Early structure models of MAO.....18 |
| 2.18 | Representation of MAO showing the substitution of one bridging methylgroup by X ligand extracted from $\text{racEt}(\text{Ind})_2\text{ZrCl}_2$ (X = Cl, NMe ₂ , CH ₂ Ph).....19 |
| 2.19 | Structure of $\text{Et}[\text{Ind}]_2\text{ZrCl}_2$ supported on silica.....30 |
| 2.20 | Structure of $\text{Et}[\text{Ind}]_2\text{ZrCl}_2$ supported on alumina.....30 |
| 2.21 | Reaction of silica and metallocene during catalyst supporting.....31 |
| 2.22 | Alkylation of supported metallocene MAO.....31 |
| 2.23 | Effect of surface hydroxyl groups on ionic metallocene catalysts.....32 |

| Figure | Page |
|--|------|
| 2.24 Structure of some silica supported metallocene catalysts..... | 34 |
| 2.25 Mechanism for supporting metallocene catalysts on silica using Spacer molecules..... | 35 |
| 2.26 Modification of silica with $\text{Cp}(\text{CH}_2)_3\text{Si}(\text{OCH}_2\text{CH}_3)_3$ and preparation of supported metallocene catalyst..... | 36 |
| 3.1 Flow diagram of research methodology..... | 40 |
| 3.2 Inert gas supply system..... | 43 |
| 3.3 Schlenk line..... | 44 |
| 3.4 Schlenk tube..... | 44 |
| 3.5 Diagram of system in slurry phase polymerization..... | 45 |
| 4.1 Pore size distribution of different SiO_2 -based supports..... | 50 |
| 4.2 XRD patterns of different SiO_2 -based supports..... | 51 |
| 4.3 Raman spectra of different SiO_2 -based supports..... | 52 |
| 4.4 SEM micrographs of different SiO_2 -based supports..... | 53 |
| 4.5 A typical spectrum of the supported dMMAO from EDX analysis used to measure the average $[\text{Al}]_{\text{dMMAO}}$ concentration on different SiO_2 -based supports..... | 54 |
| 4.6 SEM/EDX mapping for Al distributions on different SiO_2 -based supports after dMMAO impregnation..... | 55 |
| 4.7 TGA profiles of supported dMMAO on different SiO_2 -based supports..... | 56 |
| A-1 ^{13}C NMR spectrum of ethylene/1-hexene copolymer produce with homogenous..... | 79 |
| A-2 ^{13}C NMR spectrum of ethylene/1-octene copolymer produce with homogenous | 79 |
| A-3 ^{13}C NMR spectrum of ethylene/1-decene copolymer produce with homogenous | 80 |
| A-4 ^{13}C NMR spectrum of ethylene/1-hexene copolymer produce with SiO_2 (LP) | 80 |
| A-5 ^{13}C NMR spectrum of ethylene/1-octene copolymer produce with SiO_2 (LP)..... | 81 |

| Figure | Page |
|---|------|
| A-6 ^{13}C NMR spectrum of ethylene/1-decene copolymer produce with SiO_2 (LP)..... | 81 |
| A-7 ^{13}C NMR spectrum of ethylene/1-hexene copolymer produce with SiO_2 (SP)..... | 82 |
| A-8 ^{13}C NMR spectrum of ethylene/1-octene copolymer produce with SiO_2 (SP) | 82 |
| A-9 ^{13}C NMR spectrum of ethylene/1-decene copolymer produce with SiO_2 (SP)..... | 83 |
| A-10 ^{13}C NMR spectrum of ethylene/1-hexene copolymer produce with Si-Al (BP)..... | 83 |
| A-11 ^{13}C NMR spectrum of ethylene/1-octene copolymer produce with Si-Al (BP)..... | 84 |
| A-12 ^{13}C NMR spectrum of ethylene/1-decene copolymer produce with Si-Al (BP) | 84 |
| B-1 DSC curve of ethylene/1-hexene copolymer produce with homogenous..... | 86 |
| B-2 DSC curve of ethylene/1-octene copolymer produce with homogenous | 86 |
| B-3 DSC curve of ethylene/1-decene copolymer produce with homogenous | 87 |
| B-4 DSC curve of ethylene/1-hexene copolymer produce with SiO_2 (LP)..... | 87 |
| B-5 DSC curve of ethylene/1-octene copolymer produce with SiO_2 (LP)..... | 88 |
| B-6 DSC curve of ethylene/1-decene copolymer produce with SiO_2 (LP)..... | 88 |
| B-7 DSC curve of ethylene/1-hexene copolymer produce with SiO_2 (SP)..... | 89 |
| B-8 DSC curve of ethylene/1-octene copolymer produce with SiO_2 (SP) | 89 |

| Figure | Page |
|--|------|
| B-9 DSC curve of ethylene/1-decene copolymer produce with SiO ₂ (SP)..... | 90 |
| B-10 DSC curve of ethylene/1-hexene copolymer produce with Si-Al (BP)..... | 90 |
| B-11 DSC curve of ethylene/1-octene copolymer produce with Si-Al (BP)..... | 91 |
| B-12 DSC curve of ethylene/1-decene copolymer produce with Si-Al (BP) | 91 |
| C-1 EDX profiles of [Al] _{Al₂O₃} on Si-Al (BP) supports..... | 93 |
| C-2 EDX mapping of Si-Al (BP)..... | 93 |
| C-3 EDX profiles of [Al] _{dMMAO} on SiO ₂ (LP) supports..... | 94 |
| C-4 EDX mapping of dMMAO/SiO ₂ (LP) | 94 |
| C-5 EDX profiles of [Al] _{dMMAO} on SiO ₂ (SP) supports..... | 95 |
| C-6 EDX mapping of dMMAO/SiO ₂ (SP)..... | 95 |
| C-7 EDX profiles of [Al] _{dMMAO} on Si-Al (BP) supports..... | 96 |
| C-8 EDX mapping of dMMAO/Si-Al (BP) supports | 96 |
| C-9 EDX mapping of LLDPE (EH)/Si-Al (BP)..... | 97 |
| C-10 EDX mapping of LLDPE (EO)/Si-Al (BP)..... | 98 |
| C-11 EDX mapping of LLDPE (ED)/Si-Al (BP)..... | 99 |

CHAPTER I

INTRODUCTION

For years, polyolefins are one of the largest businesses in plastic industry. They are used in almost every field - from food packaging to sophisticated engineering and are a fast growing segment of the polymer industry with the highest amount of nearly 4 million tons a year. This already impressive market is still in full growth, with Foxely (1998) predicting growth rates of about 30% for PP and about 18% for PE products for the period from 2000 to 2005 [1]. The production of polyolefins is estimated to be around 140 million tons in 2010 [2]. Linear low-density polyethylene (LLDPE) which produces by ethylene copolymer of higher α -olefins such as 1-butene, 1-hexene, and 1-octene is industrially important commercial polyolefins and a petrochemical product [3]. As far, industrial efforts have been directed towards finding novel and efficient polymerization catalysts for the synthesis of the desired copolymer. The driving force in the LLDPE growth can be attributed to metallocene-catalyzed LLDPE resin. The demand for metallocene-catalyzed polyethylene is predicted to increase 45% between 1996 and 2000 and eventually grow to 5.9 million tons in the year 2010 [4].

In 1957, Natta and Breslow discovered the first homogeneous Ziegler-Natta catalyst [5]. The ethylene polymerization with titanocene catalyst Cp_2TiCl_2 and the alkylaluminum chloride as cocatalyst exhibited a low polymerization activity. In 1980's, new cocatalyst was discovered by Kaminsky and coworkers [6]. While studying a homogeneous $\text{Cp}_2\text{ZrCl}_2/\text{Al}(\text{CH}_3)_3$ polymerization system, water was unpected introduced into the reactor leading to an utmost active ethylene polymerization system. The hydrolysis of the trimethylaluminum, $\text{Al}(\text{CH}_3)_3$ is cause of formation the cocatalyst methylaluminoxane (MAO) which precede to the high activity [5].

Metallocene-based catalysts are dramatically different from previous generations of catalysts. For example, metallocene catalysts can be tailored to produce polyolefins with special stereoregularities and a high degree of tacticity. Moreover,

owing to their homogeneous nature every molecule has an active site and thus metallocene catalysts can be many times more active than Ziegler–Natta and Phillips catalysts and can produce high molecular weight polymers and copolymers, characterized by a narrow molecular weight distribution (≈ 2) and homogeneous chemical composition [7]. It has been mentioned that silica is the most widely used support for metallocene catalysts so far. It is known that the copolymerization of ethylene with higher 1-olefins is a commercial importance for productions of elastomer and linear low-density polyethylene (LLDPE). Metallocene catalysts with MAO have been studied for such a copolymerization. In fact, zirconocene catalysts along with MAO have been reported for a potential use to polymerize ethylene with 1-olefins [8,9].

Significant effort has also gone into heterogenizing the catalyst system by supporting the metallocene and cocatalyst onto an organic support. Nevertheless, as most of the existing polymerization plants use slurry- or gas-phase processes with heterogeneous catalyst systems, these soluble catalysts are unsuitable for the production of polyolefins on an industrial scale. To overcome this problem, metallocenes can be immobilized on inert supports. Remarkably, using immobilized metallocenes should result in the formation of uniform polymer particles with narrow size distribution and high bulk density compared to those provided by Ziegler–Natta-supported catalysts [10]. To overcome the preparation complexities of traditionally supported metallocene catalysts, metallocene can be supported in situ, which eliminates the need for a supporting step before polymerization. The reasons for the heterogenization of the metallocene are, for example, slower deactivation of the metallocene, avoidance of reactor fouling, less cocatalyst required, good and uniform polymer morphology, high polymer density and requirements of the commercial polymerization processes [11]. Therefore, binding these metallocene catalysts onto suitable inorganic supports can provide a promising way to overcome those drawbacks.

The role of a support material is to prevent the occurrence of sintering processes by providing a large surface area onto which the particles of active phase

can become anchored. Because of the anchoring process the small particles of active phase become stabilized and will resist sintering much more strongly. There is a wide variety of support materials onto which active phases can be stabilized. The most common support materials are simple metal oxides, such as aluminas, silicas and titanias, although zirconias and cerias also find application [12]. Silica has been the most widely used for supported metallocene catalysts so far. However, the property of silica solely was found to be partially unsuitable for the overall catalyst performance. In order to modify the property of the supports, some additives or modifiers are required [13].

The activities and selectivities of the polymerization catalysts are markedly dependent on their pore structure of support. Generally, the metal dispersion is enhanced with the increased surface area of support. But, if the support has large surface area, it usually has small pores. Undoubtedly, the intra-pellet diffusion efficiency, of reactants and products, is poor for small-pore catalysts. On the other hand, while showing improved inside-pore diffusion efficiency, a catalyst with large pore sizes has a specific surface area and is not beneficial to disperse support metal, leading to low metal dispersion and low catalytic activity. The distinct bimodal pore structure support, which contains large pores and small pores at the same time, contributes high diffusion efficiency by the large pores and contributes to higher dispersion of supported metal by the small pores, which enlarged the surface area of the support. Furthermore, it is able to diminish the diffusion resistance by its large pores. Many researchers are interested in obtaining bimodal polyethylene using bicomponent catalyst or support [14-16].

The objectives of this investigation was synthesis of various SiO_2 -based supports having different pore size distribution such as unimodal [Si(Q-50) and Si(P-10)] and bimodal $\text{SiO}_2\text{-Al}_2\text{O}_3$ and investigate on catalytic activities during the copolymerization of ethylene with α -olefins such as 1-hexene, 1-octene, 1-decene using various SiO_2 -based supported MMAO with zirconocene catalysts.

This thesis was divided into five chapters. Chapter I involved an overview of the use of metallocene catalyst for the polyolefin industry. In Chapter II, knowledge and open literature dealing with metallocene catalysis for olefin polymerization were presented. The literature review was accentuated metallocene catalyst system used for copolymerization of ethylene with α -olefins. The experimental procedure as well as the instrument and techniques used for characterizing the resulting polymers were also described in Chapter III.

In Chapter IV, the results on ethylene and α -olefins copolymerization using various unimodal SiO₂ and bimodal silica-alumina-supported zirconocene/dMMAO catalysts were presented. The influences of various pore structures of support on the catalytic activity and polymer properties were investigated. The characteristics support and catalyst precursors using N₂ physisorption, X-ray diffraction (XRD), Thermogravimetric analysis (TGA), Raman spectroscopy, Scanning electron microscopy (SEM), and Energy-dispersive x-ray spectrometer (EDX) and obtained copolymer using Differential scanning calorimetry (DSC) and ¹³C-nuclear magnetic resonance (¹³C-NMR).

Finally, conclusions of this work and some recommendations for future research work were provided in Chapter V.

สถาบันวิทยบริการ
จุฬาลงกรณ์มหาวิทยาลัย

CHAPTER II

LITERATURE REVIEW

2.1 Polymerization of olefins

Until 1953, processes for olefin polymerization were based on a radical process at high pressures and high temperatures. Polymerization of ethylene under these conditions (2000-3000 bars; 150-230°C) yields low-density polyethylene (LDPE, **Figure 2.1**), a low melting, highly branched polyethylene, containing both long- and short chain branches [17]. With propylene only atactic, low molecular weight material can be obtained. Ziegler found that ethylene could also be polymerized using TiCl_4 and alkylaluminium. The process yields linear polyethylene (HDPE, **Figure 2.1**) with a high molecular weight. Natta proved that the same type of catalyst also polymerizes propylene [18]. The resulting polymer mixture is predominantly isotactic with additional polymer fractions that are of a lower stereoregularity or atactic. Copolymerizations of ethylene with 1-hexene/1-octene with the titanium Ziegler catalysts result in copolymers in which the degree of incorporation of the α -olefin varies over the molecular weight distribution. Upon reaction of a vanadium compound, e.g. $\text{V}(\text{acac})_3$ (acac = acetylacetonato) or VCl_4 , with an alkylaluminium cocatalyst a catalyst for the production of EP (copolymer of ethylene and propylene) and EPDM (ethylene-propylene-diene elastomers) is obtained [19]. The homogeneous system shows high initial activity, but is rapidly deactivated [20]. An important advantage is that the comonomers are randomly incorporated in the polymer over the full range of the molecular weight distribution.

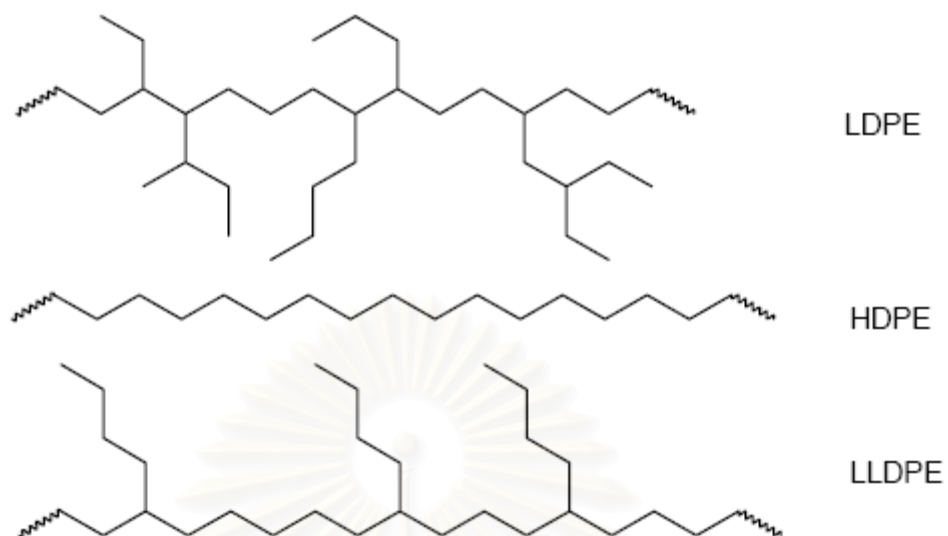


Figure 2.1 Examples of polyethenes: LDPE, HDPE and LLDPE (copolymer of ethene and 1-hexene)

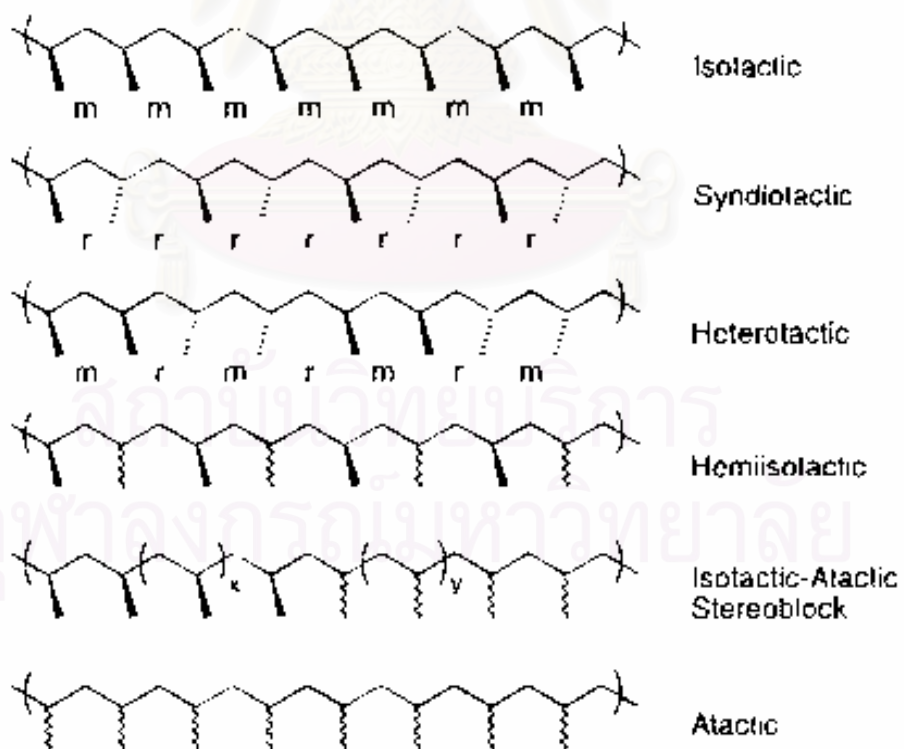


Figure 2.2 Common polymer tacticities [2]

The heterogeneity of Z-N (Ziegler Natta) systems and Phillips/Union Carbide type catalysts makes them very attractive for industrial application, and most polyolefin materials are still produced by means of heterogeneous catalysts [21]. These heterogeneous systems combine high activity with an easy processability of the resulting product mixture and good polymer particle morphology. The catalyst systems contain various types of active sites with different geometries and activities, which often leads to polymers with broad or polymodal molecular weight distributions or to mixtures of different types of polymers (e.g. mixtures of atactic and isotactic polypropene) [22]. Many improvements on the classical Z-N type catalysts have been made over the last 30 years, and modern Z-N systems allow a much better control of polymer properties. Most of these improvements were achieved by empirical methods [23].

In 1957 the first articles on homogeneous titanium-based olefin polymerization were published by Breslow and Newburg [5] and by Natta, Pino and co-workers [24]. When reacting Cp_2TiCl_2 with Et_2AlCl (DEAC) under conditions similar to those used with Z-N systems, a catalyst that polymerizes ethylene is obtained. The first homogeneous systems showed a low activity, when compared to classical Z-N systems and were also not active in polymerization of higher olefins. In contrast to heterogeneous systems, homogeneous catalysts have a single type of well-defined active sites. Although heterogeneous catalysts are in general industrially more practical, a higher control of properties of the catalyst, and more detailed kinetic and mechanistic studies are possible with well-defined molecular catalysts ("single site" catalysts) [6].

2.2 Mechanisms of homogeneous, catalytic olefin polymerization

The geometric and electronic structure of the active species affect the properties of the resulting polymer, such as molecular weight, molecular weight distribution, region and stereoselectivity (for the homopolymerization of α -olefins) and the incorporation of the other monomers. (for copolymerizations).

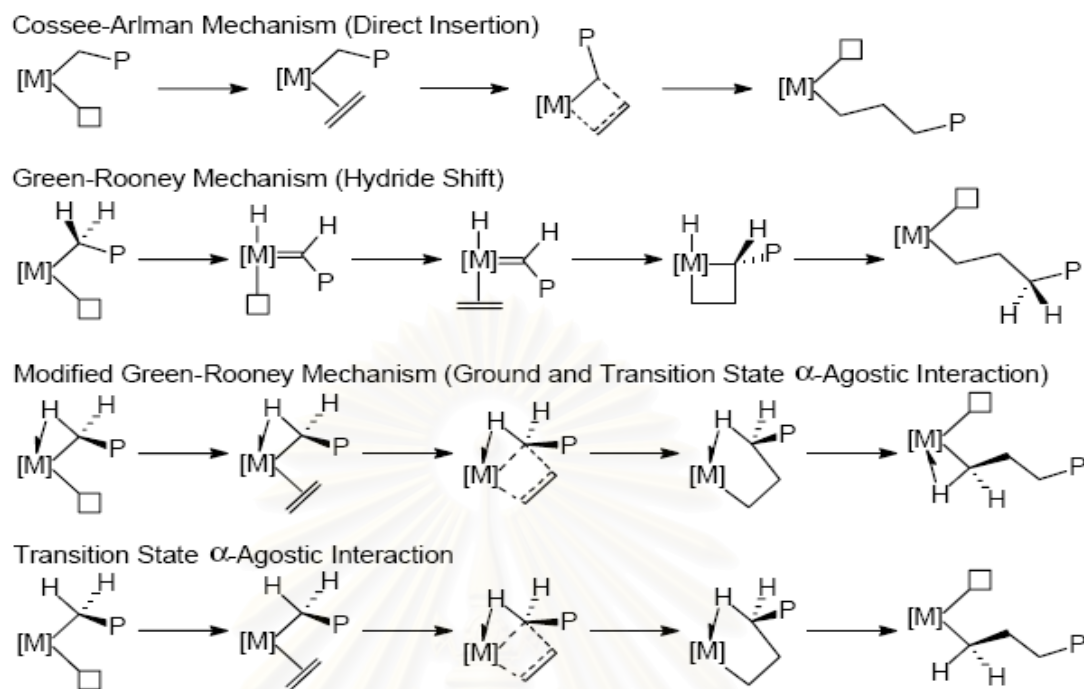


Figure 2.3 Scheme of migratory insertion mechanism, in which the metal-bound alkyl group migrates to the alkene

It is now generally accepted that this active species is an electron deficient, preferably cationic metal alkyl species. For heterogeneous systems the active sites are at dislocations and edges of the crystals, for homogeneous catalysts the active site is enclosed by a set of ancillary ligands. The cationic metal species are electronically balanced by a preferably weakly nucleophilic, weakly coordinating counter anion. Cossee and Arlman were the first to propose a mechanism for catalytic olefin polymerization [25]. They proposed that the polymer chain is growing via a *cis*-insertion of the olefin into a metal-carbon bond, migratory insertion mechanism, in which the metal-bound alkyl group migrates to the alkene shown in **Figure 2.3**

2.2.1 Chain transfer - molecular weight and molecular weight distribution

Besides chain growth, chain transfer processes are also important in olefin polymerization. The rate of chain growth over chain transfer determines molecular weight and molecular weight distribution of the resulting polymer, which

are important factors for material and processing properties. These rates are determined by the catalytic centre and its surrounding ligand (and sometimes by the cocatalyst), and they provide essential information about the polymerization mechanism.

For chain transfer several mechanisms have been revealed, which include termination reactions by β -H, β -CH₃ and H-transfer to monomer (**Figure 2.4**) chain transfer to aluminum (e.g. when an aluminum activator or scavenger is used, (**Figure 2.5**), and σ -bond metathesis between the M-alkyl bond and a C-H bond of an alkene or a solvent molecule. Also chain transfer between catalyst active sites has been suggested (in a dual site ethene/1-hexene copolymerisation).

In industrial polyolefin production, often chain transfer agents such as H₂ are added to the polymerizing mixture to gain a better control of polymer molecular weights [26]. In absence of alkylaluminium the main mechanism for chain transfer is via β -H abstraction. Two different mechanisms for β -H abstraction have been observed (**Figure 2.4**), which differ in the rate determining step (r.d.s.) of the chain transfer. In both cases polymers are obtained with olefinic end-groups. When the β -H transfer to monomer is rate determining (route 1, **Figure 2.4**), the rate of chain termination increases with increasing olefin concentration. Since also the chain growth (rate of insertion) is 1st order in olefin, molecular weights are independent of monomer concentration for these systems. When the rate determining step is the β -H transfer to metal (route 2, **Figure 2.4**) the rate of termination is independent of monomer concentration (0th order in olefin), and molecular weights increase with increasing monomer concentration. When MAO or other alkyls aluminium is present in the reaction medium, another mechanism of chain transfer can be observed. Especially in MAO with a high Me₃Al (TMA) content a considerable amount of chain transfer to aluminum may occur although this

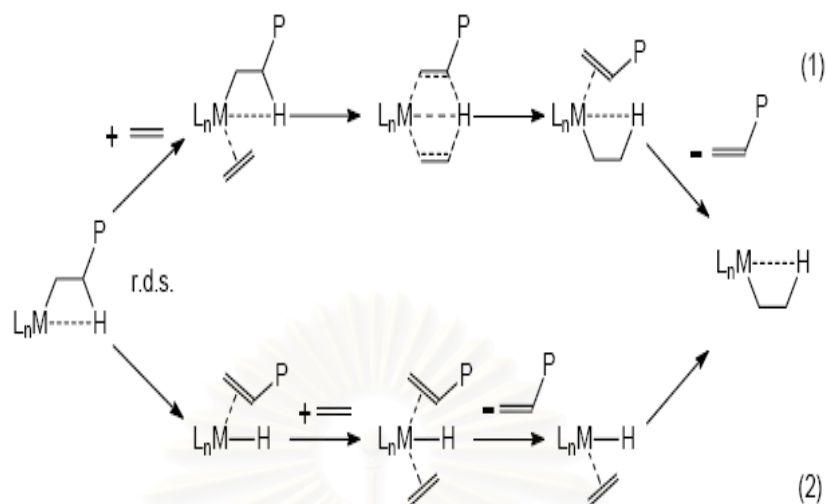


Figure 2.4 Scheme of termination reactions by β -H, β -CH₃ and H-transfer to monomer

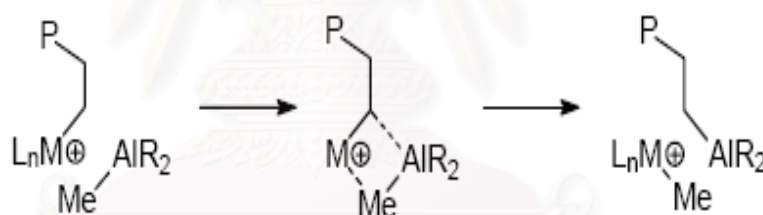


Figure 2.5 Scheme of chain transfer to aluminum

transmetallation has also been observed in TMA-free MAO [27]. As opposed to the mechanisms responsible for chain transfers to monomer, which give olefinic end groups, chain transfers to aluminum give, after hydrolysis, polymers with aliphatic end groups.

2.3 Background on Polyolefin Catalysts

Polyolefins can be produced with free radical initiators, Phillips type catalysts, Ziegler-Natta catalysts and metallocene catalysts. Ziegler-Natta catalysts have been most widely used because of their broad range of application. However, Ziegler-Natta catalyst provides polymers having broad molecular weight distribution (MWD) and composition distribution due to multiple active sites formed [28].

Metallocene catalysts have been used to polymerize ethylene and α -olefins commercially. The structural change of metallocene catalysts can control composition distribution, incorporation of various comonomers, MWD and stereoregularity [29].

2.3.1 Catalyst Structure

Metallocene is a class of compounds in which cyclopentadienyl or substituted cyclopentadienyl ligands are π -bonded to the metal atom. The stereochemistry of biscyclopentadienyl (or substituted cyclopentadienyl)-metal bis (unibidentate ligand) complexes can be most simply described as distorted tetrahedral, with each η^5 -L group (L = ligand) occupying a single co-ordination position, as in **Figure 2.6** [30].

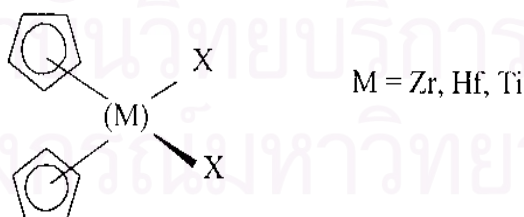


Figure 2.6 Molecular structure of metallocene

Representative examples of each category of metallocenes and some of zirconocene catalysts are shown in **Table 2.1** and **Figure 2.7**, respectively.

Table 2.1 Representative Examples of Metallocenes [30]

| Category of metallocenes | Metallocene Catalysts |
|--|--|
| [A] Nonstereorigid metallocenes | 1) Cp_2MCl_2 (M = Ti, Zr, Hf) 2) Cp_2ZrR_2 (M = Me, Ph, CH_2Ph , CH_2SiMe_3) 3) $(\text{Ind})_2\text{ZrMe}_2$ |
| [B] Nonstereorigid ring-substituted metallocenes | 1) $(\text{Me}_5\text{C}_5)_2\text{MCl}_2$ (M = Ti, Zr, Hf) 2) $(\text{Me}_3\text{SiCp})_2\text{ZrCl}_2$ |
| [C] Stereorigid metallocenes | 1) $\text{Et}(\text{Ind})_2\text{ZrCl}_2$ 2) $\text{Et}(\text{Ind})_2\text{ZrMe}_2$ 3) $\text{Et}(\text{IndH}_4)_2\text{ZrCl}_2$ |
| [D] Cationic metallocenes | 1) $\text{Cp}_2\text{MR}(\text{L})^+[\text{BPh}_4]^-$ (M = Ti, Zr) 2) $[\text{Et}(\text{Ind})_2\text{ZrMe}]^+[\text{B}(\text{C}_6\text{F}_5)_4]^-$ 3) $[\text{Cp}_2\text{ZrMe}]^+[(\text{C}_2\text{B}_9\text{H}_{11})_2\text{M}]^-$ (M = Co) |
| [E] Supported metallocenes | 1) $\text{Al}_2\text{O}_3\text{-Et}(\text{IndH}_4)_2\text{ZrCl}_2$ 2) $\text{MgCl}_2\text{-Cp}_2\text{ZrCl}_2$ 3) $\text{SiO}_2\text{-Et}(\text{Ind})_2\text{ZrCl}_2$ |

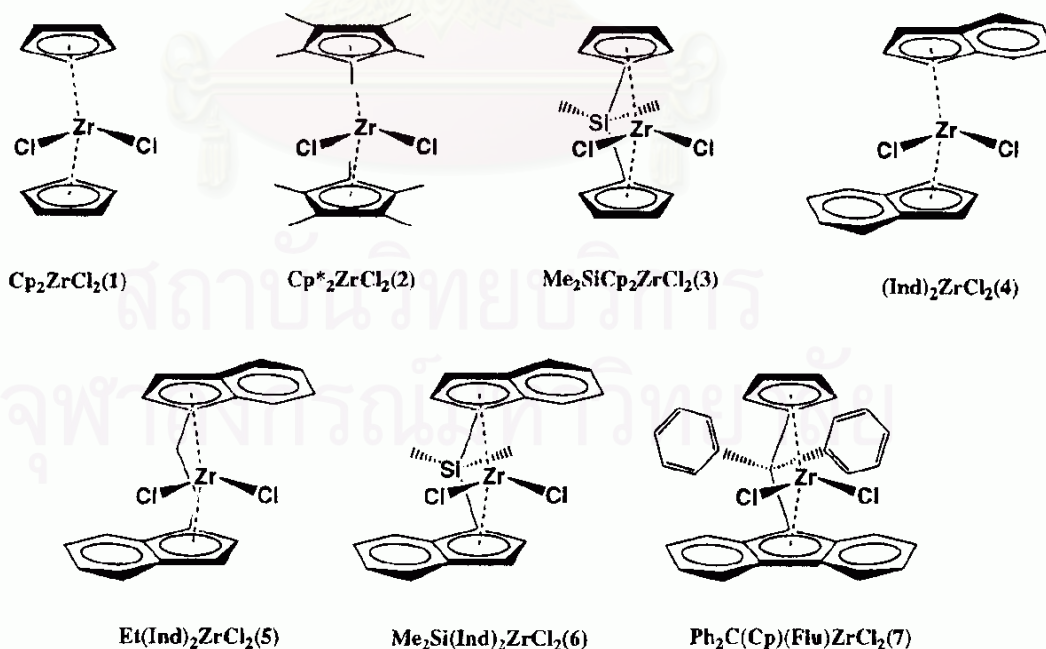


Figure 2.7 Some of zirconocene catalysts structure [31]

Composition and types of metallocene have several varieties. When the two cyclopentadienyl (Cp) rings on either side of the transition metal are unbridged, the metallocene is nonstereorigid and it is characterized by C_{2v} symmetry. The Cp_2M ($M = \text{metal}$) fragment is bent back with the centroid-metal-centroid angle θ about 140° due to an interaction with the other two σ bonding ligands [32]. When the Cp rings are bridged (two Cp rings arranged in a chiral array and connected together with chemical bonds by a bridging group), the stereorigid metallocene, so-called ansa-metallocene, could be characterized by either a C_1 , C_2 , or C_s symmetry depending upon the substituents on two Cp rings and the structure of the bridging unit as schematically illustrated in **Figure 2.8** [30].

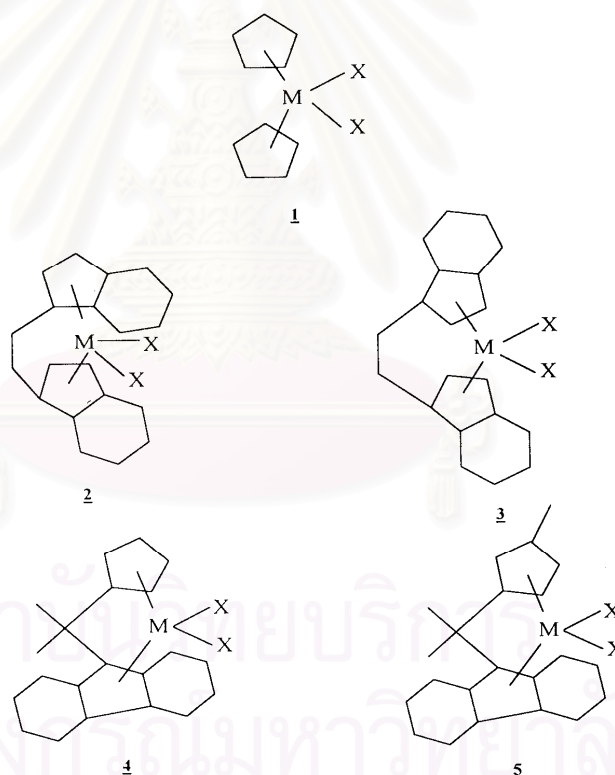


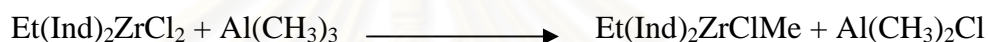
Figure 2.8 Scheme of the different metallocene complex structures [30]. Type 1 is C_{2v} -symmetric; Type 2 is C_2 -symmetric; Type 3 is C_s -symmetric; Type 4 is C_s -symmetric; Type 5 is C_1 -symmetric.

2.3.2 Polymerization Mechanism

The mechanism of catalyst activation is not clearly understood. However, alkylation and reduction of the metal site by a cocatalyst (generally alkyl aluminum or alkyl aluminoxane) is believed to generate the cationic active catalyst species.

First, in the polymerization, the initial mechanism started with formation of cationic species catalyst that is shown below.

Initiation



Propagation proceeds by coordination and insertion of new monomer unit in the metal carbon bond. Cossee mechanism is still one of the most generally accepted polymerization mechanism (**Figure 2.9**) [33]. In the first step, monomer forms a complex with the vacant coordination site at the active catalyst center. Then through a four-centered transition state, bond between monomer and metal center and between monomer and polymer chain are formed, increasing the length of the polymer chain by one monomer unit and generating another vacant site.

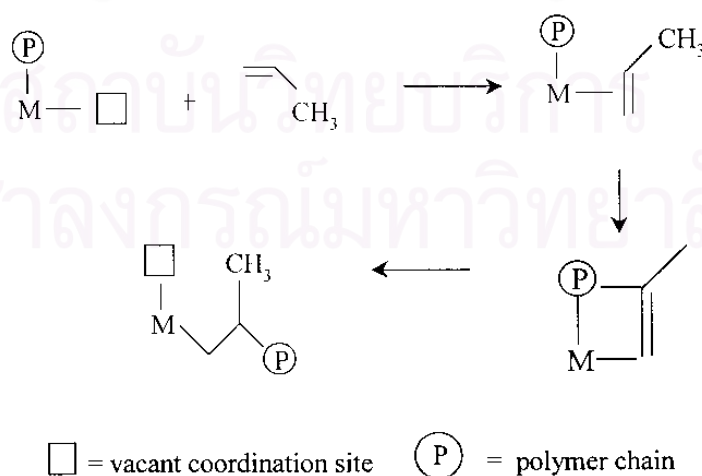


Figure 2.9 Cossee mechanism for Ziegler-Natta olefin polymerization [33].

The trigger mechanism has been proposed for the polymerization of α -olefin with Ziegler-Natta catalysts [2]. In this mechanism, two monomers interact with one active catalytic center in the transition state. A second monomer is required to form a new complex with the existing catalyst-monomer complex, thus trigger a chain propagation step. No vacant site is involved in this model. The trigger mechanism has been used to explain the rate enhancement effect observed when ethylene is copolymerized with α -olefins.

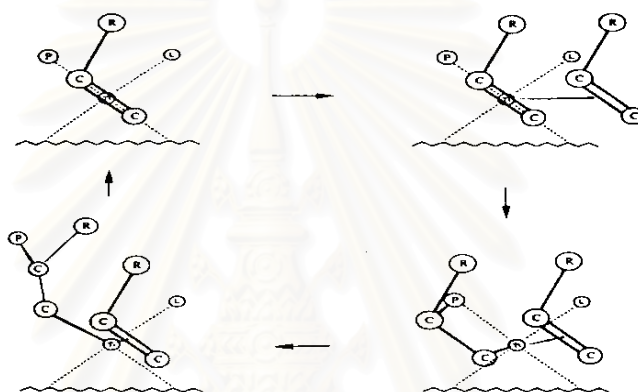


Figure 2.10 The propagation step according to the trigger mechanism [2].

After that, the propagation mechanism in polymerization shown in **Figure 2.11**

Propagation

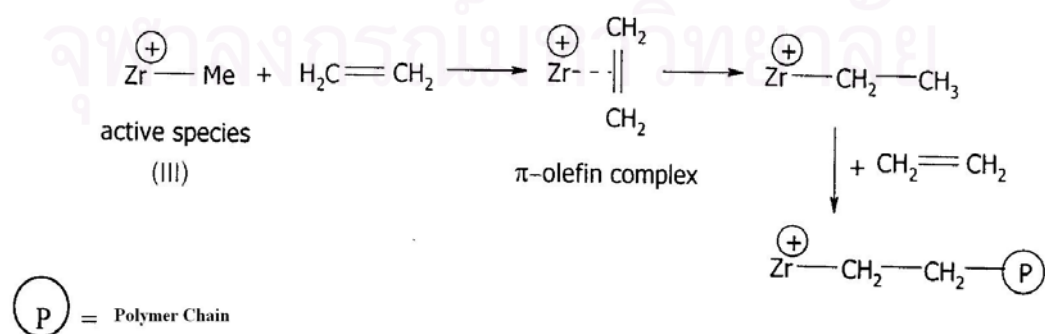


Figure 2.11 Propagation mechanism in polymerization

Finally, the termination of polymer chains can be formed by 1) chain transfer via β -H elimination, 2) chain transfer via β -Me elimination, 3) chain transfer to aluminum, 4) chain transfer to monomer, and 5) chain transfer to hydrogen (**Figure 2.7-2.11**) [30]. The first two transfer reactions form the polymer chains containing terminal double bonds.

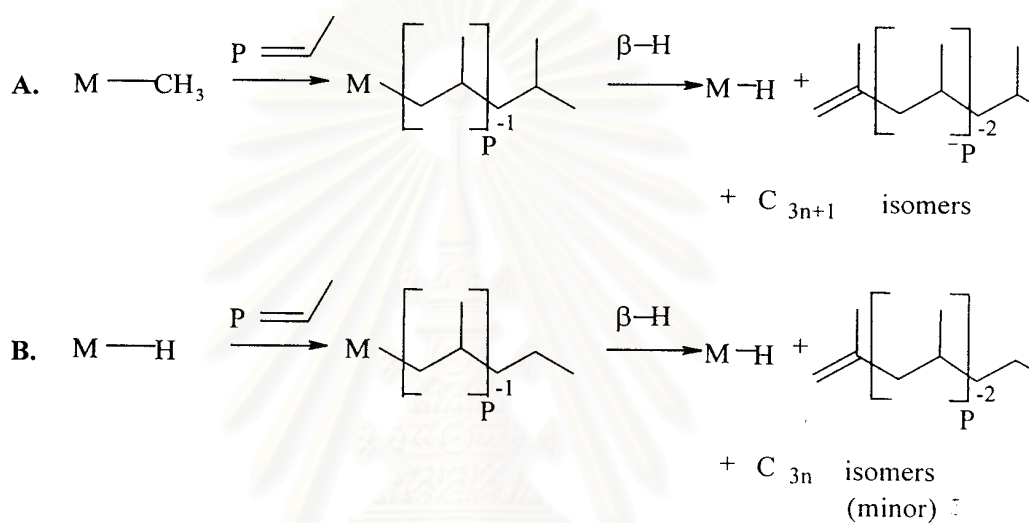


Figure 2.12 Chain transfer via β -H elimination [30]

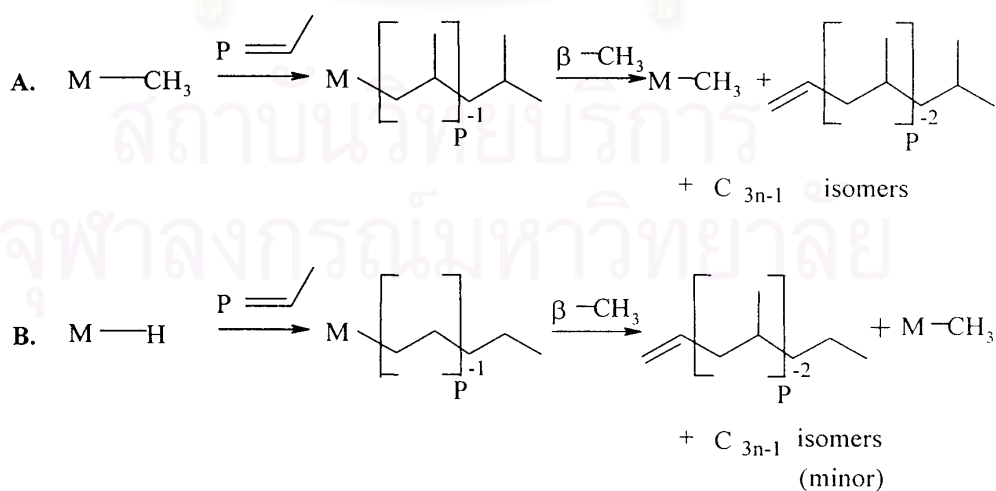


Figure 2.13 Chain transfer via β -CH₃ elimination [30]

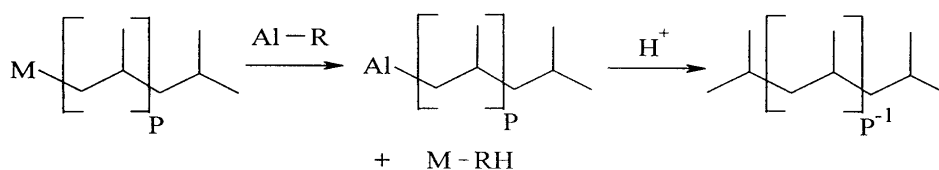


Figure 2.14 Chain transfer to aluminum [30]

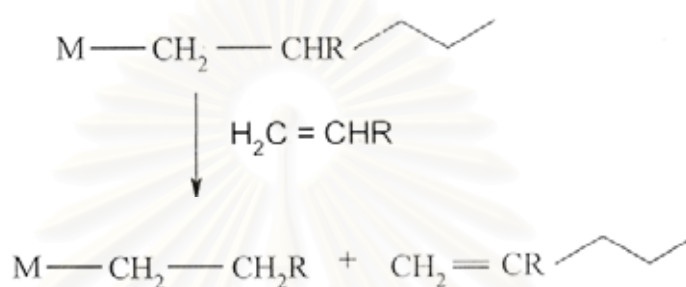


Figure 2.15 Chain transfer to monomer [30]

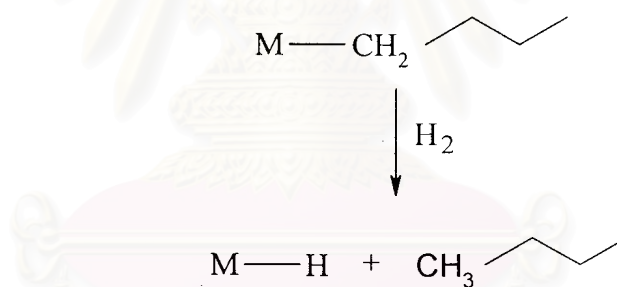


Figure 2.16 Chain transfer to hydrogen [30]

2.3.3 Cocatalysts

Metallocene catalysts have to be activated by a cocatalyst. The most common types of cocatalysts are alkylaluminums including methylaluminoxane (MAO), trimethylaluminum (TMA), triethylaluminum (TEA), triisobutylaluminum (TIBA) and cation forming agents such as $(\text{C}_6\text{H}_5)_3\text{C}^+(\text{C}_6\text{F}_5)_4\text{B}^-$ and $\text{B}(\text{C}_6\text{F}_5)_3$ [34].

Among these, MAO is a very effective cocatalyst for metallocene. However, due to the difficulties and costs involved in the synthesis of MAO, there has been considerable effort done to reduce or eliminate the use of MAO. Due to difficulties in separation, most commercially available MAO contains a significant fraction of TMA (about 10-30%) [35]. This TMA in MAO could be substantially eliminated by toluene-evaporation at 25°C.

Indeed, the difficulties encountered to better understand the important factors for an efficient activation are mainly due to the poor knowledge of the MAO composition and structure. Several types of macromolecular arrangements, involving linear chains, monocycles and/or various three-dimensional structures have been successively postulated. These are shown in **Figure 2.17**. In recent work, a more detailed image of MAO was proposed as a cage molecule, with a general formula $\text{Me}_{6m}\text{Al}_4\text{mO}_{3m}$ (m equal to 3 or 4) [36].

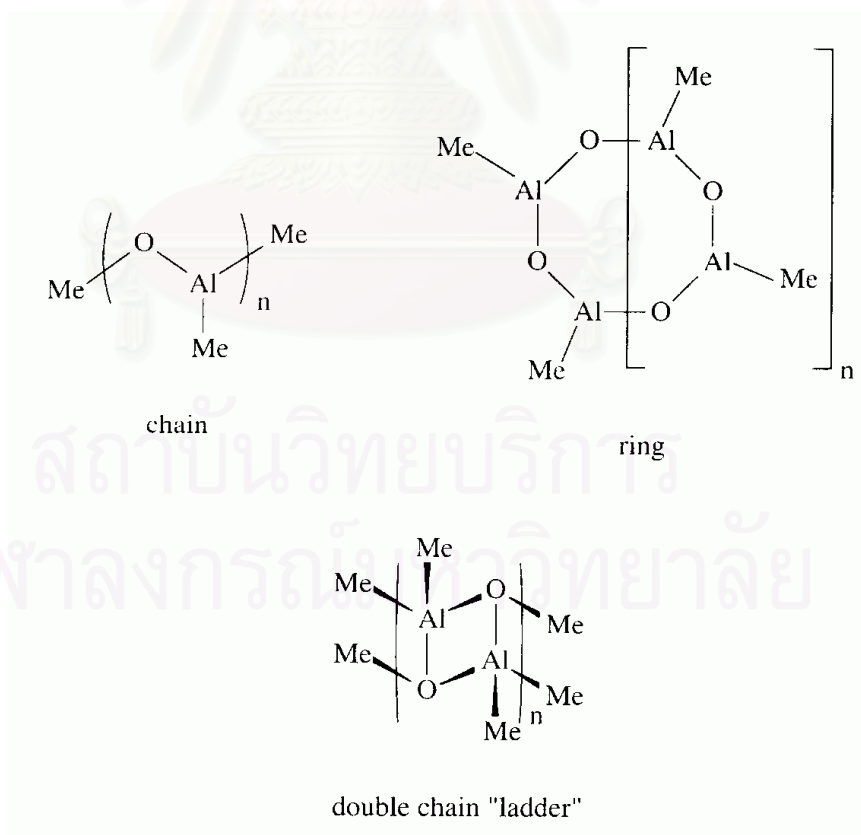


Figure 2.17 Early structure models for MAO [36]

In the case of $\text{rac-Et(Ind)}_2\text{ZrMe}_2$ as precursor, the extracted methyl ligands do not yield any modification in the structure and reactivity of the MAO counter-anion, thus allowing zirconium coordination site available for olefin that presented in **Figure 2.18** [37].

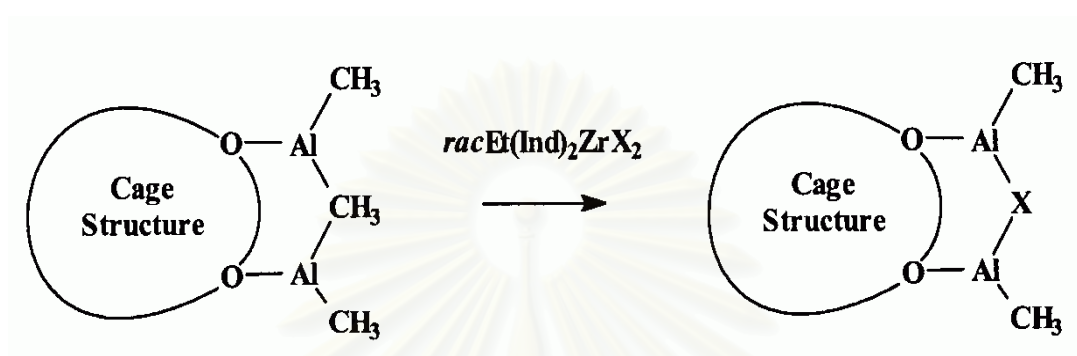


Figure 2.18 Representation of MAO showing the substitution of one bridging methyl group by X ligand extracted from $\text{racEt(Ind)}_2\text{ZrCl}_2$ ($\text{X}=\text{Cl}$, NMe_2 , CH_2Ph) [37].

Cam and Giannini [38] investigated the role of TMA present in MAO by a direct analysis of $\text{Cp}_2\text{ZrCl}_2/\text{MAO}$ solution in toluene- d_8 using $^1\text{H-NMR}$. Their observation indicated that TMA might be the major alkylating agent and that MAO acted mainly as a polarization agent. However, in general it is believed that MAO is the key cocatalyst in polymerizations involving metallocene catalysts. The role of MAO included 1) alkylation of metallocene, thus forming catalyst active species, 2) scavenging impurities, 3) stabilizing the cationic center by ion-pair interaction and 4) preventing bimetallic deactivation of the active species.

The homogeneous metallocene catalyst cannot be activated by common trialkylaluminum only. However, Soga *et al.* [39] were able to produce polyethylene with modified homogeneous Cp_2ZrCl_2 activated by common trialkylaluminum in the presence of $\text{Si}(\text{CH}_3)_3\text{OH}$. Their results show that for an “optimum” yield aging of the catalyst and $\text{Si}(\text{CH}_3)_3\text{OH}$ mixture for four hours is required. However, MWD of the produced polymers is bimodal although the polymers obtained in the presence of MAO have narrow MWD.

Ethylene/ α -olefins copolymers with bimodal CCD were produced with homogeneous Cp_2ZrCl_2 with different cocatalysts such as MAO and mixture of TEA/borate or TIBA/borate [40]. It seemed that the active species generated with different cocatalysts have different activities and produce polymers with different molecular weights.

2.3.4 Catalyst Activity

The ethylene polymerization rate of the copolymerization reaction with the catalyst system $\text{SiO}_2/\text{MAO}/\text{rac-Me}_2\text{Si} [2\text{-Me-4-Ph-Ind}]_2\text{ZrCl}_2$ was studied by Fink *et al.* [41]. The temperature was varied from 40 to 57°C. Small amount of hexene in the reaction solution increased the polymerization rate. The extent of the "comonomer effect" depended on the polymerization temperature. At 57°C the maximum activity of the ethylene/hexene copolymerization was 8 times higher than the homopolymerization under the same conditions. At 40°C the highest reaction rate for the copolymerization is only 5 times higher than that for the ethylene homopolymerization. For the polymer properties of the ethylene/ α -olefin copolymerization, the molecular weights of the polymers decreased with increasing comonomer incorporation. Ethylene/hexene copolymers produced by a metallocene catalyst also have the same melting point and glass transition temperature.

Series of ethylene copolymerization with 1-hexene or 1-hexadecene over four different siloxy-substituted ansa-metallocene/methylaluminoxane (MAO) catalyst systems were studied by Seppala *et al.* [42]. Metallocene catalysts $\text{rac-Et}[2\text{-(t-BuMe}_2\text{SiO)Ind}]_2\text{ZrCl}_2$ (1), $\text{rac-Et}[1\text{-(t-BuMe}_2\text{SiO)Ind}]_2\text{ZrCl}_2$ (2), $\text{rac-Et}[2\text{-(i-Pr}_3\text{SiO)Ind}]_2\text{ZrCl}_2$ (3) and $\text{rac-Et}[1\text{-(i-Pr}_3\text{SiO)Ind}]_2\text{ZrCl}_2$ (4) were used. The effects of minor changes in the catalyst structure, more precisely changes in the ligand substitution pattern were studied. They found that series of polymerization with siloxy-substituted bis(indenyl) ansa-metallocene are highly active catalyst precursors for ethylene- α -olefins copolymerizations. The comonomer response of all four catalyst precursors was good. Under the same conditions the order of copolymerization ability of the catalyst was $\text{rac-Et}[2\text{-(i-Pr}_3\text{SiO)Ind}]_2\text{ZrCl}_2 >$

$\text{rac-Et}[2\text{-}(\text{t-BuMe}_2\text{SiO})\text{Ind}]_2\text{ZrCl}_2$ and $\text{rac-Et}[1\text{-}(\text{i-Pr}_3\text{SiO})\text{Ind}]_2\text{ZrCl}_2 > \text{rac-Et}[1\text{-}(\text{t-BuMe}_2\text{SiO})\text{Ind}]_2\text{ZrCl}_2$. These catalysts are able to produce high molecular weight copolymers.

2.3.5 Copolymerization

By adding a small amount of comonomer to the polymerization reactor, the final polymer characteristics can be dramatically changed. For example, the Unipol process for linear low density polyethylene (LLDPE) uses hexene and the British Petroleum process (BP) use 4-methylpentene to produce high-performance copolymers [43]. The comonomer can be affected the overall crystallinity, melting point, softening range, transparency and also structural, thermochemical, and rheological properties of the formed polymer. Copolymers can also be used to enhance mechanical properties by improving the miscibility in polymer blending [44].

Ethylene is copolymerized with α -olefin to produce polymers with lower densities. It is commonly observed that the addition of a comonomer generally increases the polymerization rate significantly. This comonomer effect is sometimes linked to the reduction of diffusion limitations by producing a lower crystallinity polymer or to the activation of catalytic sites by the comonomer. The polymer molecular weight often decreases with comonomer addition, possibly because of a transfer to comonomer reactions. Heterogeneous polymerization tends to be less sensitive to changes in the aluminum/transition metal ratio. Chain transfer to aluminum is also favored at high aluminum concentrations. This increase in chain transfer would presumably produce a lower molecular weight polymer. In addition, some researchers observed the decrease, and some observed no change in the molecular weight with increasing aluminum concentration [8].

The effect of polymerization conditions and molecular structure of the catalyst on ethylene/ α -olefin copolymerization have been investigated extensively.

Pietikainen and Seppala [45] investigated the effect of polymerization temperature on catalyst activity and viscosity average molecular weights for low molecular weight ethylene/propylene copolymers produced with homogeneous Cp_2ZrCl_2 . Soga and Kaminaka [46] compared copolymerizations (ethylene/propylene, ethylene/1-hexene, and propylene/1-hexene) with $\text{Et}(\text{H}_4\text{Ind})_2\text{ZrCl}_2$ supported on SiO_2 , Al_2O_3 or MgCl_2 . Broadness of MWD was found to be related to the combination of support types and types of monomers. The effect of silica and magnesium supports on copolymerization characteristics was also investigated by Nowlin *et al.* [47]. Their results indicated that comonomer incorporation was significantly affected by the way that support was treated based on the reactivity ratio estimation calculated with simplified Finemann Ross method. However, it should be noted that Finemann Ross method could be misleading due to linear estimation of nonlinear system.

Copolymer based on ethylene with different incorporation of 1-hexene, 1-octene, and 1-decene were investigated by Quijada [48]. The type and the concentration of the comonomer in the feed do not have a strong influence on the catalytic activity of the system, but the presence of the comonomer increases the activity compared with that in the absence of it. From ^{13}C -NMR it was found that the size of the lateral chain influences the percentage of comonomer incorporated, 1-hexene being the highest one incorporated. The molecular weight of the copolymers obtained was found to be dependent on the comonomer concentration in the feed, showing that there is a transfer reaction with the comonomer. The polydispersity (M_w/M_n) of the copolymers is rather narrow and dependent on the concentration of the comonomer incorporation.

Soga *et al.* [49] noted that some metallocene catalysts produce two-different types of copolymers in terms of crystallinity. They copolymerized ethylene and 1-alkenes using 6 different catalysts such as Cp_2ZrCl_2 , Cp_2TiCl_2 , Cp_2HfCl_2 , $\text{Cp}_2\text{Zr}(\text{CH}_3)_2$, $\text{Et}(\text{Ind H}_4)_2\text{ZrCl}_2$ and $i\text{-Pr}(\text{Cp})(\text{Flu})\text{ZrCl}_2$. Polymers with bimodal crystallinity distribution (as measured by TREF-GPC analysis) were produced with some catalytic systems. Only $\text{Cp}_2\text{TiCl}_2\text{-MAO}$ and $\text{Et}(\text{H}_4\text{Ind})_2\text{ZrCl}_2\text{-MAO}$ produced polymers that have unimodal crystallinity distribution. The results seem to indicate

that more than one active site type are present in some of these catalysts. However, it is also possible that unsteady-state polymerization conditions might have caused the broad distributions since the polymerization times were very short (5 minutes for most cases).

Marques *et al.* [50] investigated copolymerization of ethylene and 1-octene by using the homogeneous catalyst system based on $\text{Et}(\text{Flu})_2\text{ZrCl}_2/\text{MAO}$. A study was performed to compare this system with that of $\text{Cp}_2\text{ZrCl}_2/\text{MAO}$. The influence of different support materials for the Cp_2ZrCl_2 was also evaluated, using silica, MgCl_2 , and the zeolite sodic mordenite NaM. The copolymer produced by the $\text{Et}(\text{Ind})_2\text{ZrCl}_2/\text{MAO}$ system showed higher molecular weight and narrower molecular weight distribution, compared with that produced by $\text{Cp}_2\text{ZrCl}_2/\text{MAO}$ system. Because of the extremely congested environment of the fluorenyl rings surrounding the transition metal, which hinders the beta hydrogen interaction, and therefore, the chain transference. Moreover, the most active catalyst was the one supported on SiO_2 , whereas the zeolite sodic mordenite support resulted in a catalyst that produced copolymer with higher molecular weight and narrower molecular weight distribution. Both homogeneous catalytic systems showed the comonomer effect, considering that a significant increase was observed in the activity with the addition of a larger comonomer in the reaction medium.

The effect of different catalyst support treatments in the 1-hexene/ethylene copolymerization with supported metallocene catalyst was investigated by Soares *et al.* [51]. The catalysts in the study were supported catalysts containing SiO_2 , commercial MAO supported on silica (SMAO) and MAO pretreated silica (MAO/silica) with Cp_2HfCl_2 , $\text{Et}(\text{Ind})_2\text{HfCl}_2$, Cp_2ZrCl_2 and $\text{Et}(\text{Ind})_2\text{ZrCl}_2$. All the investigated supported catalysts showed good activities for the ethylene polymerization (400-3000 kg polymer/mol metal.h). Non-bridged catalysts tend to produce polymers with higher molecular weight when supported on to SMAO and narrow polydispersity. The polymer produced with Cp_2HfCl_2 supported on silica has only a single low crystallinity peak. On the other hand, Cp_2HfCl_2 supported on SMAO and MAO/silica produced ethylene/1-hexene copolymers having bimodal

CCDs. For the case of Cp_2ZrCl_2 and $\text{Et}(\text{Ind})_2\text{ZrCl}_2$, only unimodal CCDs were obtained. It seems that silica-MAO-metallocene and silica-metallocene site differ slightly in their ability to incorporate comonomer into the growing polymer chain, but not enough to form bimodal CCDs.

Soares *et al.* [52] studied copolymerization of ethylene and 1-hexene. It was carried out with different catalyst systems (homogeneous $\text{Et}(\text{Ind})_2\text{ZrCl}_2$, supported $\text{Et}(\text{Ind})_2\text{ZrCl}_2$ and in-situ supported $\text{Et}(\text{Ind})_2\text{ZrCl}_2$). Supported $\text{Et}(\text{Ind})_2\text{ZrCl}_2$: an $\text{Et}(\text{Ind})_2\text{ZrCl}_2$ solution was supported on SMAO. It was used for polymerization of ethylene and 1-hexene. In-situ supported $\text{Et}(\text{Ind})_2\text{ZrCl}_2$: an $\text{Et}(\text{Ind})_2\text{ZrCl}_2$ solution was directly added to SMAO in the polymerization reactor, in the absence of soluble MAO. Homogeneous $\text{Et}(\text{Ind})_2\text{ZrCl}_2$ showed higher catalytic activity than the corresponding supported and in-situ supported metallocene catalysts. The relative reactivity of 1-hexene increased in the following order: supported metallocene \approx in-situ supported metallocene $<$ homogeneous metallocene catalysts. The MWD and short chain branching distribution (SCBD) of the copolymer made with the in-situ supported metallocene were broader than those made with homogeneous and supported metallocene catalysts. They concluded that there are at least two different active species on the in-situ supported metallocene catalyst for the copolymerization of ethylene and 1-hexene.

Soares *et al.* [9] investigated copolymerization of ethylene and 1-hexene with different catalysts: homogeneous $\text{Et}(\text{Ind})_2\text{ZrCl}_2$, Cp_2HfCl_2 and $[(\text{C}_5\text{Me}_4)\text{SiMe}_2\text{N}(\text{tert-Bu})]\text{TiCl}_2$, the corresponding in-situ supported metallocene and combined in-situ supported metallocene catalyst (mixture of $\text{Et}(\text{Ind})_2\text{ZrCl}_2$ and Cp_2HfCl_2 and mixture of $[(\text{C}_5\text{Me}_4)\text{SiMe}_2\text{N}(\text{tert-Bu})]\text{TiCl}_2$. They studied properties of copolymers by using ^{13}C NMR, gel permeation chromatography (GPC) and crystallization analysis fractionation (CRYSTAF) and compared with the corresponding homogeneous metallocene. The in-situ supported metallocene produced polymers having different 1-hexene fractions, SCBD and MDW. It was also demonstrated that polymers with broader MWD and SCBD can be produced by combining two different in-situ supported metallocenes.

In addition, Soares *et al.* [53] studied copolymerization of ethylene and 1-hexene with an in-situ supported metallocene catalysts. Copolymer was produced with alkylaluminum activator and effect on MWD and SCBD was examined. They found that TMA exhibited the highest activity while TEA and TIBA had significantly lower activities. Molecular weight distributions of copolymers produced by using the different activator types were unimodal and narrow, however, short chain branching distributions were very different. Each activator exhibited unique comonomer incorporation characteristics that can produce bimodal SCBD with the use of a single activator. They used individual and mixed activator system for controlling the SCBDs of the resulting copolymers while maintaining narrow MWDs.

2.4 Metallocene Catalysts

2.4.1 Olefin Polymerization with Metallocene Catalysts

The modern organometallic chemistry has begun when apply metallocene complexes with Group IV metals to new technologies and production of new materials. Metallocene compounds are becoming an important grade of catalysts for the synthesis of organic molecules and polymers. Metallocene catalysts are operated in all living industrial plants that are presently used for polyolefin manufacture revolutionize the technology for the production of these polymers [28].

Polyethylene's properties and the appropriate technology must be used to produce products which have the required properties by customer. This requires detailed knowledge and know-how of relationships among processing conditions, polymer structure and polymer properties. For catalytic polymerization processes the catalyst, mostly in combination with a cocatalyst, and the polymerization process are observed as the polymerization technology. This means that both the process and the catalyst are an integrated completion and must be well balanced in respect to each other [29]. The catalyst or catalyst system plays the key role, as polymerization behavior such activity, molecular mass regulation, copolymerization behavior,

process control and polymer structure such molecular mass distribution, comonomer distribution, chain structure and polymer particle morphology such bulk density, particle size, particle distribution, in the choice of process and product properties [30]. The catalyst determines the polymerization behavior, the polymer structure and the polymer powder morphology in heterogeneous processes. The catalyst system must appropriate the polymerization process.

2.4.2 Catalyst Systems for Olefin Polymerization

In 1953 Karl Ziegler, who succeeded in polymerizing ethylene into high-density polyethylene (HDPE) at standard pressure and room temperature, discovered of catalysts based on titanium trichloride and diethylaluminum chloride as cocatalyst, at the Max-Planck-Institute in Mulheim. A little later, Natta, at the Polytechnical Institute of Milan, was able to indicate that an appropriate catalyst system was capable of polymerizing propene into semi-crystalline polypropene. Ziegler and Natta shared a Nobel Prize for Chemistry in 1963 for their work [2]. With this so-called Ziegler-Natta catalyst.

Ziegler-Natta catalyst has been widely used in olefin polymerization; the coordination polymerization allows the catalyst geometry around the metal center to control the polymer structure. In homogeneous polymerization, the ligand of a catalyst largely controls the geometry of an active metal center on which the polymerization reaction occurs. However, the conventional Ziegler-Natta catalysts the molecular structure of the polymers cannot be controlled well the molecular structure of the polymers because these catalysts have different nature types of catalytic sites.

Kaminsky discovered the metallocene catalyst system; it has proven to be a major breakthrough for the polyolefin industry. Metallocene catalysts show in opposite to conventional Ziegler-Natta catalytic systems, only one type of active site (single site catalyst), which produces polymers with a narrow molar mass distribution

($M_w/M_n = 2$). The molecular structure of the metallocene catalysts can be easily changed which allows control of the structure of polyolefin produced with these catalysts. Many metallocene are soluble in hydrocarbons or liquid propene. These properties allow one to predict accurately the properties of the resulting polyolefins by knowing the structure of the catalyst used during their manufacture and to control the resulting molar mass and distribution, comonomer content and tacticity by careful selection of the appropriate reactor conditions. In addition, their catalytic activity is 10-100 times higher than that of the classical Ziegler-Natta systems.

Metallocene, in combination with the conventional aluminum alkyl cocatalyst used in Ziegler systems, are indeed capable of polymerizing ethylene, but only at a very low activity. Only with the discovery and application of methylaluminoxane (MAO) by Sinn et al., 1980, was it possible to enhance the activity, surprisingly, by a factor of 10000. Therefore, MAO played a crucial part in the catalysis with metallocenes. Since this discovery of effective zirconocene-MAO catalyst systems for ethylene polymerization, development of the catalyst system has been conducted to achieve higher activity and to obtain higher molecular weight polyethylene. Modifications of metallocene ligand were investigated in non-bridged and bridged zirconocene catalysts [31].

The varying ligand of the metallocene can be change the different microstructures and characteristics in polyolefin. By combining different olefins and cycloolefins with one another, the range of characteristics can be further broadened. The production of polyolefin with tailored microstructures and chemically uniform copolymers has not yet been achieved by conventional heterogeneous catalysts [2]. However, extensive research has been concerned towards metallocene catalyst studying modifications of the catalyst system, which leads to specific changes in catalytic activity and product characteristics [31]. The development of metallocene catalysts has not yet been complete, and studies are required to increase the understanding of several important factors which affect catalytic performance, such as transition metal-olefin interaction, metal-alkyl bond stability, influence of other ligands, and steric effects of the other ligands.

2.5 Heterogeneous System

The new metallocene/MAO systems offer more possibilities in olefin polymerization compared to conventional Ziegler-Natta catalysts, such as narrow stereoregularity, molecular weight and chemical composition distributions (CCDs) through ligand design. However, only heterogeneous catalysts can be practically used for the existing gas phase and slurry polymerization processes. Without using a heterogeneous system, high bulk density and narrow size distribution of polymer particles cannot be achieved. The advantages of supporting catalysts include improved morphology, less reactor fouling, lower Al/metal mole ratios required to obtain the maximum activities in some cases the elimination of the use of MAO, and improved stability of the catalyst due to much slower deactivation by bimolecular catalyst interactions. Therefore, developing heterogeneous metallocene catalysts, that still have all the advantages of homogeneous systems, became one of the main research objectives of applied metallocene catalysis.

Steinmetz *et al.* [54] examined the particle growth of polypropylene made with a supported metallocene catalyst using scanning electron microscopy (SEM). They noticed formation of a polymer layer only on the outer surface of catalyst particles during the initial induction period. As the polymerization continued, the whole particle was filled with polymer. Particle fragmentation pattern depended on the type of supported metallocene.

2.5.1 Catalyst Chemistry

The nature of the active sites affects the polymer morphology, catalyst stability and activity, and the characteristics of the polymer produced. However, structure and chemistry of the active sites in supported catalysts are not clearly understood. Catalytic activities for supported metallocene are usually much lower than that of their counterpart homogeneous system. Formation of different active species, deactivation of catalyst during supporting procedure, and mass transfer resistance may contribute to decreased catalyst activity.

Tait *et al.* [55] reported general effects of support type, treatment, supporting procedure, and type of diluents on reaction kinetics and physical properties of polymer produced. Although the activities of supported catalysts are much lower compared to homogeneous systems. The activity of catalysts increased slightly when *o*-dichlorobenzene was introduced in toluene

The catalytic activities of supported catalyst depended on the percentage of the incorporated metallocene was reported by Quijada *et al.* [56]. However, in the case of metallocenes supported on MAO pretreated silica, depending on how the surface bound MAO complex with the catalyst, the activity can be as high as that of homogeneous system. According to the experiment by Chein *et al.* [57], if a single MAO is attached to silica, it would complex with zirconocene and lowers its activity. On the other hand, if multiple MAOs are attached to the surface silanol, the supported zirconocene will not be further complexed with MAO and have activity.

2.5.2 Supporting Methods

In the case of carriers like silica or other inorganic compounds with OH group on the surface, the resulting catalyst displayed very poor activities even combined with MAO. The reaction of metallocene complexes with the Si-OH groups might cause the decomposition of active species. Such decomposition could be suppressed by fixing MAO on the silica surface and then reacting with metallocenes [58]. Therefore, silica must be pretreated before the interaction with metallocene, to reduce the OH concentration and to prepare an adequate surface for metallocene adsorption and reaction in a non-deactivating way [59]. Metallocene immobilization methods can be divided in to three main groups. The first method is the direct support of catalyst onto an inert support. The second method involves the pretreatment of the inert support with MAO or other alkylaluminum followed by metallocene supporting. The third method, the catalyst is chemically anchored to the support, which often involves in-situ catalyst synthesis. These methods produce catalysts with distinct activities, comonomer reactivity ratios, and stereospecificities.

2.5.2.1 Direct Supporting of Inert Material

Collins *et al.* [60] reported that $\text{Et}(\text{Ind})_2\text{ZrCl}_2$, when supported on partially dehydrated silica, reacted with surface hydroxyl groups during adsorption to form inactive catalyst precursors and free ligands (**Figure 2.19**). Therefore, the activity is lower compared to the case of using dehydrated silica. **Figure 2.20** shows the proposed structure $\text{Et}(\text{Ind})_2\text{ZrCl}_2$ supported on alumina. For the case of alumina, the activity of catalyst supported on dehydrated alumina is lower than the one supported on partially dehydrated alumina. The high Lewis acidity of aluminum sites on dehydrated alumina facilitates the formation of Al-Cl bonds and Zr-O bonded species when the metallocene compound is adsorbed on these sites. However, the metal sites in this case remain inactive even after MAO addition.

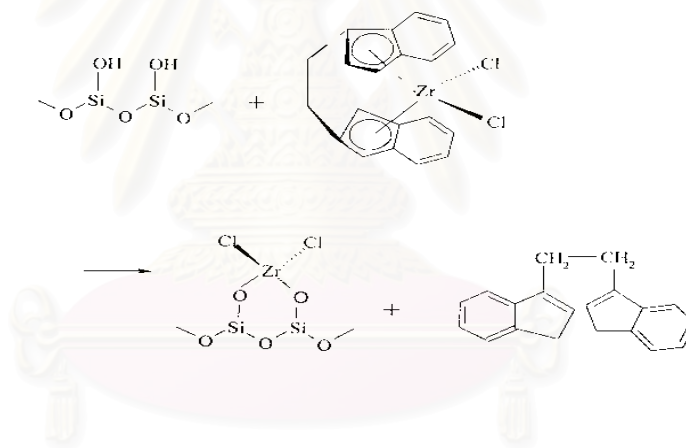


Figure 2.19 Structure of $\text{Et}(\text{Ind})_2\text{ZrCl}_2$ supported on silica [8]

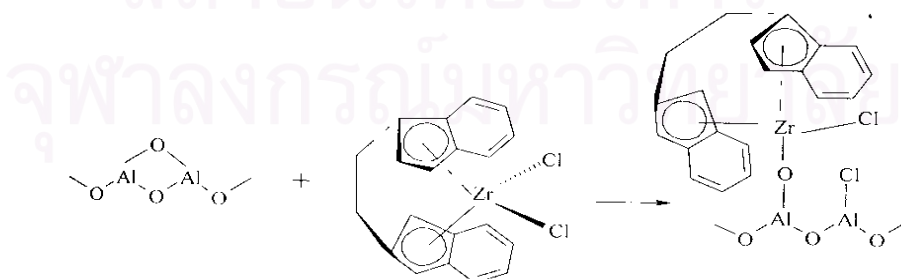


Figure 2.20 Structure of $\text{Et}(\text{Ind})_2\text{ZrCl}_2$ supported on alumina [8]

Kaminsky *et al.* [61] proposed a possible explanation for the different behavior of metallocene supported directly on to silica, homogeneous systems, or supported onto MAO-pretreated silica. It is assumed that the supporting of metallocenes on silica takes place in three stages. First, the metallocene reacts with OH groups of the silica as shown in **Figure 2.21**.

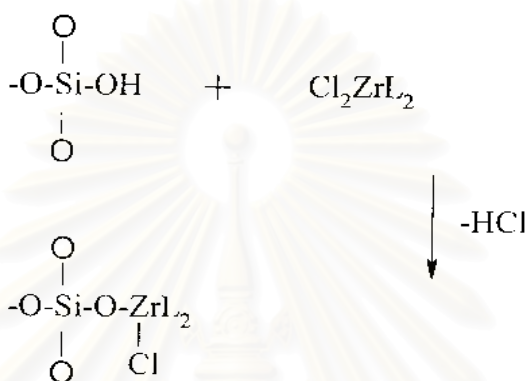


Figure 2.21 Reaction of silica and metallocene during catalyst supporting [61], where L is a ligand (Cp, Ind).

The second step is the alkylation by MAO as shown in **Figure 2.22**

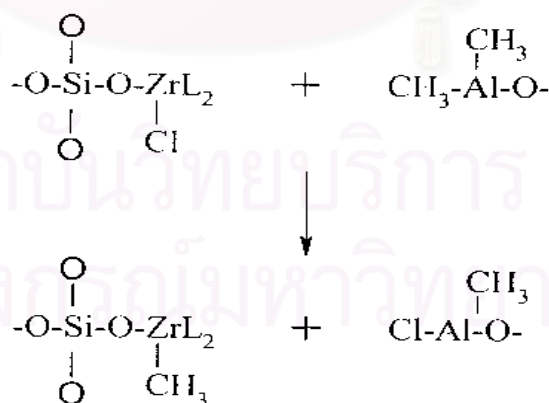


Figure 2.22 Alkylation of supported metallocene by MAO [61]

The third step is the dissociation of the $-\text{SiO}_2\text{-O-Zr-}$ bond to an ion pair to form the cation active center $(\text{SiO})^-(\text{Zr})^+$. The polydispersity of polymers produced with these supported metallocenes are reported to be relatively high ($5 \approx 8$) due to different electronic and steric interactions between the silica surface and the metal active sites. The immobilization of the zirconocene on silica inhibits bimolecular deactivation processes because the active sites are separated from each other.

As a consequence less use of MAO is required, increased molecular weights are achieved due to the reduction of β -hydrogen transfer by a second zirconocene center, and polypropylene of higher isotacticity and melting point is formed.

2.5.2.2 Supporting Catalyst on Materials Treated with Alkylaluminum

When silica is pretreated with MAO, the supporting mechanism is different. The zirconocene is complexed to MAO supported on silica, which will make the catalyst similarly to a homogeneous system. The polymers produced in this way have lower molecular weights.

Hiatky and Upton [62] reported that supporting of the aluminum-alkyl free catalysts can form 2 complexes as shown in **Figure 2.23**, (a) deactivation through coordination of Lewis-basic surface oxides to the electrophilic metal center or (b) reaction of the ionic complex with residual surface hydroxyl groups.

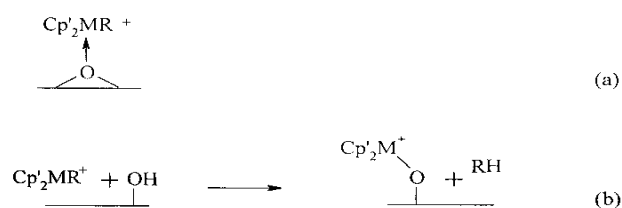


Figure 2.23 Effect of surface hydroxyl groups on ionic metallocene catalysts [62]

However, highly active supported ionic metallocene catalysts for olefin polymerization can be prepared by pretreating the support with scavenger. It is assumed that pretreatment of the support with a scavenger serves to activate the support and compatibilize it with the ionic metallocene complex.

Lee *et al.* [63] used TMA pretreated-silica as the support for metallocene catalysts. The activity of supported catalysts showed dependency to H₂O content in silica, H₂O/TMA ratio, metallocene, and cocatalyst. The supported catalyst was also able to polymerize ethylene in the absence of MAO when common alkyl aluminum was used as the cocatalyst.

The surface aluminum and metallocene loading was studied by Santos *et al.* [64]. About 7 wt% of MAO can be supported on silica when the initial amount of MAO in mixture of silica was ca. 10 wt%. Depending on silica types, saturation of MAO supported on silica can occur at lower MAO contents.

Harrison *et al.* [65] compared a variety of silica and alumina supports with different degrees of surface hydroxylation as the supports. It was shown that as the concentration of OH groups on the surface of the support increased, more MAO could be impregnated and thus catalyst with more metallocene content could be produced. The most obvious benefit of supported catalyst with more metallocene was increased activities compared to catalysts with lower concentration of surface hydroxyl groups (increased activities both in kg PE/mol Zr/hr and kg PE /g-support/h). However, at high polymerization temperatures, leaching of catalyst from the support was observed. In lower polymerization temperatures, leaching was less significant, however, the morphology and bulk density of the polymer formed were still unsuitable for use in gas-phase polymerization.

For the case of propylene polymerization, a decrease in syndiotacticity was observed by Xu *et al.* [66] when the metallocene catalyst was supported on pretreated silica.

2.5.2.3 Chemically Anchoring Catalyst on Support

Soga *et al.* [67] described a method to support zirconocenes more rigidly on SiO_2 . The supporting steps are as follows: 1) Silica was treated with SiCl_4 to substitute the OH groups with chlorine atoms. 2) The resulting silica was filtered and washed with tetrahydrofuran (THF). 3) The solid was re-suspended in THF and a lithium salt of indene, dissolved in THF, was added drop-wise. 4) The resulting solid was filtered and washed again with THF. And to re-suspended solid in THF, $\text{ZrCl}_4 \cdot 2\text{THF}$ dissolved in THF was added. The final solid part was separated by filtration, washed with THF and diethyl ether, and dried under vacuum. The supported catalyst produced in this way showed higher isospecificity than the corresponding homogenous system for propylene polymerization. MAO or ordinary alkylaluminums were used as cocatalysts. The yield was higher when MAO was used as the cocatalyst, but the molecular weight of the polypropylene was half of the molecular weight obtained when TIBA was used as the cocatalyst (3.4×10^5 g/mol and 7.2×10^5 g/mol, respectively). **Figure 2.24** shows the structure of the silica supported metallocenes.

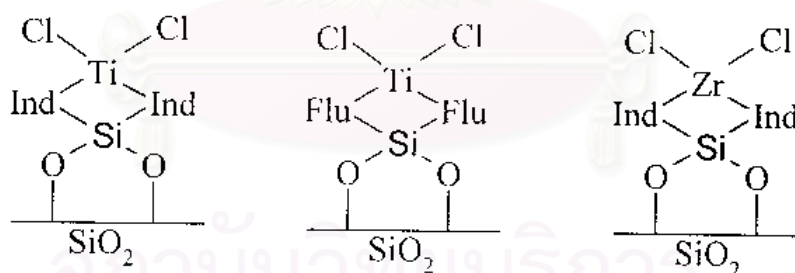


Figure 2.24 Structure of some silica supported metallocene catalysts [67]

Lee *et al.* [68] used spacer molecules in supporting metallocene catalysts onto silica to eliminate the steric hindrance near the active site caused by the silica surface (**Figure 2.25**). By distancing the active site from the silica surface, higher catalytic activities but lower polymer molecular weights were obtained in comparison with analogous silica-supported catalysts without spacer between silica and CpIndZrCl_2 .

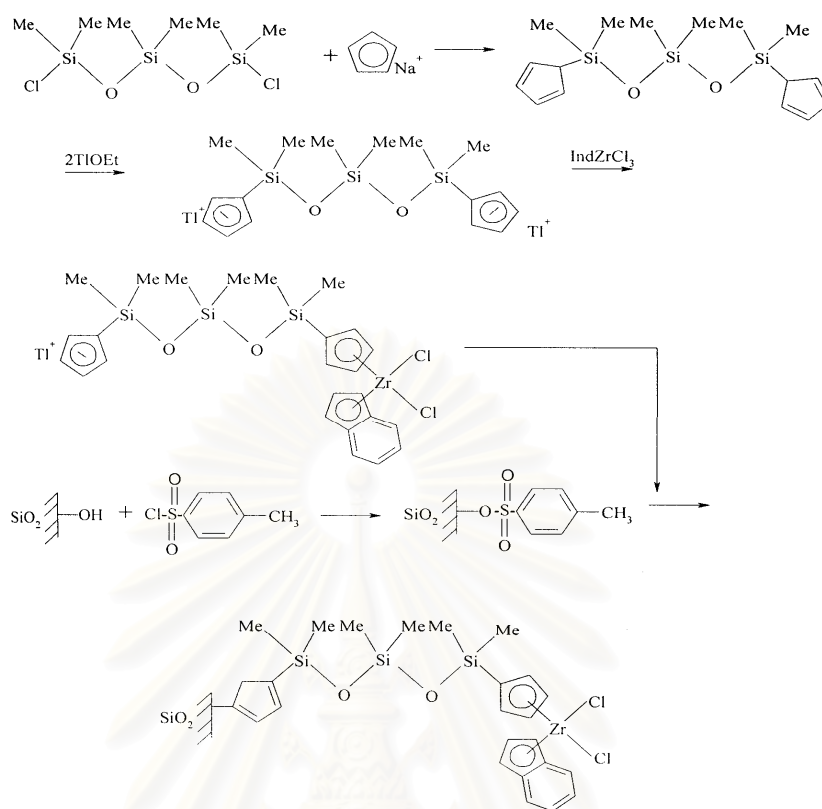


Figure 2.25 Mechanism for supporting metallocene catalysts on silica using spacer molecules [68].

Iiskola *et al.* [69] treated the surface of partially dehydroxylated silica with a silane coupling agents, Cp(CH₂)₃Si(OCH₂CH₃)₃, and then immobilized CpZrCl₃ onto cyclopentadienyl surface formed on the silica to obtain a highly active catalyst (**Figure 2.26**) for ethylene polymerization in the presence of MAO. Depending on the calcination temperature and the modification methods, the catalysts show different activities and produced polymers with different molecular weights. In general, when compared to homogeneous Cp₂ZrCl₂ systems, all the supported catalysts showed lower activities, but the polymers produced had higher molecular weights. On the other hand, when compared to homogeneous Cp₂ZrCl₂ systems, the activities of the supported catalysts were similar but molecular weights of polymer produced were lower and depended on the silica surface modification method used. The polydispersity index of the polymers ranged from 2.2 to 2.8.

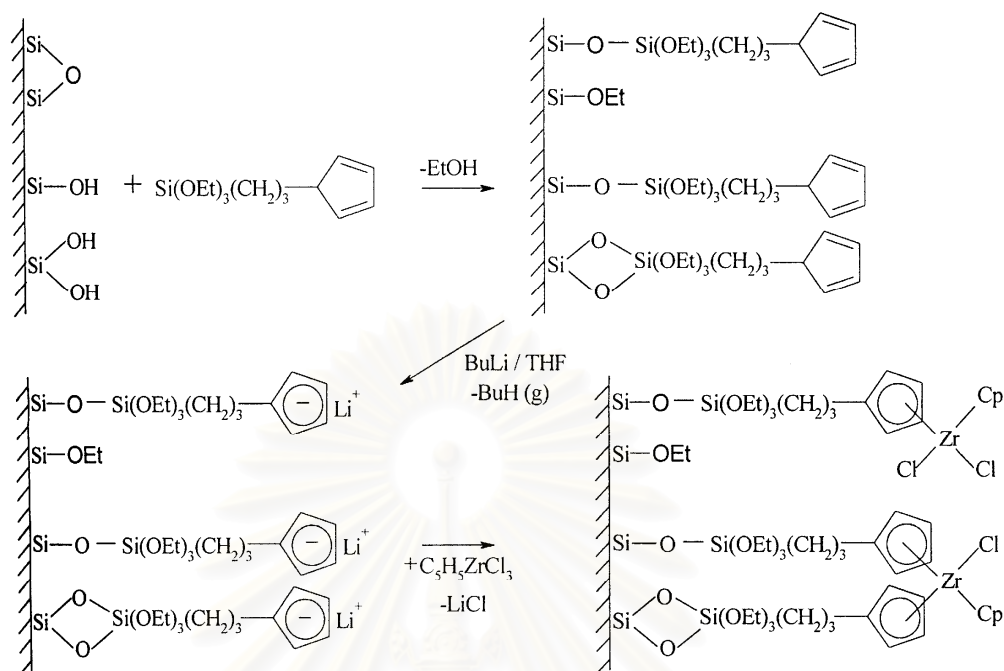


Figure 2.26 Modification of silica with $\text{Cp}(\text{CH}_2)_3\text{Si}(\text{OCH}_2\text{CH}_3)_3$ and preparation of supported metallocene catalysts [69].

2.5.2.4. Supporting on Other Supports

Lee and Yoon [70] studied ethylene and styrene homopolymerization initiated by cyclodextrin (CD) supported Cp_2ZrCl_2 or Cp^*TiCl_3 catalyst. The effect of CD pretreatment with MAO or TMA on catalyst behaviors was shown that either TMA or MAO could be used as cocatalyst for ethylene polymerization while only MAO could initiate the styrene polymerization with α -CD supported catalysts.

Marques *et al.* [71] investigated ethylene polymerization by using Y zeolite-supported Cp_2ZrCl_2 catalysts. These systems produced polyethylene with higher molecular weight and as narrow a molecular weight distribution as the homogeneous precursor, however, at relatively lower activity. The main characteristic that makes a zeolite a good support for metallocene catalyst seems to be a high Si/Al

value and therefore a low Al density on the surface of the zeolite. This suggests that the presence of isolated aluminium atoms favors the fixation of zirconocene.

Moreover, Michelotti *et al.* [72] studied copolymerization of ethylene with higher α -olefins, such as 4-methyl-1-pentene, 1-hexene, 1-octene and 1-dodecene. The catalytic behavior of various metallocene (Cp_2ZrCl_2 , $\text{Ind}_2\text{ZrCl}_2$, $\text{Et}(\text{Ind})_2\text{ZrCl}_2$, and $\text{Et}(\text{Ind})_2\text{HfCl}_2$) supported on methylalumoxane-pretreated HY zeolite ($\text{SiO}_2/\text{Al}_2\text{O}_3=5.7$) were compared.

Meshkova *et al.* [73] investigated ethylene polymerization in the presence of ZSM-5(H_2O)/TMA- $\text{Et}(\text{Ind})_2\text{ZrCl}_2$. They found that the synthesis of MAO directly on the zeolite support and the absence of free MAO may be one of the way of the reduction of supported zirconocene catalyst leaching. The positive temperature coefficient of polymerization rate as well as the increase of molecular weight and melting point of PE obtained with the zeolite supported zirconocene catalyst developed in this work compared to PE produced by homogeneous zirconocene system confirms this view.

Weiss *et al.* [74] investigated the clay minerals kaolin and montmorillonite as inorganic carriers for the polymerization of ethylene and propylene with Cp_2ZrCl_2 , Cp_2ZrHCl or Cp_2TiCl_2 catalyst and TMA as cocatalyst. The heterogeneous catalysts on kaolin were less active in ethylene polymerization than comparable homogeneous catalysts. But the heterogeneous catalysts on montmorillonite are often more active in ethylene or propylene polymerization than comparable homogeneous catalysts.

Looveren *et al.* [75] studied methylalumoxane (MAO)-MCM-41 as support in the co-oligomerization of ethene and propene with $[\text{C}_2\text{H}_4(\text{Ind})_2\text{Zr}(\text{CH}_3)_2]$. They were found that the MAO-MCM-41 was catalytically more active than the corresponding silica-based MAO derivative or the homogeneous system.

Wang et al. [76] investigated ethylene polymerization using homogeneous and heterogeneous bis(2,4-dimethylindenyl) zirconium dichloride catalyst –MAO systems. The heterogeneous catalysts on Si (MS-3040) showed the highest activity at an Al/Zr ratio of 1500, while increasing or decreasing the amount of MAO would decrease the activity. The heterogeneous of activity at Al/Zr = 1000 achieved the same level as that of homogeneous catalyst at Al/Zr = 3000, indicating that the immobilization of metallocene catalyst reduces the deactivation even in a low amount of MAO.

Van Grieken et al. [77] studied the influence of support properties in ethylene polymerization over supported MAO/(*n*BuCp)₂ZrCl₂ catalysts. They found that at the same calcination temperature, catalysts supported on SiO₂-Al₂O₃ (Si/Al = 4.8, Al = 5.48 wt%) and AlPO₄ exhibited higher polymerization activity than silica because P-OH and Al-OH hydroxyl group are more acidic than Si-OH. Their formation and the stabilization of zirconium cations (Zr⁺) are easier when support materials present acid sites.

สถาบันวิทยบริการ
จุฬาลงกรณ์มหาวิทยาลัย

CHAPTER III

EXPERIMENTAL

3.1 Objectives of the Thesis

To investigate the effect of different pore structure of SiO₂-based-supported zirconocene/dMMAO catalyst for ethylene/ α -olefin copolymerization on the polymerization behaviors.

3.2 Scopes of the Thesis

1. Preparation of alumina-silica bimodal pore supports by the incipient wetness impregnation method.
2. Preparation of supports such as SiO₂(Q-50), SiO₂(P-10), SiO₂-Al₂O₃ bimodal pore by impregnation with dried modified methylaluminoxane (dMMAO).
3. Study and characterization for the effects of supports with zirconocene catalyst on catalytic and polymer properties during ethylene and ethylene/ α -olefin copolymerization.

3.3 Research Methodology

Research Methodology of flow diagram is show in **Figure 3.1**.

All reactions were conducted under argon atmosphere using Schlenk techniques and glove box.

สถาบันวิทยบริการ
จุฬาลงกรณ์มหาวิทยาลัย

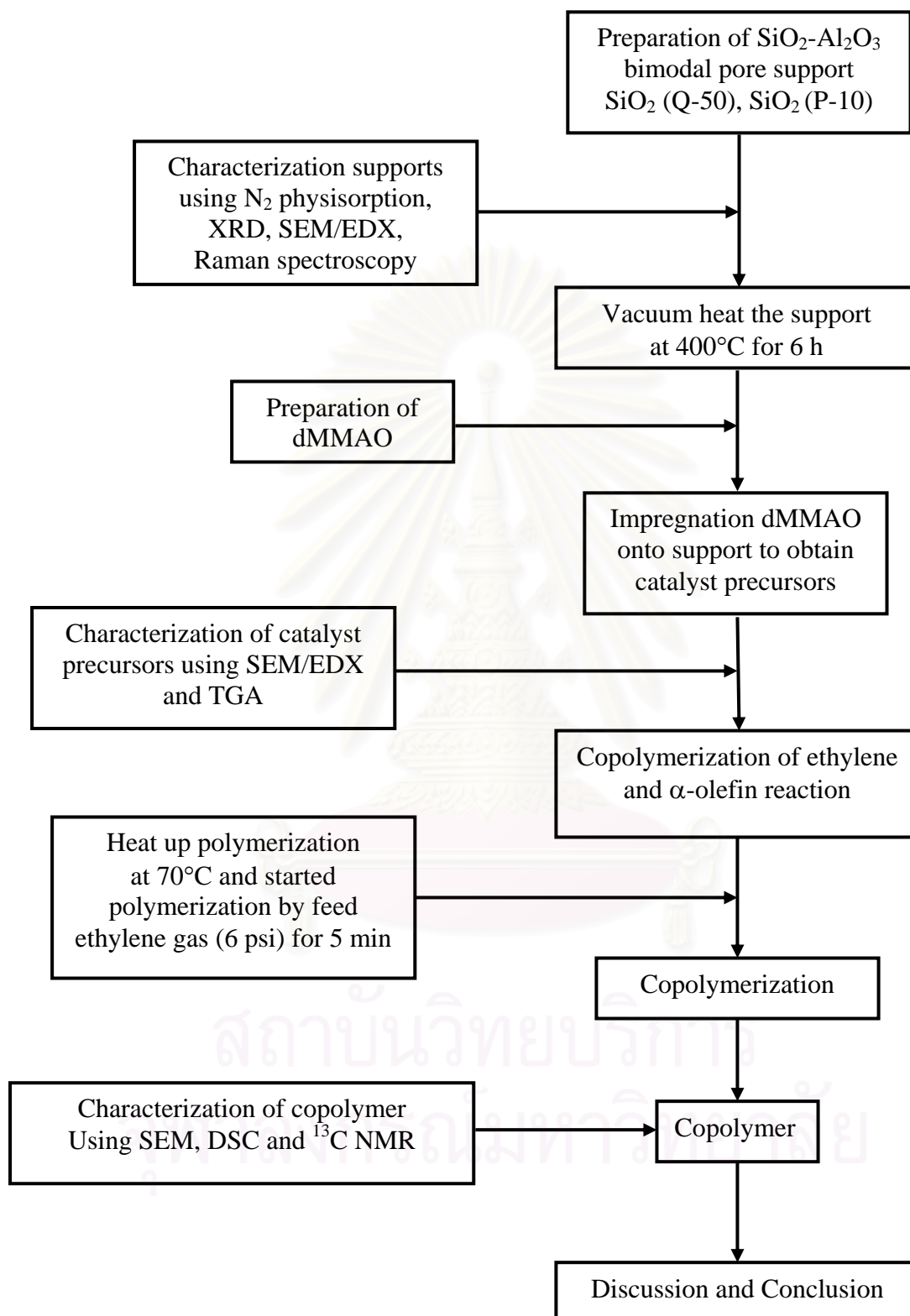


Figure 3.1 Flow diagram of research methodology

3.4 Experimental

3.4.1 Chemicals

The chemicals used in these experiments were analytical grade, but only major materials are specified as follows:

1. Silica gel from Fuji Silysia Chemical Ltd., Japan (Cariact Q-50) was calcined at 400 °C for 6 hours under vacuum.
2. Silica gel from Fuji Silysia Chemical Ltd., Japan (Cariact P-10) was calcined at 400 °C for 6 hours under vacuum.
3. Aluminium nitrate was purchased from Aldrich Chemical Company, Inc. and use as received
4. Polyethylene glycol (average mol wt. 200) was purchased from Aldrich Chemical Company, Inc. and use as received
5. Modified Methylaluminoxane (MMAO) 5.6% wt in hexane was donated from Tosoh Akso, Japan and used without further purification.
6. rac-Ethylenebis(indenyl)zirconium dichloride ($\text{Et}(\text{Ind})_2\text{ZrCl}_2$) was supplied from Aldrich Chemical Company, Inc. and used without further purification.
7. Trimethylaluminum $[\text{Al}(\text{CH}_3)_3]$ 2.0 M in toluene was supplied from Nippon Aluminum Alkyls Ltd., Japan and used without further purification.
8. Ethylene gas (99.96%) was devouted from National Petrochemical Co., Ltd., Thailand and used as received.
9. Ultra high purity argon gas (99.999%) was purchased from Thai Industrial Gas Co., Ltd., and further purified by passing through columns packed with molecular sieve 3 A, BASF Catalyst R3-11G, sodium hydroxide (NaOH) and phosphorus pentaoxide (P_2O_5) to remove traces of oxygen and moisture.
10. Toluene was devouted from EXXON Chemical Ltd., Thailand. This solvent was dried over dehydrated CaCl_2 and distilled over sodium/benzophenone under argon atmosphere before use.
11. 1-Hexene (99+%) was purchased from Aldrich Chemical Company, Inc. and purified by distilling over sodium under argon atmosphere before use.
12. 1-Octene (98%) was purchased from Aldrich Chemical Company, Inc. and used as received.

13. 1-Decene ($\geq 97\%$) was purchased from Fluka Chemie A.G. Switzerland. and used as received.

14. Hydrochloric acid (Fuming 36.7%) was supplied from Sigma.

15. Methanol (Commercial grade) was purchased from SR lab.

3.4.2 Equipments

Due to the metallocene system is extremely sensitive to the oxygen and moisture. Thus, the special equipments were required to handle while the preparation and polymerization process. For example, glove box: equipped with the oxygen and moisture protection system was used to produce the inert atmosphere. Schlenk techniques (Vacuum and Purge with inert gas) are the others set of the equipment used to handle air-sensitive product.

3.4.2.1 Cooling system

The cooling system was in the solvent distillation in order to condense the freshly evaporated solvent.

3.4.2.2 Inert gas supply

The inert gas (argon) was passed through columns of BASF catalyst R3-11G as oxygen scavenger, molecular sieve 3×10^{-10} m to remove moisture. The BASF catalyst was regenerated by treatment with hydrogen at 300 °C overnight before flowing the argon gas through all the above columns. The inert gas supply system is shown in **Figure 3.2**.

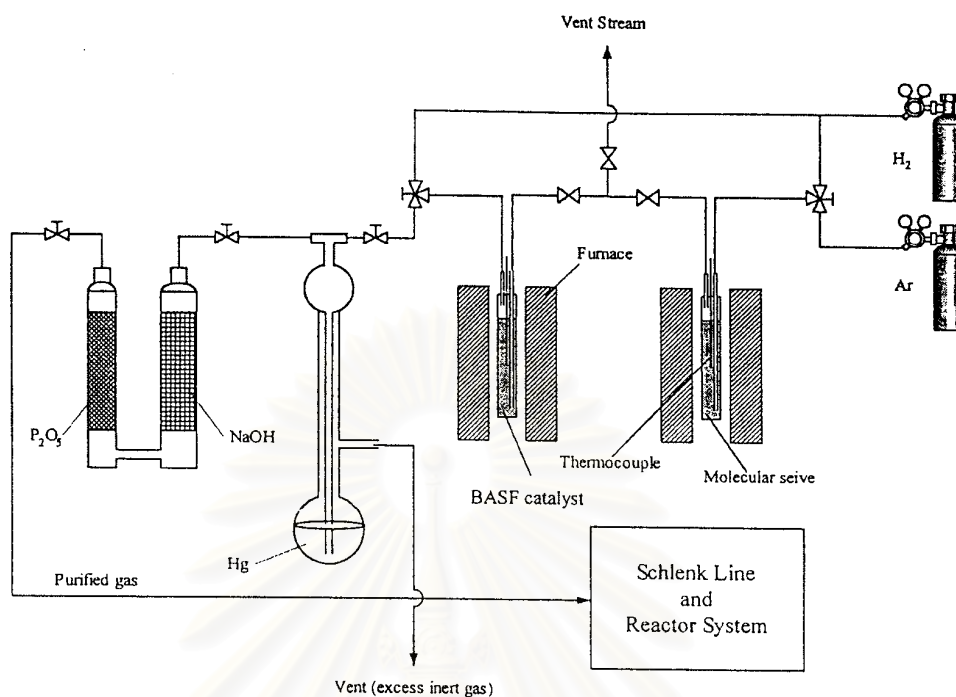


Figure 3.2 Inert gas supply system

3.4.2.3 Magnetic stirrer and heater

The magnetic stirrer and heater model RTC basis from IKA Labortechnik were used.

3.4.2.4 Reactor

A 100 ml glass flask connected with 3-ways valve was used as the copolymerization reactor for atmospheric pressure system and a 100 ml stainless steel autoclave was used as the copolymerization reactor for high pressure systems.

3.4.2.5 Schlenk line

Schlenk line consists of vacuum and argon lines. The vacuum line was equipped with the solvent trap and vacuum pump, respectively. The argon line was connected with the trap and the mercury bubbler that was a manometer tube and contain enough mercury to provide a seal from the atmosphere when argon line was evacuated. The Schlenk line was shown in **Figure 3.3**.

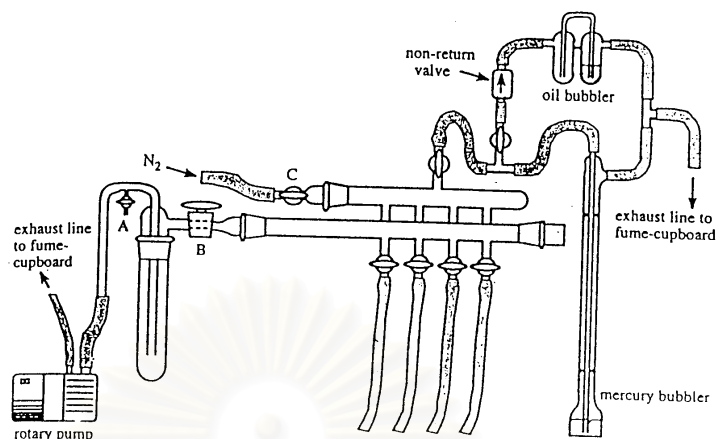


Figure 3.3 Schlenk line

3.4.2.6 Schlenk tube

A tube with a ground glass joint and side arm, which was three-way glass valve as shown in **Figure 3.4**. Sizes of Schlenk tubes were 50, 100 and 200 ml used to prepare catalyst and store materials which were sensitive to oxygen and moisture.

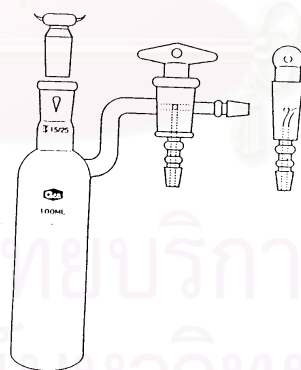


Figure 3.4 Schlenk tube

3.4.2.7 Vacuum pump

The vacuum pump model 195 from Labconco Corporation was used. A pressure of 10^{-1} to 10^{-3} mmHg was adequate for the vacuum supply to the vacuum line in the Schlenk line.

3.4.2.8 Polymerization line

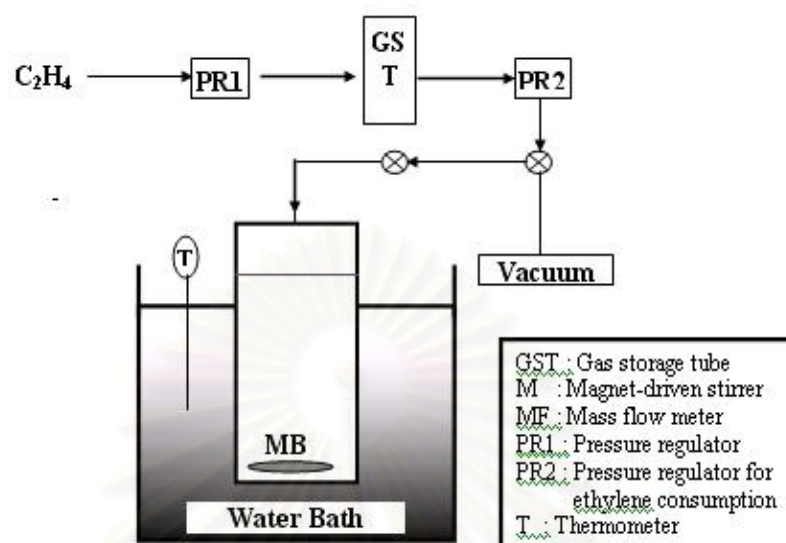


Figure 3.5 Diagram of system in slurry phase polymerization

3.4.3 Supporting Procedure

3.4.3.1 Preparation of alumina-silica bimodal pore supports

The alumina-silica bimodal pore support was synthesized according to the method described by Y. Zhang et al. [78]. The alumina-silica bimodal pore support was obtained by the incipient-wetness impregnation of the solution of aluminium nitrate. Prepare the polymer complex solution, aluminium nitrate was dissolved in a 0.3 mol/l polyethylene glycol aqueous solution stirring at 80 °C for 1 h. The solution was impregnated into silica gel (Q-50). The amounts of alumina loading was 15 wt%. The support was dried at 110 °C for 12 h and then calcined in air at 400 °C for 2 h.

3.4.3.2 Preparation of dried-MMAO (dMMAO)

Removal of TMA from MMAO was carried out according to the reported procedure [79]. The toluene solution of MMAO was dried under vacuum for 6 h at room temperature to evaporate the solvent, TMA, and Al(*i*Bu)₃ (TIBA). Then, continue to dissolve with 100 ml of heptane and the solution was evaporated under

vacuum to remove the remaining TMA and TIBA. This procedure was repeated 6-8 times and the white powder of dried MMAO (dMMAO) was obtained.

3.4.3.3 Preparation of supported dMMAO (catalyst precursor)

The $\text{SiO}_2\text{-Al}_2\text{O}_3$ support was reacted with the desired amount of dMMAO in 20 ml of toluene at room temperature for 30 min. The solvent was then removed from the mixture by evacuated. This procedure was done twice with toluene (20 ml x 2) and 3 times with hexane (20 ml x 3). Then, the solid part was dried under vacuum at room temperature. The white powder of supported cocatalyst (dMMAO/support) was then obtained. Similarly, $\text{SiO}_2(\text{Q-50})$ supported dMMAO [dMMAO/ $\text{SiO}_2(\text{Q-50})$] and $\text{SiO}_2(\text{P-10})$ supported dMMAO [dMMAO/ $\text{SiO}_2(\text{P-10})$] were prepared according to the method as described above.

3.4.4 Ethylene/ α -olefin Polymerization Procedures

The ethylene/ α -olefin copolymerization reaction was carried out in a 100 ml semi-batch stainless steel autoclave reactor equipped with magnetic stirrer. In the glove box, the desired amounts of *rac*-Et[Ind]₂ZrCl₂ and TMA were mixed and stirred for 5 min for aging. Then, toluene (to make a total volume of 30 ml) and 100 mg of dMMAO/support were introduced into the reactor. After that, the mixture of *rac*-Et[Ind]₂ZrCl₂ and TMA were injected into the reactor. The reactor was frozen in liquid nitrogen to stop reaction and then 0.018 mol of α -olefin was injected into the reactor. The reactor was evacuated to remove argon. Then, it was heated up to polymerization temperature (70°C) and the polymerization was started by feeding ethylene gas (total pressure 50 psi in the reactor) until the consumption of ethylene 0.018 mol (6 psi was observed from the pressure gauge) was reached. The reaction of polymerization was completely terminated by addition of acidic methanol. The time of reaction was recorded for purpose of calculating the activity. The precipitated polymer was washed with methanol and dried at room temperature.

3.4.5 Characterization of supports and catalyst precursor

3.4.5.1 N₂ physisorption

Measurement of BET surface area, average pore diameter and pore size distribution of MCM-41 support were determined by N₂ physisorption using a Micromeritics ASAP 2000 automated system.

3.4.5.2 X-ray diffraction (XRD)

XRD was performed to determine the bulk crystalline phases of sample. It was conducted using a SIEMENS D-5000 X-ray diffractometer with CuK_α ($\lambda = 1.54439 \times 10^{-10}$ m). The spectra were scanned at a rate 2.4 degree/min in the range $2\theta = 20-80$ degrees.

3.4.5.3 Raman spectroscopy

Raman spectroscopy was performed to determine the bulk crystalline phases of supports. The Raman spectra of supports were collected by projecting a continuous wave YAG laser of neodymium (Nd) red (1064 nm) to through the samples at room temperature. A scanning range of 200-3500 cm⁻¹ with a resolution of 8 cm⁻¹ were be applied.

3.4.5.4 Scanning electron microscopy (SEM) and energy dispersive

X-ray spectroscopy (EDX)

SEM and EDX were used to determine the morphologies and elemental distribution throughout the sample granules, respectively. The SEM of JEOL mode JSM-6400 was applied. The EDX was performed using Link Isis series 300 program.

3.4.5.5 Thermogravimetric analysis (TGA)

TGA was performed to determine the interaction force of the supported

dMMAO. It was conducted using TA Instruments SDT Q 600 analyzer. The samples of 10-20 mg and a temperature ramping from 25 to 600 °C at 2 °C /min were used in the operation. The carrier gas was N₂ UHP.

3.4.6 Characterization Method of Polymer

3.4.6.1 Differential scanning calorimetry (DSC)

The melting temperature of polymer products was determined with thermal analysis measurement. It was performed using a Perkin-Elmer DSC P7 calorimeter. The DSC measurements reported here were recorded during the second heating/cooling cycle with the rate of 20 °C min⁻¹. This procedure ensured that the previous thermal history was erased and provided comparable conditions for all samples. Approximately 10 mg of sample was used for each DSC measurement.

3.4.6.2 ¹³C NMR spectroscopy (¹³C NMR)

¹³C NMR spectroscopy was used to determine the α -olefin incorporation and copolymer microstructure. Chemical shift were referenced internally to the benzene-d₆ and calculated according to the method described by Randall [80]. Sample solution was prepared by dissolving 50 mg of copolymer in 1,2,4-trichlorobenzene and benzene-d₆. ¹³C NMR spectra were taken at 60 °C using BRUKER A400 operating at 100 MHz with an acquisition time of 1.5 s and a delay time of 4 s.

สถาบันวิทยบริการ
จุฬาลงกรณ์มหาวิทยาลัย

CHAPTER IV

RESULTS AND DISCUSSIONS

The purpose of this study is to investigate and characterize effects of different pore structures of supports on the catalyst activity and properties of copolymers during ethylene/ α -olefin polymerization with the zirconocene catalyst. The supports and supported-dMMAO (catalyst precursors) were also investigated to make better understanding about polymerization results.

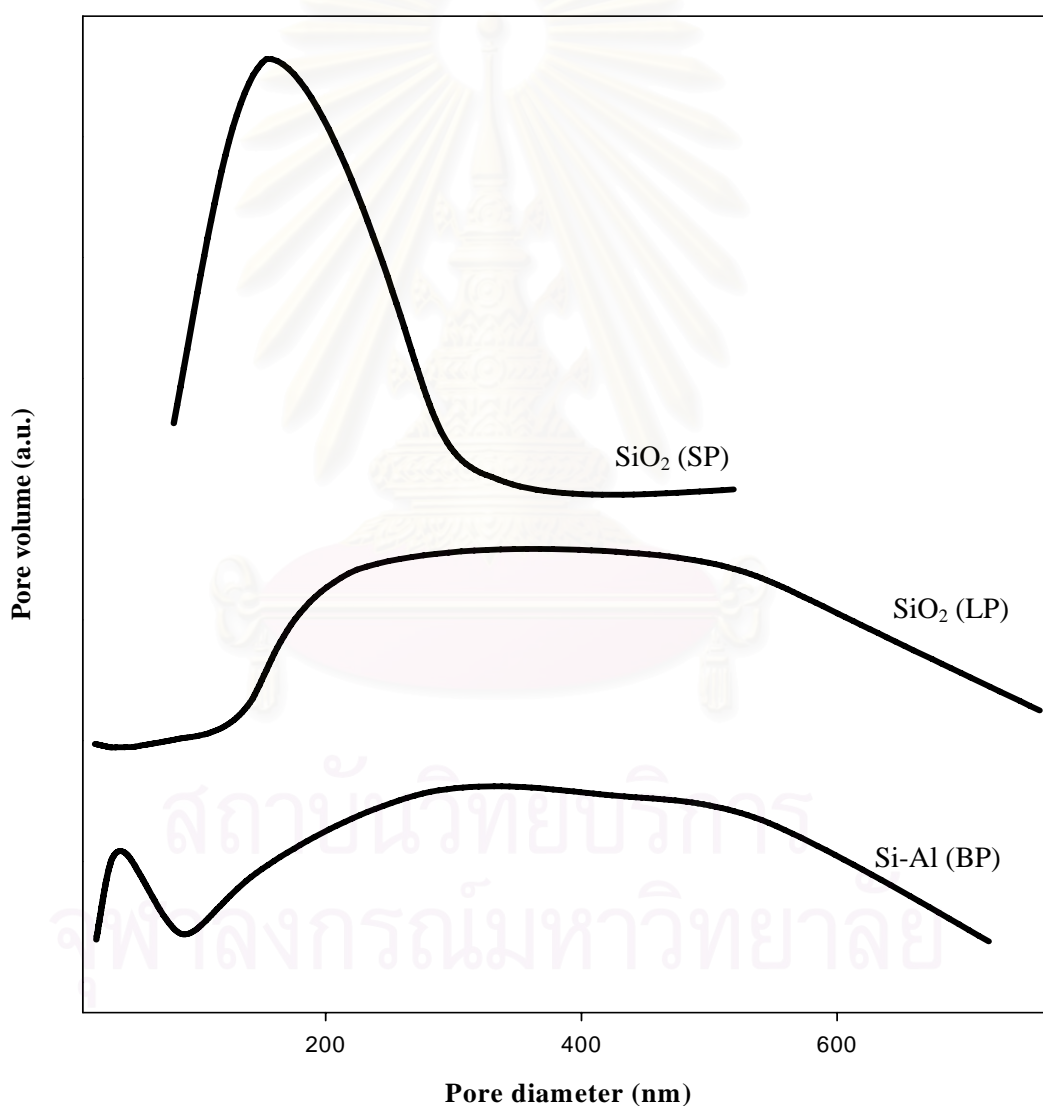
4.1 Characterization of supports and supported dMMAO

4.1.1 Characterization of supports with N₂ physisorption

The SiO₂-Al₂O₃ bimodal pore support was prepared in the same manner as that of Y. Zhang et al. [78]. After preparation of support, the supports having different pore structures such as SiO₂(Q-50), SiO₂(P-10) and SiO₂-Al₂O₃ bimodal pore were characterized before impregnation with dMMAO. The SiO₂ (Q-50) support denoted as SiO₂ (LP) having the average pore diameter of ca. 34 nm and surface area of 72.3 m²/g was obtained as seen in **Table 4.1**. The pore size distribution of the SiO₂ (LP) is shown in **Figure 4.1** indicating only the unimodal pore size distribution. In the same way, SiO₂ (P-10) denoted as SiO₂ (SP) is the unimodal support with the average pore diameter of ca. 14 nm (surface area = 256.8 m²/g). The SiO₂-Al₂O₃ bimodal pore support is assigned to the Si-Al (BP) support having the average pore diameter of ca. 8 nm (surface area = 126.7 m²/g) as also shown in **Table 4.1** and **Figure 4.1**. As seen in **Figure 4.1**, it can be observed that the SiO₂ (LP) support exhibited the large pore, the SiO₂ (SP) support exhibited the small pore and the bimodal pore size distribution for Si-Al (BP) was evident.

Table 4.1 BET surface area and average pore diameter of different SiO₂-based supports

| Support | BET surface area (m ² /g) | Average small pore diameter (nm) | Average large pore diameter (nm) | Pore volume (cm ³ /g) |
|-----------------------|--------------------------------------|----------------------------------|----------------------------------|----------------------------------|
| SiO ₂ (LP) | 72.3 | - | 33.8 | 0.26 |
| SiO ₂ (SP) | 256.8 | 13.7 | - | 1.50 |
| Si-Al (BP) | 126.7 | 3.8 | 33.6 | 0.30 |

**Figure 4.1** Pore size distribution of different SiO₂-based supports

4.1.2 Characterization of supports with X-ray diffraction (XRD)

The various supports with different pore structure were characterized before impregnation with dMMAO. The XRD patterns of supports with different pore structure are shown in **Figure 4.2**. It can be seen that all supports exhibited the similar XRD patterns indicating only a broad peak between 20-30°, as seen typically for the conventional amorphous silica.

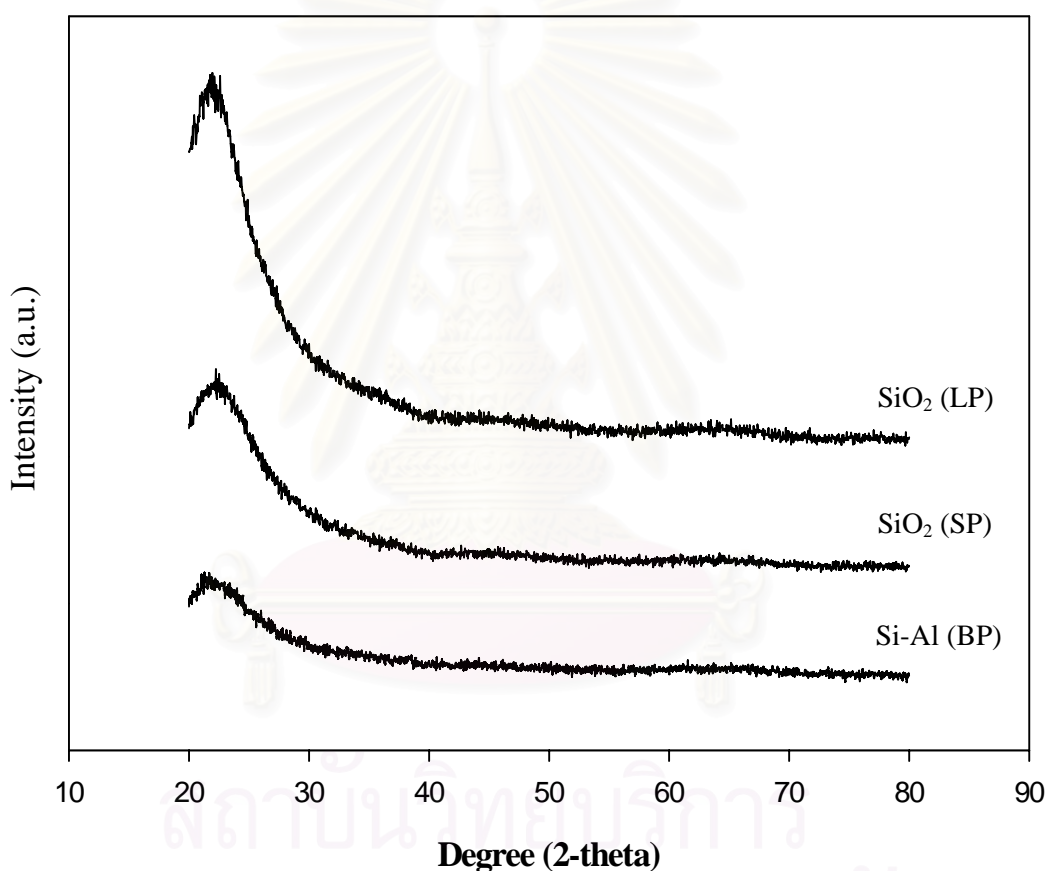


Figure 4.2 XRD patterns of different SiO₂-based supports

4.1.3 Characterization of supports with Raman spectroscopy

As confirmation, no significantly different Raman bands (**Figure 4.3**) were also observed for all supports within the Raman shift ranged between 200 and 3500 cm⁻¹.

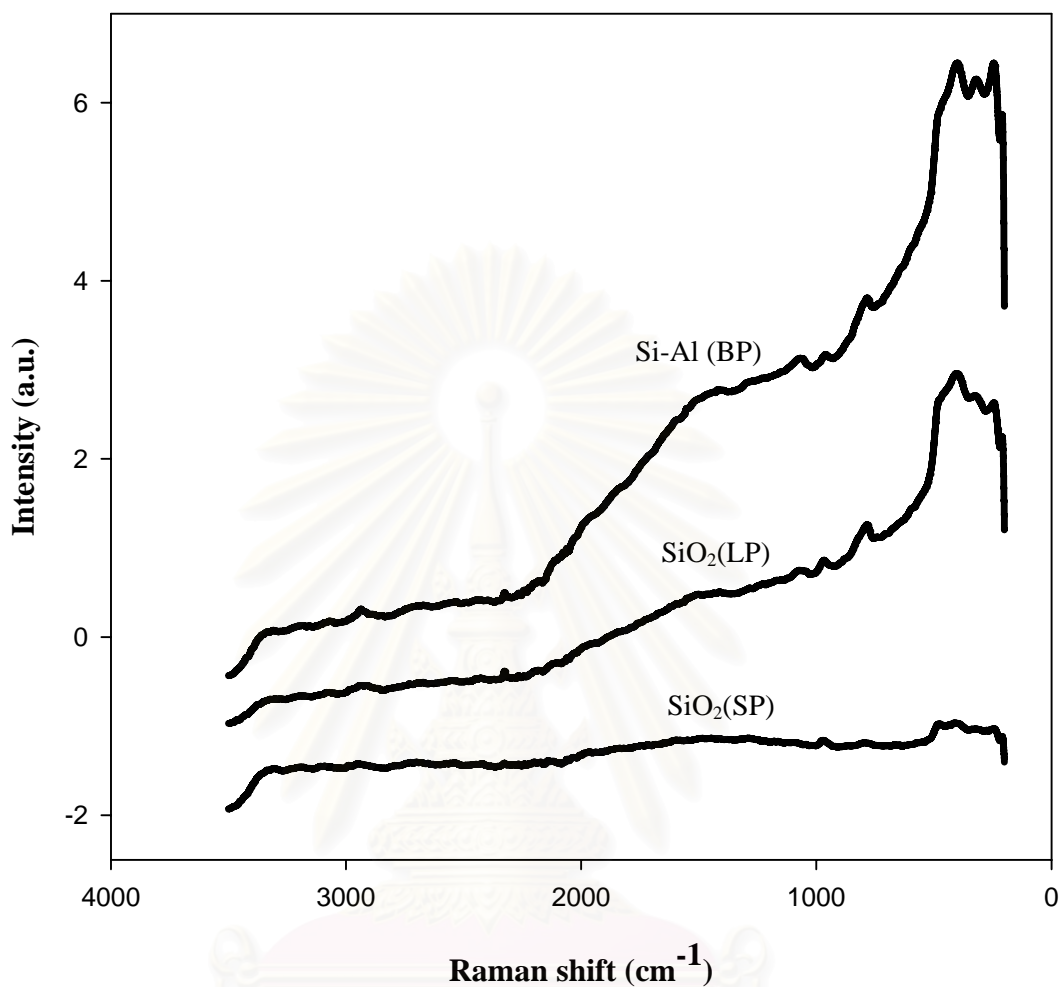


Figure 4.3 Raman spectra of different SiO₂-based supports

4.1.4 Characterization of supports and supported dMMAO with scanning electron microscope (SEM) and energy dispersive X-ray spectroscopy (EDX)

EDX and SEM were performed to determine the content of [Al]_{Al₂O₃}, [Al]_{dMMAO} and the elemental distributions and the morphologies of supports. **Figure 4.4** is SEM micrograph of various supports before impregnation of dMMAO. After impregnation of supports with dMMAO, the [Al]_{dMMAO} content was measured using EDX. The amounts of [Al]_{dMMAO} in various supports are listed in **Table 4.2**. the content of [Al]_{Al₂O₃} is 15 wt%.

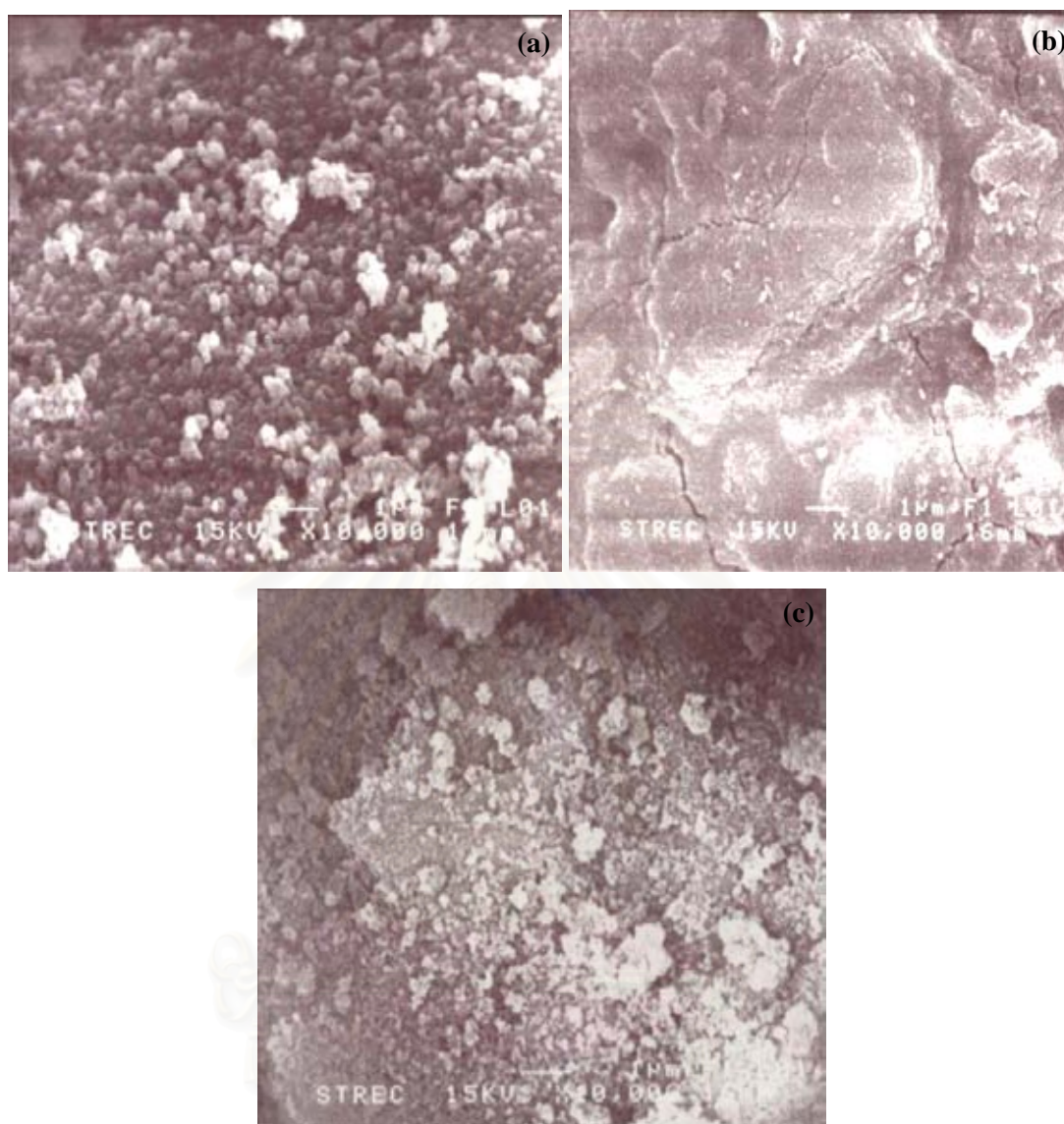


Figure 4.4 SEM micrographs of different SiO₂-based supports; (a) SiO₂(LP), (b) SiO₂(SP) and (c) Si-Al (BP)

Table 4.2 The content of [Al]_{dMMAO} on different SiO₂-based supports

| catalyst precursor | [Al] _{dMMAO} (wt%) |
|-----------------------------|-----------------------------|
| dMMAO/SiO ₂ (LP) | 18.90% |
| dMMAO/SiO ₂ (SP) | 12.90% |
| dMMAO/ Si-Al (BP) | 12.20% ^a |

^a subtracted [Al]_{Al₂O₃}

The typical measurement curve for the quantitative analysis using EDX is shown in **Figure 4.5**. It can be seen that the amount of $[Al]_{dMMAO}$ in various supports were varied due to the adsorption ability of each support. It revealed that $SiO_2(LP)$ exhibited the highest amount of $[Al]_{dMMAO}$ being present among other supports probably because surface of $SiO_2(LP)$ was most roughish. Besides the content of $[Al]_{dMMAO}$ in supports, one should consider the distribution of $[Al]_{dMMAO}$ in the supports. The elemental distribution was also performed using EDX mapping on the external surface. The support morphology and the $[Al]_{dMMAO}$ distribution in the various supports are shown in **Figure 4.6**. As seen, all samples exhibited good distribution of Al without any changes in the support morphology.

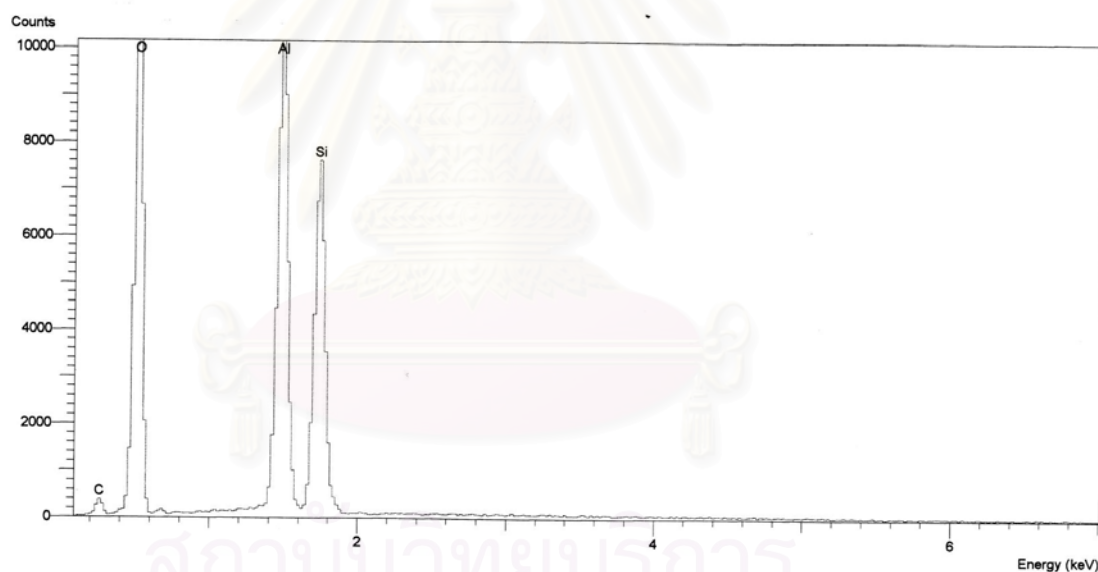


Figure 4.5 A typical spectrum of the supported dMMAO from EDX analysis used to measure the average $[Al]_{dMMAO}$ concentration on different SiO_2 -based supports

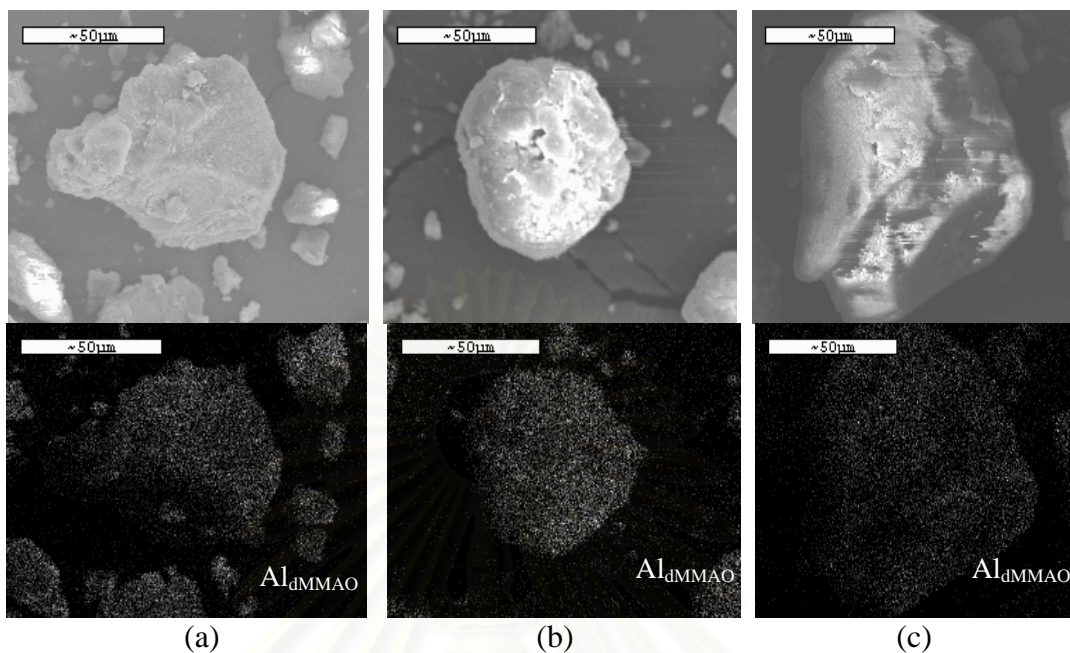


Figure 4.6 SEM/EDX mapping for Al distributions on different SiO₂-based supports after dMMAO impregnation (a) SiO₂ (LP), (b) SiO₂ (SP) and (c) Si-Al (BP) supports

4.1.5 Characterization of supports and supported dMMAO with Thermogravimetric analysis (TGA)

In this study, dMMAO was dispersed by impregnation onto the various supports. The degree of interaction between the support and the cocatalyst (dMMAO) can be determined by the TGA measurement. The TGA provide information on the degree of interaction for the dMMAO bound to the support in terms of weight loss and removal temperature. The TGA profiles of [Al]_{dMMAO} on various supports are shown in **Figure 4.7** indicating the similar profiles for various supports. The species having strong interaction with the support was removed at 596 °C. It was observed that the weight loss of [Al]_{dMMAO} present on Si-Al (BP), SiO₂ (SP) and SiO₂ (LP) supports were in the order of 13.7% < 20.8% < 21.4%, respectively. This indicated that [Al]_{dMMAO} present on Si-Al (BP) support had the strongest interaction > SiO₂ (SP) > SiO₂ (LP) support.

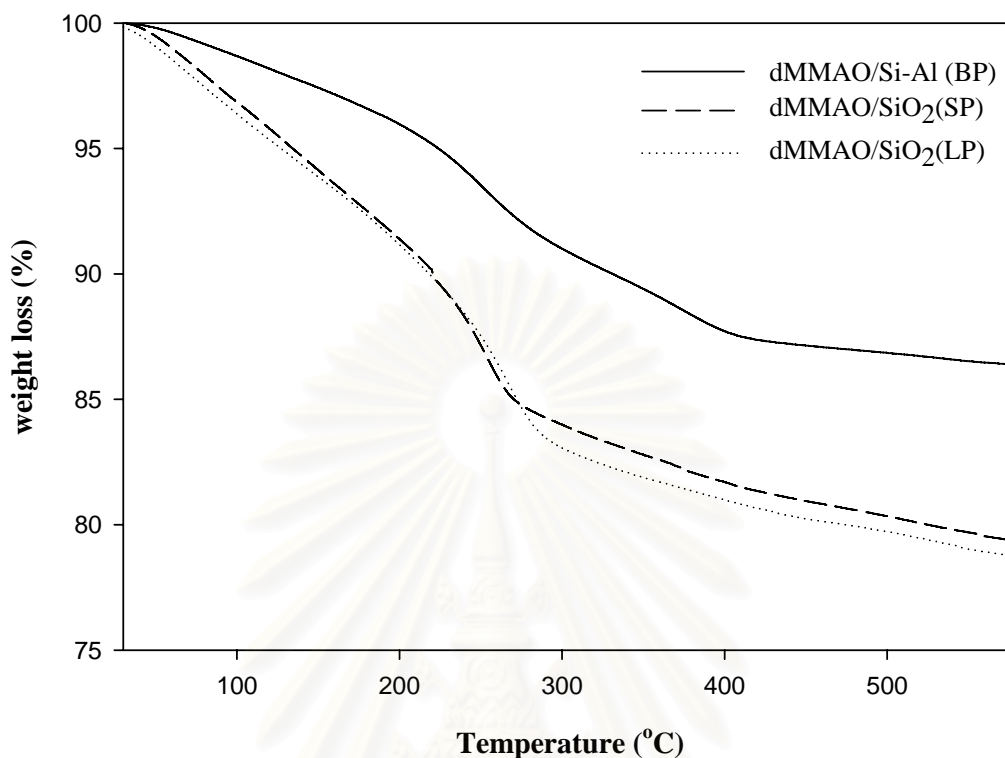


Figure 4.7 TGA profiles of supported dMMAO on different SiO₂-based supports

4.2 Characteristics and catalytic properties of ethylene/1-octene copolymerization

The various supports [SiO₂ (LP), SiO₂ (SP) and Si-Al (BP)] after impregnation with dMMAO [dMMAO/SiO₂ (LP), dMMAO/SiO₂ (SP) and dMMAO/Si-Al (BP)] were used and investigated for catalytic activities. The ethylene/1-octene copolymerization via various supported dMMAO with (*rac*-Et[Ind]₂ZrCl₂) was performed in order to determine the characteristics and catalytic properties of copolymer influenced by the various supports. Dried modified methylaluminoxane (dMMAO) was used as cocatalyst which all supports were fixed the [Al]_{dMMAO}/[Zr]_{cat} ratios of 1135. The copolymerization were performed in toluene at 70 °C feeding 0.018 mol of ethylene gas (6 psi was observed from the pressure gauge), pressure in reactor = 50 psi, 0.018 ml of 1-octene and zirconium concentration 10×10^{-5} M with total solution volume of 30 ml.

4.2.1 The effect of various supports on the catalytic activity

The catalytic activities via various supports and the homogeneous system are listed in **Table 4.3**.

Table 4.3 Copolymerization activities

| System | Polymerization time (sec) | Polymerization yield ^a (g) | Catalytic Activity ^b (kg Pol.mol.Zr ⁻¹ ·h ⁻¹) |
|-----------------------|---------------------------|---------------------------------------|---|
| homogeneous | 128 | 1.47 | 27496 |
| SiO ₂ (LP) | 134 | 1.21 | 21745 |
| SiO ₂ (SP) | 202 | 0.86 | 10174 |
| Si-Al (BP) | 307 | 0.61 | 4731 |

^a The polymer yield was fixed [limited by ethylene fed and 1-octene used (0.018 mole equally)].

^b Activities were measured at polymerization temperature of 70°C, [Ethylene] = 0.018 mole, [Al]_{dMMAO} / [Zr]_{cat} = 1135, [Al]_{TMA} / [Zr]_{cat} = 2500, in toluene with total volume = 30 ml and [Zr]_{cat} = 5×10⁻⁵ M.

For comparative studies, the polymerization activities towards copolymerization of ethylene/1-octene upon the presence of different supports were measured. The polymerization activities of the homogeneous and the different supported systems are listed in **Table 4.3**. The polymerization activities were in the order of homogeneous system > SiO₂ (LP) > SiO₂ (SP) > Si-Al (BP). As known, the activities of the supported system were apparently lower than homogeneous one due to supporting effect [81-82]. Among the supported systems, the polymerization activity obtained from the SiO₂ (LP) was the highest. This was presumably due to the largest amount of [Al]_{dMMAO} present (18.9 wt%) on the support as seen from the EDX measurement. This indicated that the greater amounts of dMMAO resulted in more active species being present during polymerization [83-85]. It was proposed that dMMAO possibly had many functions, such as alkylating agent, a stabilizer for a cationic metallocene alkyl and/or counter-ion, an ionizing and/or reducing agent for the transition element, and a scavenger for the metallocene catalytic system. However, one of the most important roles of this alkylaluminumoxane is apparently to

prevent the formation of $ZrCH_2CH_2Zr$ species, which is formed via a bimolecular process [86]. The polymerization activities obtained from the SiO_2 (SP) and Si-Al (BP) exhibited lower activities due to less amount of $[Al]_{dMMAO}$ present (12.9 and 12.2 wt%, respectively). It should be noted that although the Si-Al (BP) had a slightly lower amount of $[Al]_{dMMAO}$ than that of the SiO_2 (SP), the polymerization activity obtained from the former was much lower (almost three times). Thus, the lower polymerization activity can not be attributed to only the $[Al]_{dMMAO}$ concentration, but also to other factor, such as the interaction between the $[Al]_{dMMAO}$ and the support [87]. Based on this study, dMMAO was dispersed by impregnation onto the different supports prior to polymerization. The degree of interaction between the support and dMMAO can be determined by the TGA measurement. In order to give a better understanding, we propose the interaction of support and dMMAO based on the review paper by Severn et al. [88]. They explained that the connection of the support and cocatalyst occurred via the $O_{support} \sim Al_{cocatalyst}$ linkage. In particular, the TGA can only provide useful information on the degree of interaction for the dMMAO bound to the support in terms of weight loss and removal temperature. The stronger interaction can result in it being more difficult for the dMMAO bound to the support to react with metallocene during activation processes, leading to lower polymerization activity for polymerization. Base on TGA, this indicated that $[Al]_{dMMAO}$ present on the Si-Al (BP) had the strongest interaction and thus the lowest observed polymerization activity.

4.2.2 The effect of various supports on the melting temperatures of copolymers

The melting temperatures (T_m) of copolymer were evaluated by the differential scanning calorimeter (DSC) are shown in **Table 4.4**. DSC curves of the copolymer are also shown in Appendix B

Table 4.4 Melting temperatures of copolymers obtained different SiO₂-based supports

| System | T _m (°C) | Crystallinity (%) |
|-----------------------|---------------------|-------------------|
| Homogeneous | n.o. | n.o. |
| SiO ₂ (LP) | n.o. | n.o. |
| SiO ₂ (SP) | n.o. | n.o. |
| Si-Al (BP) | 94 | 6.57 |

n.o. refers to not observe

From the characterization of copolymer in **Table 4.4**, it appeared only the melting temperatures (T_m) of copolymer obtained from the Si-Al (BP) exhibited the melting temperature at 94°C. The absence of T_m for copolymers obtained from SiO₂ (LP) and SiO₂ (SP) supports indicated non-crystalline copolymers produced. The non-crystalline copolymers were attributed to the higher degree of 1-octene incorporation.

4.2.3 The effect of various supports on the incorporation of copolymers

The quantitative analysis of triad distribution for all copolymers was conducted on the basis assignment of the ¹³C NMR spectra of ethylene/1-octene (EO) copolymer and calculated according to the method of Randall [80]. The characteristics of ¹³C NMR spectra (as shown in appendix A) for all copolymers were similar indicating the copolymer of ethylene/1-octene. The triad distribution of all polymers is shown in **Table 4.5**. It was found that ethylene incorporation in all systems gave copolymers with similar triad distribution. It was also shown a little probability to produce the dyad of OO, which is the characteristic of this zirconocene in homogeneous system [81]. No triad of EOO in the copolymers was found. Only the random copolymers can be produced in all systems. In addition, the 1-octene incorporations in both SiO₂ (LP) and SiO₂ (SP) supports were 18 and 21 mol%, which was similar to that in the homogeneous system (22 mol%). Apparently, the copolymer obtained from the Si-Al (BP) support exhibited the lowest degree of 1-octene insertion resulting in the observation of T_m based on DSC measurement.

Table 4.5 ^{13}C NMR analysis of ethylene/1-octene copolymer

| System | Triad distribution of copolymer | | | | | | 1-octene insertion (mol %) |
|-----------------------|---------------------------------|-----|-------|-------|-------|-------|----------------------------|
| | OOO | EOO | EOE | EEE | OEO | OEE | |
| Homogeneous | 0 | 0 | 0.214 | 0.591 | 0.043 | 0.152 | 22 |
| SiO ₂ (LP) | 0 | 0 | 0.176 | 0.471 | 0.043 | 0.310 | 18 |
| SiO ₂ (SP) | 0 | 0 | 0.212 | 0.418 | 0.056 | 0.314 | 21 |
| Si-Al (BP) | 0 | 0 | 0.063 | 0.790 | 0 | 0.147 | 6 |

E refers to ethylene monomer and O refers to 1-octene comonomer

4.3 The effect of various comonomers with different supports

4.3.1 The effect of various comonomers with different supports on the catalytic activity

Then, the different supports after impregnation with dMMAO were used and investigated for catalytic activities upon different comonomers employed (1-hexene, 1-octene and 1-decene). Copolymerization of ethylene/1-hexene (EH) and ethylene/1-decene (ED) with different SiO₂-based-supported dMMAO with zirconocene catalyst was performed in order to determine the catalytic activities influenced by the different supports coupled with comonomers. The dMMAO was used as cocatalyst which the $[\text{Al}]_{\text{dMMAO}}/[\text{Zr}]_{\text{cat}}$ molar ratio of 1135. The copolymerization was performed in toluene at 70°C using ethylene consumption of 0.018 mol (pressure in reactor 50 psi), 0.018 ml of α -olefin, 100 mg of catalyst precursor and zirconium concentration 5.0×10^{-5} M with total solution volume of 30 ml. The resulted reaction study is shown in **Table 4.6**.

Table 4.6 Catalytic activities of different SiO₂-based -supported dMMAO with zirconocene catalyst during ethylene/ α -olefin copolymerization

| system | comonomer | Polymerization time (s) | Polymer yield ^a (g) | Catalytic Activity ^b (kg Pol.mol.Zr ⁻¹ •h ⁻¹) |
|-----------------------|-----------|-------------------------|--------------------------------|---|
| homogeneous | 1-hexene | 99 | 1.2231 | 29651 |
| | 1-octene | 128 | 1.4665 | 27496 |
| | 1-decene | 141 | 1.6785 | 28570 |
| SiO ₂ (LP) | 1-hexene | 150 | 1.1171 | 17874 |
| | 1-octene | 134 | 1.2141 | 21745 |
| | 1-decene | 116 | 1.0108 | 20914 |
| SiO ₂ (SP) | 1-hexene | 153 | 0.8671 | 13601 |
| | 1-octene | 202 | 0.8564 | 10174 |
| | 1-decene | 136 | 1.2903 | 22769 |
| Si-Al (BP) | 1-hexene | 281 | 0.622 | 5312 |
| | 1-octene | 307 | 0.6052 | 4731 |
| | 1-decene | 261 | 0.497 | 4570 |

^a The polymer yield was fixed [limited by ethylene fed and 1-olefins used (0.018 mole equally)].

^b Activities were measured at polymerization temperature of 70°C, [Ethylene] = 0.018 mole, [Al]_{dMMAO} / [Zr]_{cat} = 1135, [Al]_{TMA} / [Zr]_{cat} = 2500, in toluene with total volume = 30 ml and [Zr]_{cat} = 5×10⁻⁵ M.

For copolymerization of ethylene with three different comonomers, it was obvious that comonomer affected activities upon different supports. For Si-Al (BP), comonomer almost had not effect because strong interaction is more pronounced. In homogeneous system, comonomer had only slight effect with the absence of supports. Monomer movement was not hindered by immobilization. An immobilization made the pathway to catalytic sites narrow. An effect of comonomer influenced very little on activities of SiO₂ (LP) because rough surface of the support was appropriate with all comonomers. For the SiO₂ (SP), comonomers had pronounced effect on activities. The comonomer effect was often associated with polymerization rate enhancement. Higher- α -olefin was sometimes linked to the reduction of diffusion limitations by producing a lower crystallinity polymer [8] and increase the gap between the cationic active species and counter anion more separated

[89]. Thus, it is more easily to monomer to raise the propagation rate to polymer chain before the chain was terminated and increase the number of catalytic sites. Therefore 1-decene apparently exhibited the highest activity.

4.3.2 The Effect of different comonomers on the melting temperatures of copolymers with different supports

The melting temperatures (T_m) of copolymer were evaluated by differential scanning calorimeter (DSC) and are shown in **Table 4.7**. DSC curves of the copolymer are also shown in Appendix B.

Table 4.7 Melting temperatures, % crystallinity of copolymers obtained from different SiO₂-based supports with different comonomer

| system | comonomer | T_m (°C) | % crystallinity |
|-----------------------|-----------|------------|-----------------|
| homogeneous | 1-hexene | n.o. | n.o. |
| | 1-octene | n.o. | n.o. |
| | 1-decene | n.o. | n.o. |
| SiO ₂ (LP) | 1-hexene | n.o. | n.o. |
| | 1-octene | n.o. | n.o. |
| | 1-decene | n.o. | n.o. |
| SiO ₂ (SP) | 1-hexene | n.o. | n.o. |
| | 1-octene | n.o. | n.o. |
| | 1-decene | n.o. | n.o. |
| Si-Al (BP) | 1-hexene | 87.2 | 2.16 |
| | 1-octene | 94.3 | 6.57 |
| | 1-decene | n.o. | n.o. |

n.o. refers to not observe

From in **Table 4.7**, it was found that, T_m is proportional to the crystallinity of polymer. The melting temperatures T_m was observed in Si-Al (BP) support. The non-crystalline polymers obtained were attributed to the high degree of α -olefin insertion.

4.3.3 The effect of various supports on incorporation of copolymer the with different comonomers

^{13}C NMR spectroscopy was used to determine comonomer incorporation and polymer microstructure. The quantitative analysis of triad distribution for all copolymers was conducted and calculated according to the method of Randall [80]. The result obtained for the triad sequence distribution of copolymer is shown in **Table 4.8**. Both supported and homogeneous systems were similar indicating the copolymer of EH EO and ED. It indicated that 1-hexene exhibited higher comonomer incorporation compared with other comonomers in same systems and no triad of α -olefin (HHH, OOO and DDD) in the copolymers was found.

In homogeneous system, ethylene incorporation in all comonomers gave copolymers with similar triad distribution. It was also shown a little probability to produce the dyad of HH, OO and DD. Comonomer incorporations were between 16 and 36 mol%. The incorporation of this system was similar. In the Si-Al (BP) support, obtained triad distribution was similar. It indicated a slight probability to produce the dyad of HH, OO and DD. The incorporation of this system was low corresponding to low activities. For the SiO_2 (LP) support, it revealed a little probability to produce the dyad of HH, OO and DD. The incorporation of this system was between 13 and 38 mol%. Hexene incorporation was the highest among other comonomers due to incorporation inside the pore. Thus, the decreased degree of insertion for 1-octene and 1-decene was evident. For the SiO_2 (SP) support, it was also shown a little probability to produce the dyad of HH, OO and DD. The incorporation of this system was between 20 and 42 mol%. The similar trend was observed as seen for the SiO_2 (LP) support. However, the degree of insertion of comonomers was higher than that of the former because incorporation occurred on the external surface of support.

Table 4.8 ^{13}C NMR analysis of ethylene/ α -olefins copolymer

| system | comonomer | Triad distribution of copolymer | | | | | | Mol % of C in copolymer |
|-----------------------|-----------|---------------------------------|-------|-------|-------|-------|-------|----------------------------|
| | | CCC | ECC | ECE | EEE | CEC | CEE | |
| homogeneous | 1-hexene | 0 | 0.200 | 0.157 | 0.377 | 0.044 | 0.222 | 36 |
| | 1-octene | 0 | 0 | 0.214 | 0.591 | 0.043 | 0.152 | 22 |
| | 1-decene | 0 | 0 | 0.164 | 0.379 | 0.045 | 0.412 | 16 |
| SiO ₂ (LP) | 1-hexene | 0 | 0.265 | 0.120 | 0.375 | 0.047 | 0.193 | 38 |
| | 1-octene | 0 | 0 | 0.176 | 0.471 | 0.043 | 0.310 | 18 |
| | 1-decene | 0 | 0 | 0.135 | 0.499 | 0.035 | 0.331 | 13 |
| SiO ₂ (SP) | 1-hexene | 0 | 0.327 | 0.094 | 0.395 | 0.017 | 0.167 | 42 |
| | 1-octene | 0 | 0 | 0.212 | 0.418 | 0.056 | 0.314 | 21 |
| | 1-decene | 0 | 0 | 0.204 | 0.394 | 0.051 | 0.351 | 20 |
| Si-Al (BP) | 1-hexene | 0 | 0 | 0.077 | 0.782 | 0 | 0.141 | 8 |
| | 1-octene | 0 | 0 | 0.063 | 0.790 | 0 | 0.147 | 6 |
| | 1-decene | 0 | 0 | 0 | 0.744 | 0 | 0.256 | 0 |

E refers to ethylene monomer and C refers to H (1-hexene), O (1-octene) and D (1-decene) comonomer

CHAPTER V

CONCLUSIONS & RECOMMENDATIONS

5.1 CONCLUSIONS

In the first part, the impact of various SiO₂-based supported-dMMAO on the catalytic activities during copolymerization of ethylene/1-octene was investigated. It was found that the activities of the supported system were lower than the homogeneous one due to the supporting effect. In supported system, the polymerization activity obtained from the large pored silica [SiO₂ (LP)] was the highest among other small pored silica [SiO₂ (SP)] and bimodal pored silica-alumina [Si-Al (BP)] supports. The high activity can be attributed to large amount of dMMAO present coupled with moderate interaction between the dMMAO and support. The strong interaction of dMMAO and Si-Al (BP) was the major factor that caused the decrease in polymerization activity. It is worth noting that all copolymers produced exhibited the similar triad distribution, but had different degree of 1-octene insertion.

In the second part, the impact of comonomers employed under corresponding condition as mentioned in the first part was further investigated. It was found that base on polymerization activities, it was found that effect of comonomer present on different support in order to SiO₂ (SP) > SiO₂ (LP) > Homo > Si-Al (BP).

5.2 RECOMMENDATIONS

- Other bimodal supports should be further investigated.
- The modification of supports should be studied.
- Interaction between the support and cocatalyst under in situ condition should be further determined.

REFERENCES

- [1] McKenna, T.F. and Soares, J.B.P. Single particle modelling for olefin polymerization on supported catalysts: A review and proposals for future developments. **Chemical Engineering Science** 56 (2001): 3931-3949.
- [2] Kaminsky, W. and Laban, A. Metallocene catalysis. **Applied Catalysis A: General** 222 (2001): 47-61.
- [3] Park, H.W.; Chung, J.S; Baeck, S.H. and Song, I.K. Physical property and chemical composition distribution of ethylene-hexene copolymer produced by metallocene/Ziegler-Natta hybrid catalyst. **Journal of Molecular Catalysis A: Chemical** 255 (2006): 69-73.
- [4] Britto, M.L.; Galland, G.B.; dos Santos, J.H.Z. and Forte, M.C. Copolymerization of ethylene and 1-hexene with $\text{Et}(\text{Ind})_2\text{ZrCl}_2$ in hexane. **Polymer** 42 (2001): 6355-6361.
- [5] Breslow, D. S. and Newburg, N. R. Bis-(cyclopentadienyl) titaniumdichloride-Alkylaluminum complexes as catalysts for the polymerization of ethylene. **Journal of American Chemical Society** 79 (1957): 5072-5073.
- [6] Sinn, H. and Kaminsky, W. Ziegler-Natta Catalyst. **Advances in Organometallic Chemistry** 18 (1980): 99-149.
- [7] Zhang, J.; Wang, X. and Jin, G.-X. Polymerized metallocene catalysts and late transition metal catalysts for ethylene polymerization. **Coordination Chemistry Reviews** 250 (2006): 95-109.
- [8] Shan, C.L.P.; Soares, J.B.P. and Penlidis, A. Ethylene/1-octene copolymerization studies with in situ supported metallocene catalysts: Effect of polymerization parameters on the catalyst activity and polymer microstructure. **Journal of Polymer Science Part A: Polymer Chemistry** 40 (2002): 4426-4451.
- [9] Chu, K.J.; Shan, C.L.P.; Soares, J.B.P. and Penlidis, A. Copolymerization of ethylene and 1-hexene with in-situ supported $\text{Et}[\text{Ind}]_2\text{ZrCl}_2$. **Macromolecule Chemical and Physics** 200 (1999): 2372-2376.

- [10] Ribeiro, M.R.; Deffieux, A. and Portela, M.F. Supported Metallocene Complexes for Ethylene and Propylene Polymerizations: Preparation and Activity. **Industrial and Engineering Chemistry Research** 36 (1997): 1224-1237.
- [11] Lee, K.S.; Oh, C.-G.; Yim, S.-K. and Ihm, J. Characteristics of zirconocene catalysts supported Al-MCM-41 for ethylene polymerization. **Journal of Molecular Catalysis A: Chemical** 159 (2000): 301-308.
- [12] De Jong, K.P. and Geus, J.W. Carbon Nanofibers: Catalytic Synthesis and Applications. **Catalysis Reviews - Science and Engineering** 42 (2000): 481-510.
- [13] Jongsomjit, B.; Kaewkrajang, P. and Praserttham, P. Effect of silane-modified /MAO-supported Et[Ind]₂Cl₂ metallocene catalyst on copolymerization of ethylene. **European Polymer Journal** 40 (2004): 2813-2817.
- [14] Reb, A. and Alt, H.G. Diastereomeric amido functionalized ansa half-sandwich complexes of titanium and zirconium as catalyst precursors for ethylene polymerization to give resins with bimodal molecular weight distributions. **Journal of Molecular Catalysis A: Chemical** 174 (2001): 35-49.
- [15] Kim, J.D. and Soares, J.B.P. Copolymerization of ethylene and α -olefins with combined metallocene catalysts III. Production of polyolefins with controlled microstructures. **Journal of Polymer Science, Part A: Polymer Chemistry** 38 (2000): 1427-1432.
- [16] Wang, Q.; Yang, H.X. and Fan, Z.Q. Efficient Activators for an Iron Catalyst in the Polymerization of Ethylene. **Macromolecular Rapid Communications** 23 (2002): 639-642.
- [17] Smedberg, A.; Hjertberg, T. and Gustafsson, B. Characterization of an unsaturated low-density polyethylene. **Journal of Polymer Science, Part A: Polymer Chemistry** 41 (2003): 2974-2984.

- [18] Natta, G. and Pino, P. Crystalline high polymers of α -olefins. **Journal of the American Chemical Society** 77 (1955): 1708-1710.
- [19] Gambarotta, S. Coord. Vanadium-based Ziegler-Natta: Challenges, promises, problems. **Coordination Chemistry Reviews** 237 (2003): 229-243.
- [20] Ma, Y.; Reardon, D.F.; Gambarotta, S. and Yap, G.P.A. Vanadium-Catalyzed Ethylene-Propylene Copolymerization: The Question of the Metal Oxidation State in Ziegler-Natta Polymerization Promoted by (β -diketonate)₃V. **Organometallics** 18 (1999): 2773-2781.
- [21] Kashiwa, N. The discovery and progress of MgCl₂-supported TiCl₄ catalysts. **Journal of Polymer Science, Part A: Polymer Chemistry** 42 (2004): 1-8.
- [22] Kissin, Y.V. Multicenter nature of titanium-based Ziegler-Natta catalysts: Comparison of ethylene and propylene polymerization reactions. **Journal of Polymer Science, Part A: Polymer Chemistry** 41 (2003): 1745-1758.
- [23] Hlatky, G. Heterogeneous single-site catalysts for olefin polymerization. **Chemical Reviews** 100 (2000): 1347-1376.3
- [24] Natta, G.; Pino, P. and Mazzanti, G. A crystallizable organometallic complex containing titanium and aluminum. **Journal of the American Chemical Society** 79 (1957): 2975-2976.
- [25] Arlman, E.J. and Cossee, P. Ziegler-Natta Catalysis III. Stereospecific Polymerization of Propene with the Catalyst System TiCl₃-AlEt₃. **Journal of Catalysis** 3 (1964): 99-104.
- [26] Chung, T.-C. and Xu, G. US 6248837 B1, 2001 assigned to **The Penn State Research Foundation**
- [27] Fujita, M.; Seki, Y. and Miyatake, T. Synthesis of Ultra-High-Molecular-Weight Poly(α -olefin)s by Thiobis(phenoxy)titanium/Modified Methylaluminoxane System. **Journal of Polymer Science, Part A: Polymer Chemistry** 42 (2004): 1107-1111.
- [28] Kashiwa, N. and Imuta, J. Recent progress on olefin polymerization catalysts. **Catalysis Surveys from Japan** 1 (1997): 125-142.

- [29] Sinclair, K. B. and Wilson, R. B. Metallocene catalysis - A revolution in olefin polymerization. **Chemistry & Industry** 7 (1994): 857-862.
- [30] Gupta, V. K.; Satish, S. and Bhardwaj, I. S. Metallocene complexes of group 4 elements in the polymerization of monoolefins. **Journal of Macromolecular Science - Reviews in Macromolecular Chemistry and Physics** C34, No.3 (1994): 439-514.
- [31] Naga, N. and Imanishi, Y. Copolymerization of ethylene and cyclopentene with zirconocene catalysts: Effect of ligand structure of zirconocenes. **Macromolecular Chemistry and Physics** 203 (2002): 159-165.
- [32] Lauher, J. W. and Hoffmann, R. Structure and chemistry of bis(cyclopentadienyl)-ML_n complexes. **Journal of the American Chemical Society** 98 (1976): 1729-1742.
- [33] Castonguay, L. A. and Rappe, A. K. Ziegler-Natta catalysis. A theoretical study of the isotactic polymerization of propylene. **Journal of the American Chemical Society** 114 (1992): 5832-5842.
- [34] Yang, X.; Stern, C. L. and Marks, T. J. "Cation-like" homogeneous olefin polymerization catalysts based upon zirconocene alkyls and tris(pentafluorophenyl)borane. **Journal of the American Chemical Society** 113 (1991): 3623-3625.
- [35] Chien, J. C. W. and Wang, B. P. Metallocene-Methylaluminoxane catalysts for olefin polymerization. Trimethylaluminum as coactivator. **Journal of Polymer Science Part A: Polymer Chemistry** 26 (1988): 3089-3102.
- [36] Pedoutour, J. N.; Radhakrishnan, K.; Cramail, H. and Deffieux, A. Use of "TMA-depleted" MAO for the activation of zirconocenes in olefin polymerization. **Journal of Molecular Catalysis A: Chemical** 185 (2002): 119-125.
- [37] Pedoutour, J. N.; Cramail, H. and Deffieux, A. Influence of X ligand nature in the activation process of racEt(Ind)₂ZrX₂ by methylaluminoxane. **Journal of Molecular Catalysis A: Chemical** 176 (2001): 87-94.

- [38] Cam, D. and Giannini, U. **Makromolekular Chemistry** 193 (1992): 1049-1055.
- [39] Soga, K.; Kim, H. J. and Shiono, T. Polymerization of ethylene with homogeneous metallocene catalysts activated by common trialkylaluminums and $\text{Si}(\text{CH}_3)_3\text{OH}$. **Macromolekular Rapid Communications** 14 (1993): 765-770.
- [40] Katayama, H.; Shiraishi, H.; Hino, T.; Ogane, T., and Imai, A. The effect of aluminum compounds in the copolymerization α - olefins. **Macromolekular Symposia** 97 (1995): 109-118.
- [41] Przybyla, C.; Tesche, B., and Fink, G. Ethylene hexene copolymerization with the heterogeneous catalyst system $\text{SiO}_2/\text{MAO}/\text{rac-Me}_2\text{Si}[2\text{-Me-4-Ph-Ind}](2)\text{ZrCl}_2$: The filter effect. **Macromolekular Rapid Communications** 20 (1999): 328-332.
- [42] Harkki, O.; Lehmus, P.; Leino, R.; Luttikhedde, H. J. G.; Nasman, J. H. and Seppala, J. V. Copolymerization of ethylene with 1-hexene or 1-hexadecane over siloxy-substituted metallocene catalysts. **Macromolekular Chemistry and Physics** 200 (1999): 1561-1565.
- [43] Cheruvu, S. **US Pat 5608019** (1997).
- [44] Albano, C.; Sánchez, G., and Ismayel, A. Influence of a copolymer on the mechanical properties of a blend of PP and recycled and non-recycled HDPE. **Polymer Bulletin** 41 (1998): 91-98.
- [45] Pietikainen, P. and Seppala, J.V. Low molecular weight ethylene/propylene copolymers. Effect of process parameters on copolymerization with homogeneous Cp_2ZrCl_2 catalyst. **Macromolecules** 27 (1994): 1325-1328.
- [46] Soga, K. and Kaminaka, M. Polymerization of propene with the heterogeneous catalyst system $\text{Et}[\text{IndH}_4]_2\text{ZrCl}_2/\text{MAO}/\text{SiO}_2$ combined with trialkylaluminium. **Macromolekular Rapid Communications** 13 (1992): 221-224.
- [47] Nowlin, T. E.; Kissin, Y. V. and Wagner, K. P. High activity Ziegler-Natta catalysts for the preparation of ethylene copolymers. **Journal of Polymer Science Part A: Polymer Chemistry** 26 (1988): 755-764.

- [48] Chu, K. J.; Soares, J. B. P. and Penlidis, A. Variation of molecular weight distribution (MWD) and short chain branching distribution (SCBD) of ethylene/ 1-hexene copolymers produced with different in-situ supported metallocene catalysts. **Macromolecular Chemistry and Physics** 201 (2000): 340-348.
- [49] Soga, K.; Uozumi, T.; Arai, T. and Nakamura, S. Heterogeneity of active species in metallocene catalysts. **Macromolecular Rapid Communications** 16 (1995): 379-385.
- [50] De Fatima V. ; Marques, M. ; Conte, A., ; De Resende, F. C. and Chaves, E. G. Copolymerization of ethylene and 1-octene by homogeneous and different supported metallocenic catalysts. **Journal of Applied Polymer Science** 82 (2001): 724-730.
- [51] Kim, J. D. and Soares, J. B. P. Copolymerization of ethylene and 1-hexene with supported metallocene catalysts: Effect of support treatment. **Macromolecular Rapid Communications** 20 (1999): 347-350.
- [52] Chu, K. J.; Soares, J. B. P. and Penlidis, A. Polymerization mechanism for in situ supported metallocene catalysts. **Journal of Polymer Science Part A: Polymer Chemistry** 38 (2000): 462-468.
- [53] Shan, C. L. P.; Chu, K. J.; Soares, J., and Penlidis, A. Using alkylaluminium activators to tailor short chain branching distributions of ethylene/ 1-hexene copolymers produced with in-situ supported metallocene catalysts. **Macromolecular Chemistry and Physics** 201 (2000): 2195-2202.
- [54] Steinmetz, B.; Tesche, B.; Przybyla, C.; Zechlin, J. and Fink, G. Polypropylene growth on silica-supported metallocene catalysts: A microscopic study to explain kinetic behavior especially in early polymerization stages. **Acta Polymerica** 48 (1997): 392-399.
- [55] Tait, P. J. T. and Monterio, M. G. K. **Mecton'96**, Houston, TX, USA June (1996).
- [56] Quijada, R.; Rojas, R.; Alzamora, L.; Retuert, J. and Rabagliati, F. M. Study of metallocene supported on porous and nonporous silica for the polymerization of ethylene. **Catalysis letters** 46 (1997): 107-112.

- [57] Chen, Y. X.; Rausch, M.D. and Chein, J. C. W. Heptane-Soluble Homogeneous Zirconocene Catalyst - Synthesis of a Single Diastereomer, Polymerization Catalysis, and Effect of Silica Supports. **Journal of Polymer Science Part A: Polymer Chemistry** 33 (1995): 2093-2108.
- [58] Ban, H.; Arai, T.; Ahn, C. H.; Uozumi, T. and Soga, T. **Recent Development in Heterogeneous Metallocene Catalyst**
- [59] Ferreira, M. L., Belelli, P. G., Juan, A., and Damiani, D. E. Theoretical and experimental study of the interaction of methylaluminoxane (MAO)-low temperature treated silica: Role of trimethylaluminium (TMA). **Macromolecular Chemistry and Physics** 201 (2000): 1334-1344.
- [60] Collins, S.; Kelly, W. M. and Holden, D.A. Polymerization of propylene using supported, chiral, ansa-metallocene catalysts: Production of polypropylene with narrow molecular weight distributions. **Macromolecules** 25 (1992): 1780-1785.
- [61] Kaminsky, W.; Renner, F. and Winkelbach, H. **Mecton'94**, Houston, TX, USA, May (1994).
- [62] Hlatky, G. G. and Upton, D. J. Supported ionic metallocene polymerization catalysts. **Macromolecules** 29 (1996): 8019-8020.
- [63] Lee, D. H.; Shin, S. Y. and Lee, D. H. Ethylene polymerization with metallocene and trimethylaluminum-treated silica. **Macromolecular Symposia** 97 (1995): 195-203.
- [64] Dos Santos, J. H. Z.; Dorneles, S.; Stedile, F.; Dupont, J.; Forte, M. M. C. and Baumovl, I. J. R. Silica supported zirconocenes and Al-based cocatalysts: Surface metal loading and catalytic activity. **Macromolecular Chemistry and Physics** 198 (1997): 3529-3537.
- [65] Harrison, D.; Coulter, I. M.; Wang, S.; Nistala, S.; Kuntz, B. A.; Pigeon, M.; Tian, J. and Collins, S. Olefin polymerization using supported metallocene catalysts: Development of high activity catalysts for use in slurry and gas phase ethylene polymerizations. **Journal of Molecular Catalysis A: Chemical** 128 (1998): 65-77.

- [66] Xu, J.; Deng, Y.; Feng, L.; Cui, C. and Chen, W. Temperature rising elution fractionation of syndiotactic polypropylene prepared by homogeneous and supported metallocene catalysts **Polymer Journal** 30 (1998): 824-827.
- [67] Soga, K.; Kim, H. J. and Shiono, T. Highly isospecific SiO₂-supported zirconocene catalyst activated by ordinary alkylaluminiums. **Macromolecular Rapid Communications** 15 (1994): 139-144.
- [68] Lee, D.; Yoon, K. and Noh, S. Polymerization of ethylene by using zirconocene catalyst anchored on silica with trisiloxane and pentamethylene spacers. **Macromolecular Rapid Communications** 18 (1997): 427-431.
- [69] Iiskola, E. I.; Timonen, S.; Pakkanen, T. T.; Harkki, O.; Lehmus, P. and Seppala, J. V. Cyclopentadienyl surface as a support for zirconium polyethylene catalysts. **Macromolecules** 30 (1997): 2853-2859.
- [70] Lee, D. and Yoon, K. **Macromolecular Symposia** 97 (1995): 185-193.
- [71] De Fatima V.; Marques, M.; Henriques, C. A.; Monteiro, J. L. F.; Menezes, S. M.C. and Coutinho, F. M. B. Ethylene polymerization with Cp₂ZrCl₂ supported on dealuminated Y zeolite. **Polymer Bulletin** 39 (1997): 567-571.
- [72] Michelotti, M.; Altomare, A.; Ciardelli, F. and Roland, E. Zeolite supported polymerization catalysts: Copolymerization of ethylene and α -olefins with metallocenes supported on HY zeolite. **Journal of Molecular Catalysis A: Chemical** 129 (1998): 241-248.
- [73] Meshkova, I. N.; Ushakova, T. M.; Ladygina, T. A.; Kovalena, N. Y. and Novokshonova, L. A. Ethylene polymerization with catalysts on the base of Zr-cenes and methylaluminoxanes synthesized on zeolite support. **Polymer Bulletin** 44 (2000): 461-468.
- [74] Weiss, K.; Wirth-Pfeifer, C.; Hofmann, M.; Botzenhardt, S.; Lang, H.; Bruning, K. and Meichel, E. Polymerisation of ethylene or propylene with heterogeneous metallocene catalysts on clay minerals. **Journal of Molecular Catalysis A: Chemical** 182-183 (2002): 143-149.

- [75] Looveren, L. K. V.; Geysen, D. F.; Vercruyse, K. A.; Wouters, B. H.; Grobet, P. J. and Jacobs, P. A. Methylalumoxane MCM-41 as Support in the Co-Oligomerization of Ethene and Propene with $[\{C_2H_4(1\text{-indenyl})_2\} Zr(CH_3)_2]$. **Angewandte Chemie (International Edition in English)** 37 (1998): 517-520.
- [76] Wang, W.; Fan, Z.Q. and Feng, L.X. Ethylene polymerization and ethylene/1-hexene copolymerization using homogeneous and heterogeneous unbridged bisindenyl zirconocene catalysts. **European Polymer Journal** 41 (2005): 2380-2387.
- [77] Van Grieken, R.; Carrero, A.; Suarez, I. and Paredes, B. Ethylene polymerization over supported MAO/ $(nBuCp)_2ZrCl_2$ catalysts : influence of support properties. **European Polymer Journal** 43 (2007): 1267-1277.
- [78] Zhang, Y.; Koike, M.; Yang, R.; Hinchiranan, S.; Vitidsant, T. and Tsubaki, N. Multi-functional alumina-silica bimodal pore catalyst and its application for Fischer-Tropsch synthesis. **Applied Catalysis A: General** 292 (2005): 252–258.
- [79] Hagimoto, H.; Shiono, T. and Ikeda, T. Supporting Effects of Methylaluminoxane on the Living Polymerization of Propylene with a Chelating (Diamide)dimethyltitanium Complex. **Macromolecular Chemistry and Physics** 205 (2004): 19–26.
- [80] Randall, J. C. A review of high resolution liquid ^{13}C nuclear magnetic resonance characterization of ethylene-based polymers. **Journal of Macromolecular Science, Reviews in Macromolecular Chemistry and Physics** C29 (1989): 201-315.
- [81] Jongsomjit, B.; Kaewkrajang, P.; Wanke, S.E. and Prasertdam, P. A comparative study of ethylene/ α -olefin copolymerization with silane-modified silica-supported MAO using zirconocene catalysts. **Catalysis Letters** 94 (2004): 205-208.

- [82] Jongsomjit, B.; Ngamposri, S. and Prasertthdam, P. Catalytic activity during copolymerization of ethylene and 1-hexene via mixed TiO₂/SiO₂-supported MAO with rac-Et[Ind]₂ZrCl₂ metallocene catalyst. **Molecules** 10 (2005): 672-678.
- [83] Jongsomjit, B.; Chaichana, E. and Prasertthdam, P. Effect of nano-SiO₂ particle size on the formation of LLDPE/SiO₂ nanocomposite synthesized via in situ polymerization with metallocene catalyst. **Chemical Engineering Science** 62 (2007): 899–905.
- [84] Jongsomjit, B.; Panpranot, J. and Prasertthdam, P. Effect of nanoscale SiO₂ and ZrO₂ as the fillers on the microstructure of LLDPE nanocomposites synthesized via in situ polymerization with zirconocene. **Materials Letters** 61 (2007): 1376-1379.
- [85] Jongsomjit, B.; Desharun, C. and Prasertthdam, P. Study of LLDPE/alumina nanocomposites synthesized by in situ polymerization with zirconocene/d-MMAO catalyst. **Catalyst Communications** 9 (2008): 522-528.
- [86] Jongsomjit, B.; Kaewkrajang, P.; Shiono, T. and Prasertthdam, P. Supporting Effects of Silica-Supported Methylaluminoxane (MAO) with Zirconocene Catalyst on Ethylene/1-Olefin Copolymerization Behaviors for Linear Low-Density Polyethylene (LLDPE) Production. **Industrial and Engineering Chemistry Research** 43 (2004): 7959-7963.
- [87] Jongsomjit, B.; Ketloy, C. and Prasertthdam, P. Characteristics and catalytic properties of [t-BuNSiMe₂Flu]TiMe₂/dMMAO catalyst dispersed on various supports towards ethylene/1-octene copolymerization. **Applied Catalysis A General** 327 (2007): 270-277.
- [88] Severn, J.R.; Chadwick, J.C.; Duchateau, R. and Friderichs, N. "Bound but Not Gagged"-Immobilizing Single-Site α -Olefin Polymerization Catalysts. **Chemical Review** 105 (2005): 4073-4147.
- [89] Chan, M.S.W.; Vanka, K.; Pye, C.C. and Ziegler, T. Density Functional Study on Activation and Ion-pair Formation in Group IV Metallocene and Related Olefin Polymerization Catalysts. **Organometallics** 18 (1999) 4624-4636.

- [90] Galland G.B.; Quijada P.; Mauler R.S. and De Menezes S.C. Determination of reactivity ratios for ethylene/ α -olefin copolymerization catalysed by the $C_2H_4[Ind]_2ZrCl_2$ /methylaluminoxane system. **Macromolecular Rapid Communications** 17 (1996): 607-613.
- [91] Liu, S.; Yu, G. and Huang B. Polymerization of ethylene by zirconocene $B(C_6F_5)_3$ catalysts with aluminum compounds. **Journal of Applied Polymer Science** 66 (1997): 1715-1720.



สถาบันวิทยบริการ
จุฬาลงกรณ์มหาวิทยาลัย



APPENDICES

สถาบันวิทยบริการ
จุฬาลงกรณ์มหาวิทยาลัย



APPENDIX A
(Nuclear magnetic resonance)

สถาบันวิทยบริการ
จุฬาลงกรณ์มหาวิทยาลัย

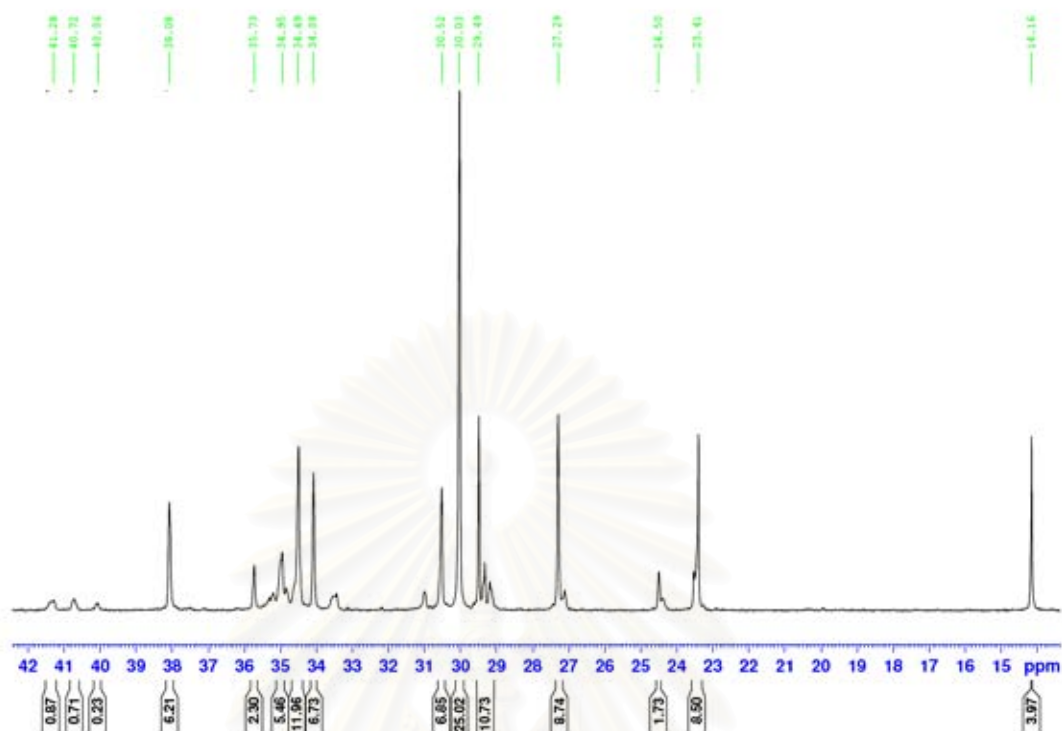


Figure A-1 ^{13}C NMR spectrum of ethylene/1-hexene copolymer produce with homogenous

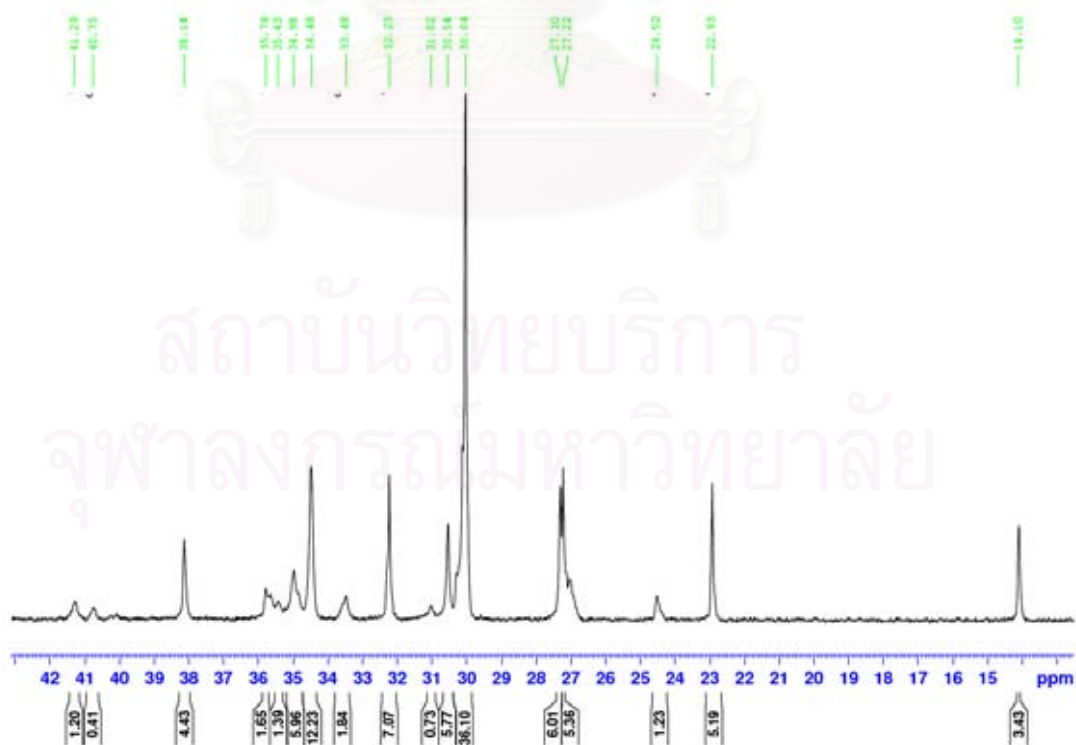


Figure A-2 ^{13}C NMR spectrum of ethylene/1-octene copolymer produce with homogenous

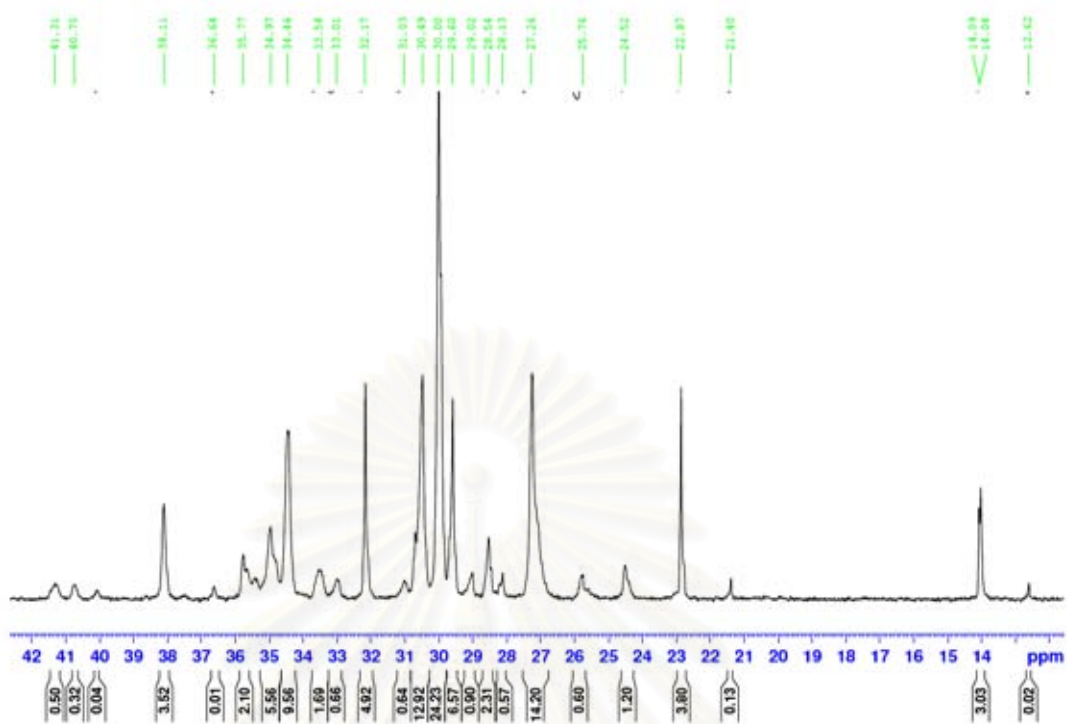


Figure A-3 ^{13}C NMR spectrum of ethylene/1-decene copolymer produce with homogenous

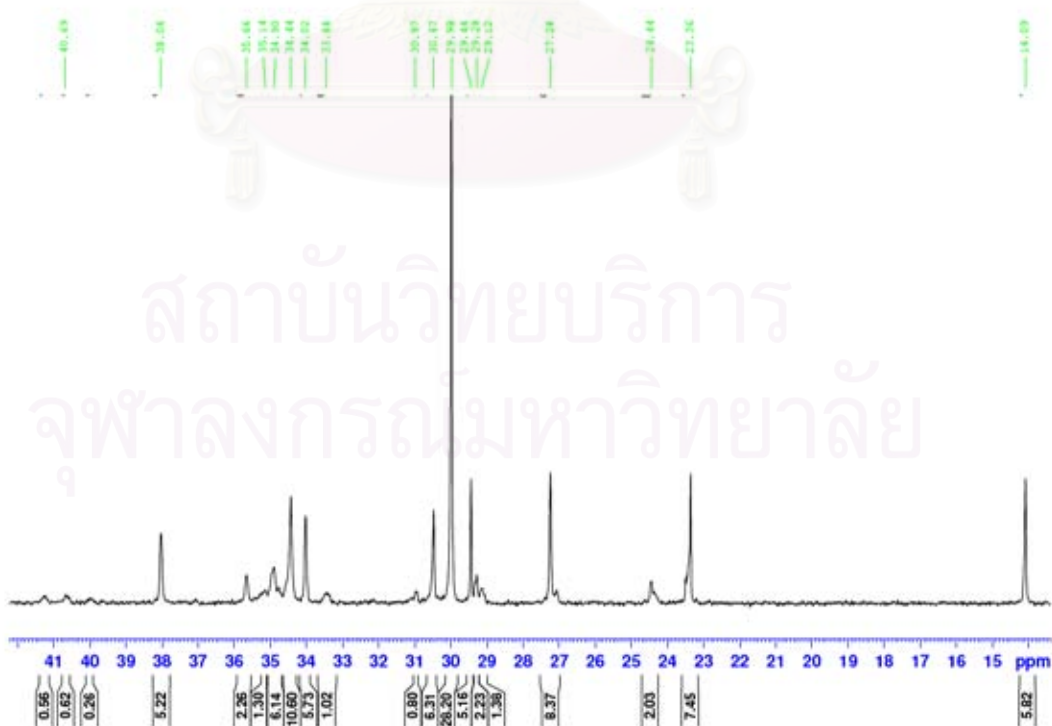


Figure A-4 ^{13}C NMR spectrum of ethylene/1-hexene copolymer produce with SiO_2 (LP)

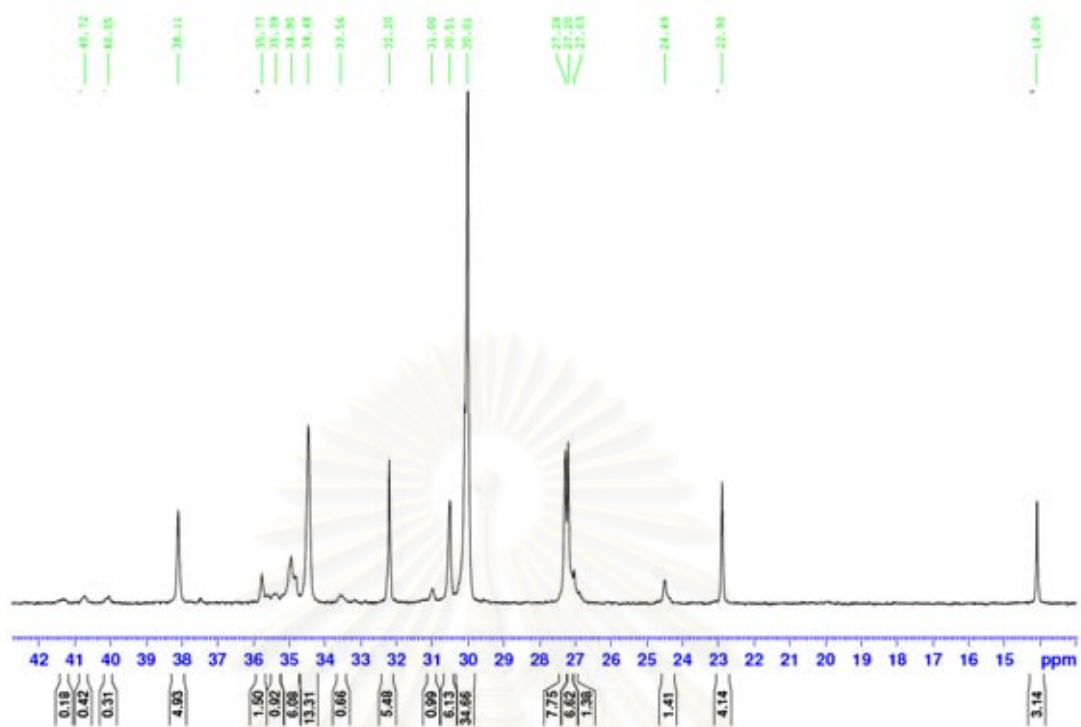


Figure A-5 ^{13}C NMR spectrum of ethylene/1-octene copolymer produce with SiO_2 (LP)

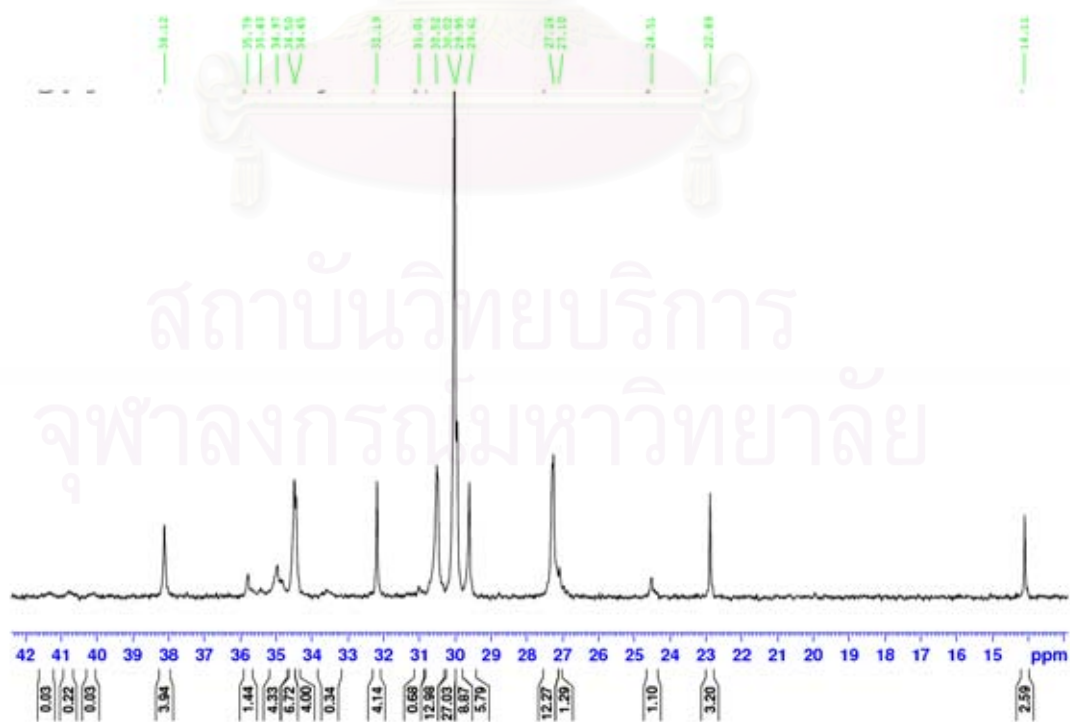


Figure A-6 ^{13}C NMR spectrum of ethylene/1-decene copolymer produce with SiO_2 (LP)

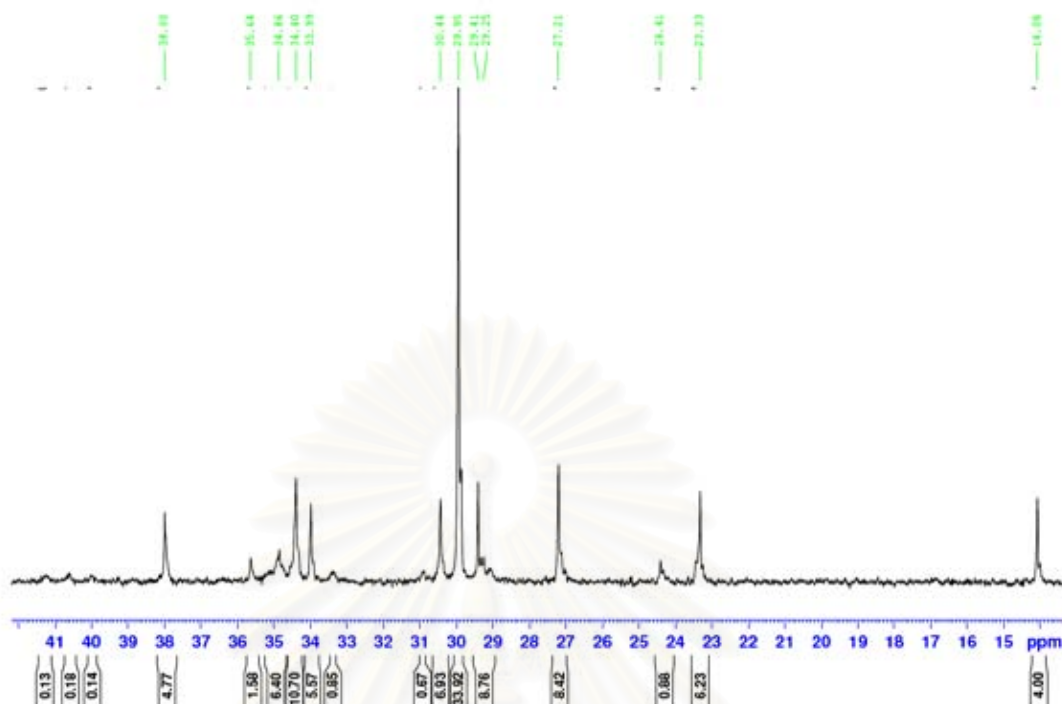


Figure A-7 ^{13}C NMR spectrum of ethylene/1-hexene copolymer produce with SiO_2 (SP)

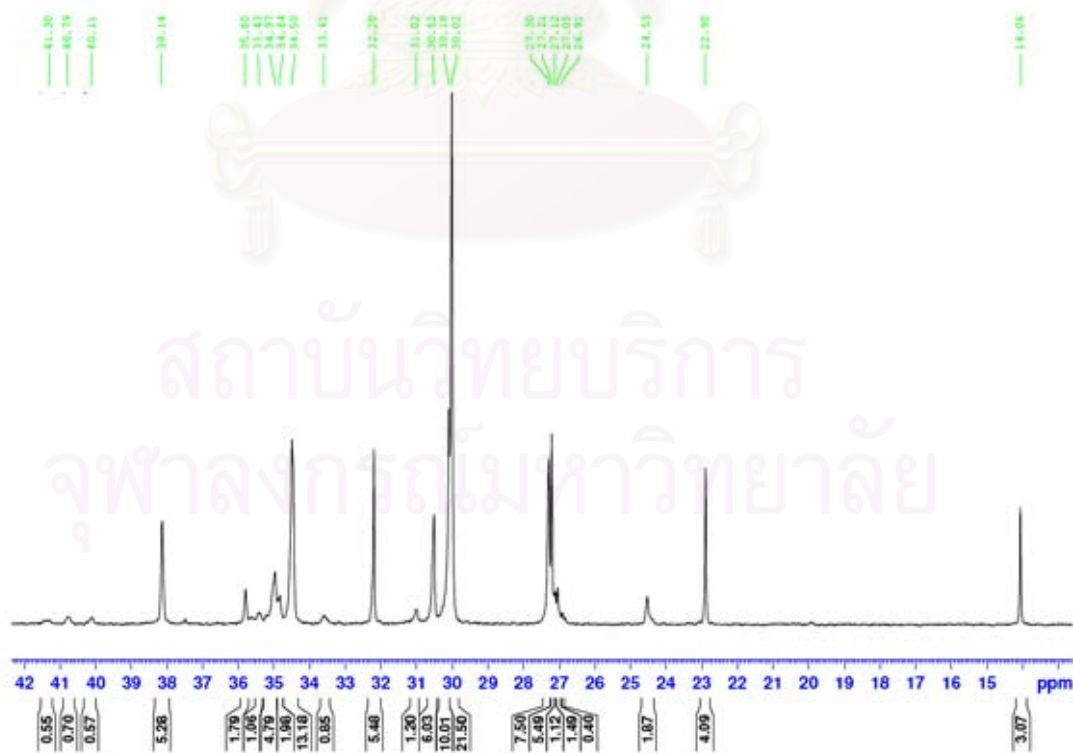


Figure A-8 ^{13}C NMR spectrum of ethylene/1-octene copolymer produce with SiO_2 (SP)

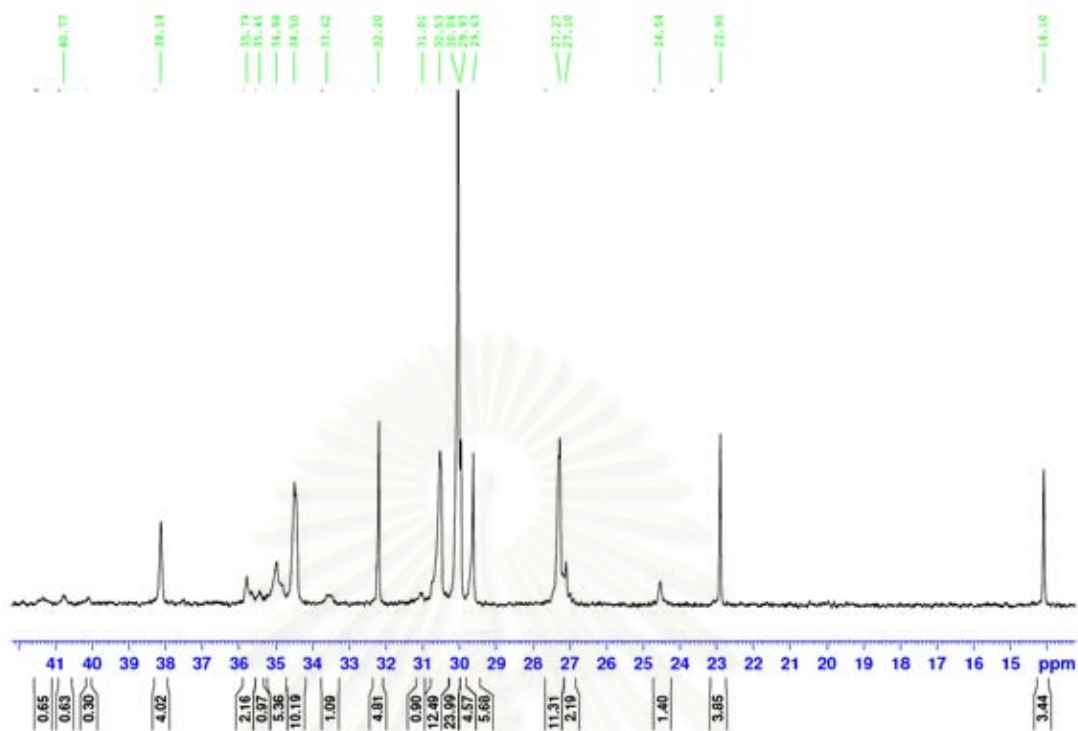


Figure A-9 ^{13}C NMR spectrum of ethylene/1-decene copolymer produced with SiO_2 (SP)

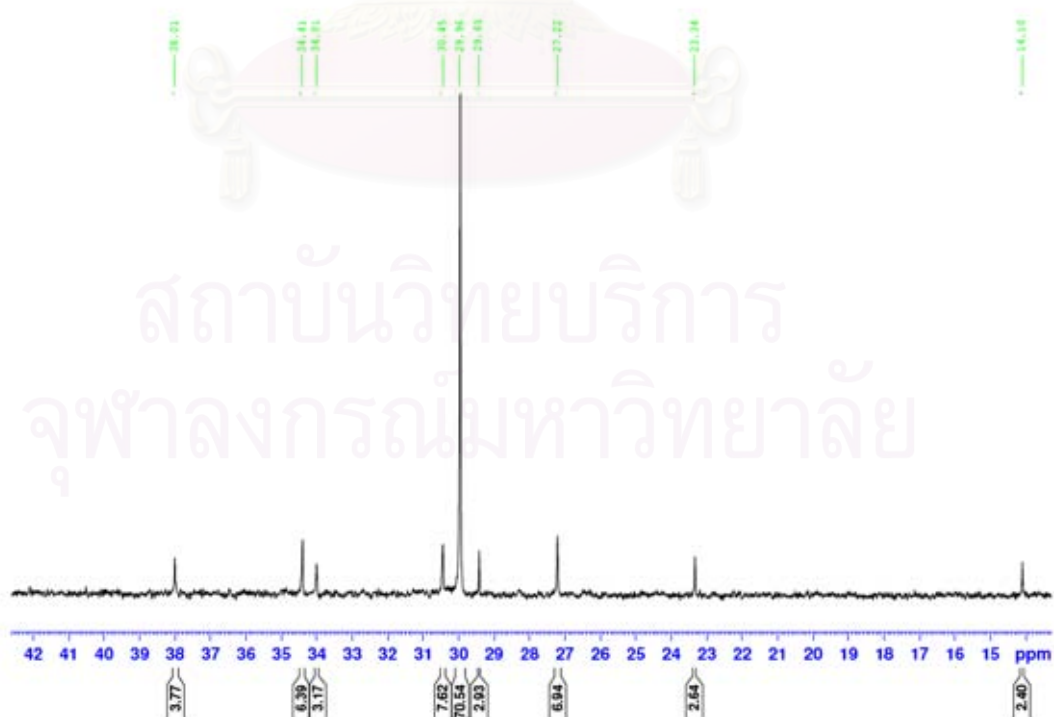


Figure A-10 ^{13}C NMR spectrum of ethylene/1-hexene copolymer produced with Si-Al (BP)

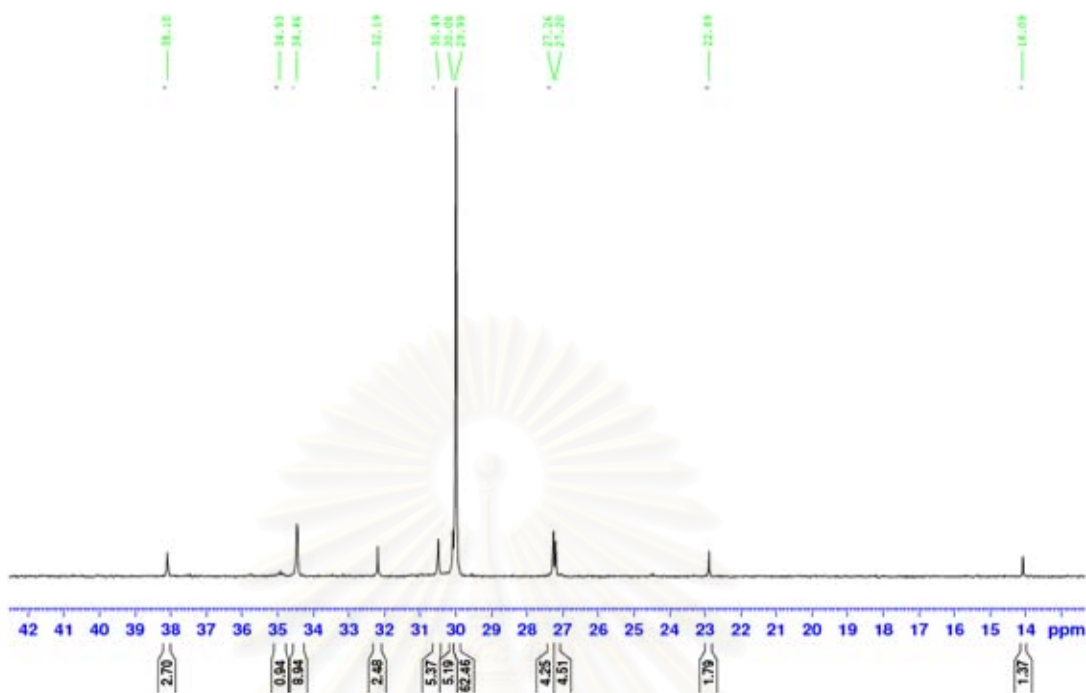


Figure A-11 ^{13}C NMR spectrum of ethylene/1-octene copolymer produce with Si-Al (BP)

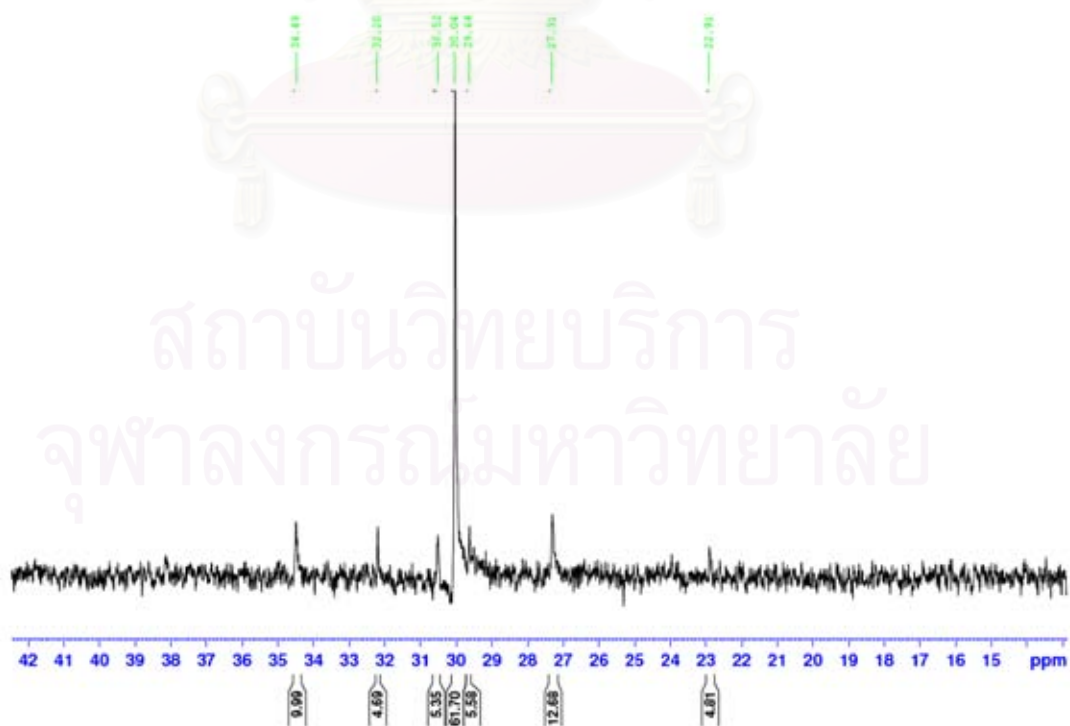
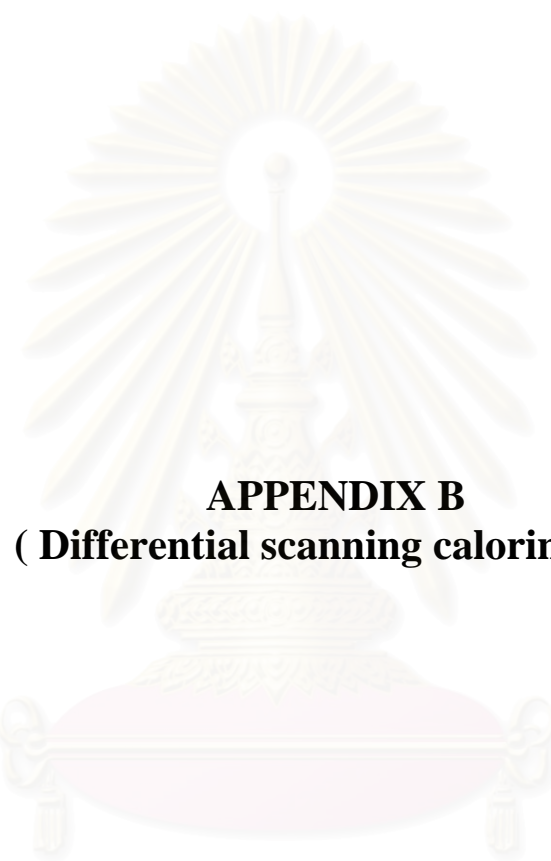


Figure A-12 ^{13}C NMR spectrum of ethylene/1-decene copolymer produce with Si-Al (BP)



APPENDIX B
(Differential scanning calorimeter)

สถาบันวิทยบริการ
จุฬาลงกรณ์มหาวิทยาลัย

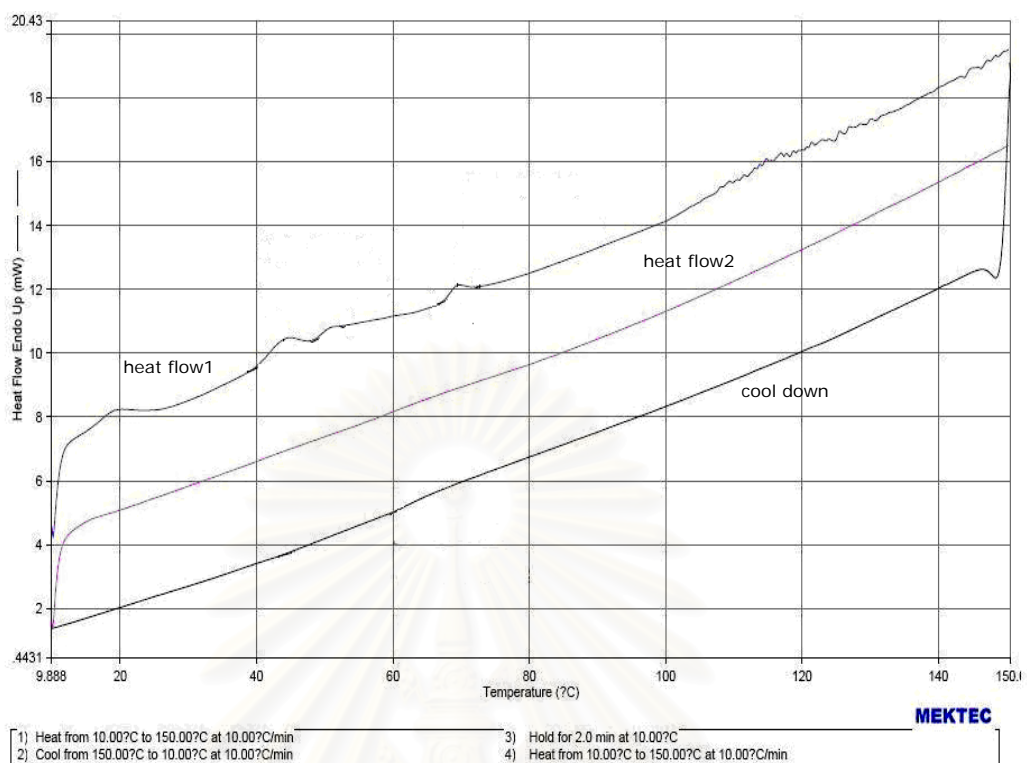


Figure B-1 DSC curve of ethylene/1-hexene copolymer produce with homogenous

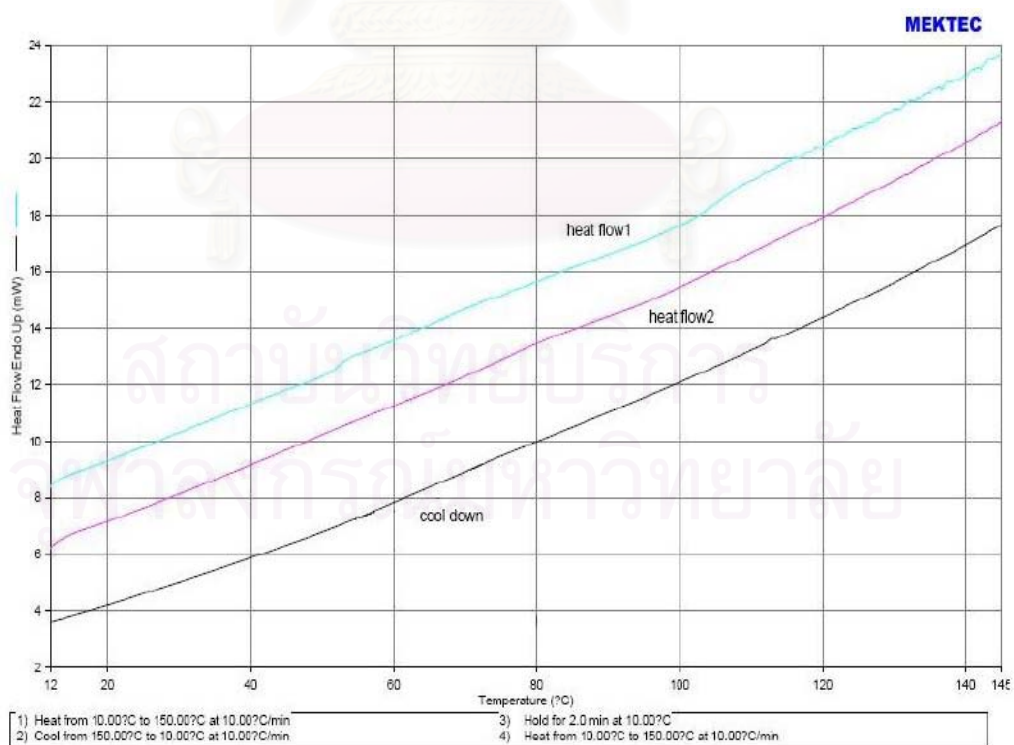


Figure B-2 DSC curve of ethylene/1-octene copolymer produce with homogenous

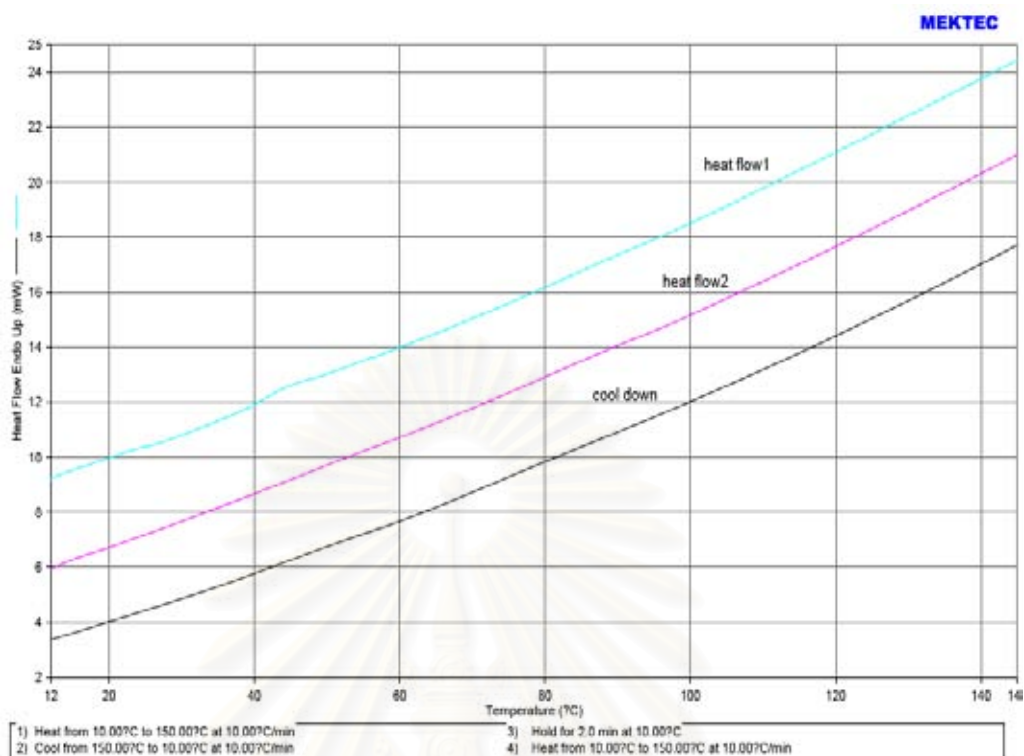


Figure B-3 DSC curve of ethylene/1-decene copolymer produce with homogenous

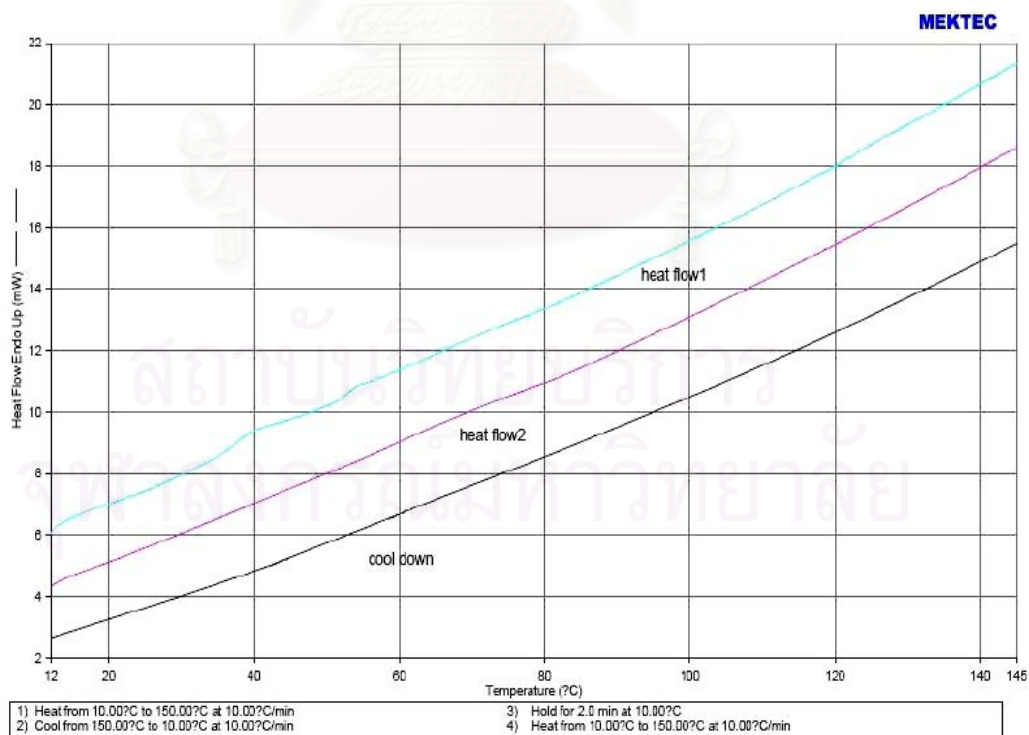


Figure B-4 DSC curve of ethylene/1-hexene copolymer produce with SiO₂ (LP)

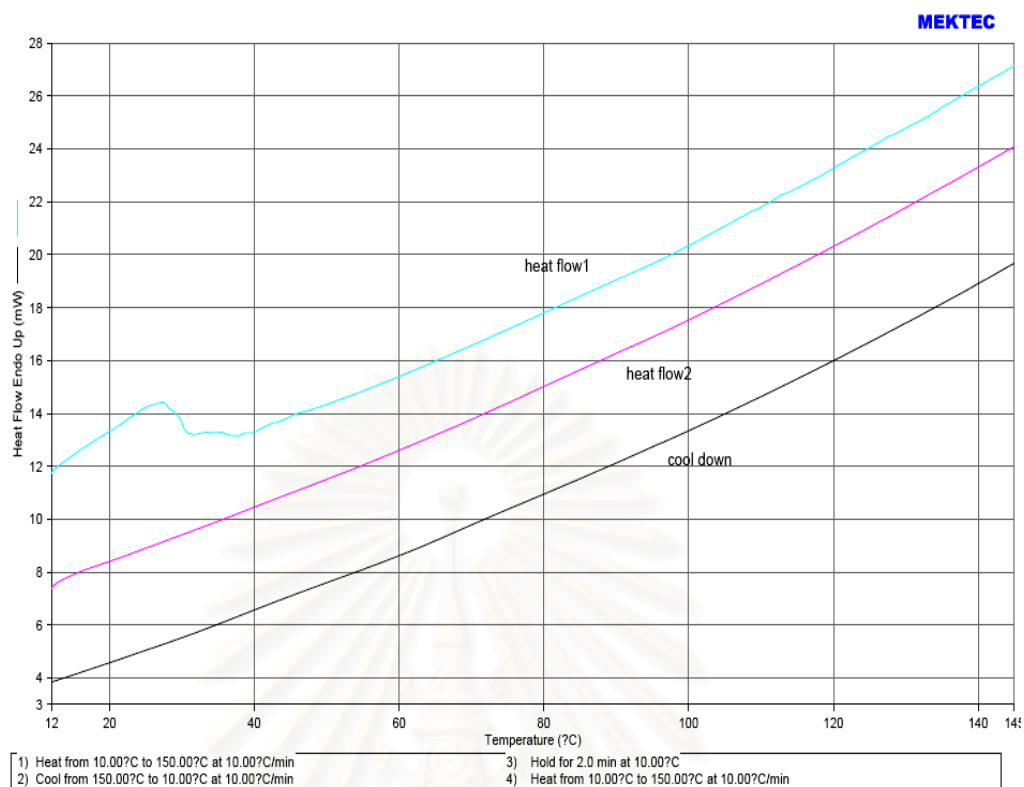


Figure B-5 DSC curve of ethylene/1-octene copolymer produce with SiO₂ (LP)

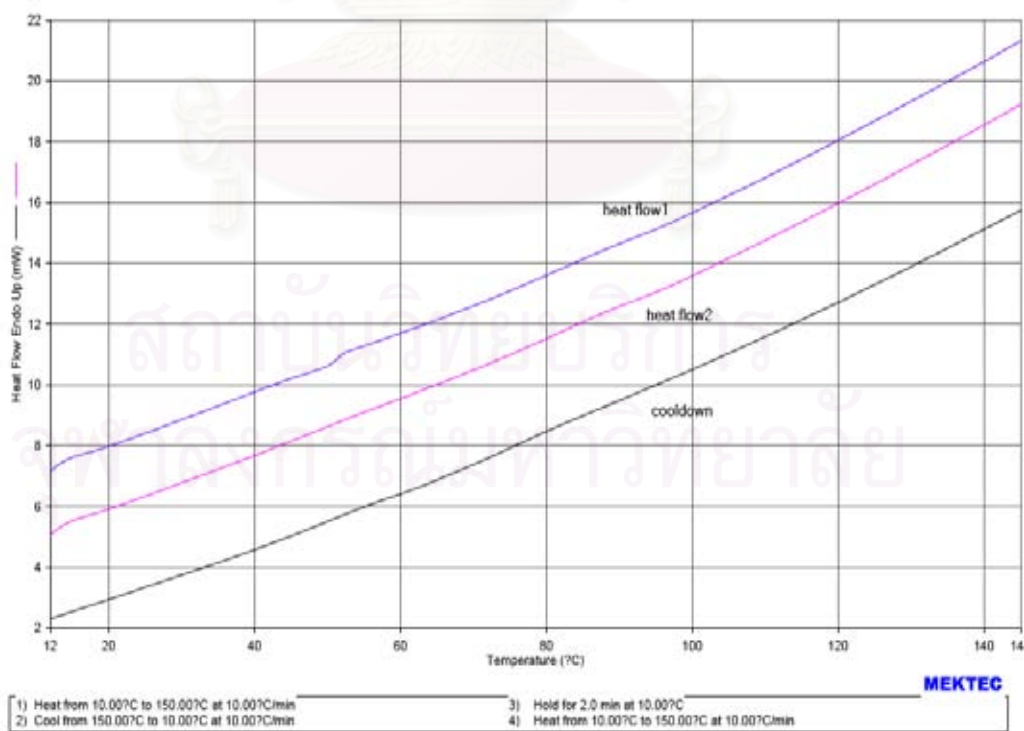


Figure B-6 DSC curve of ethylene/1-decene copolymer produce with SiO₂ (LP)

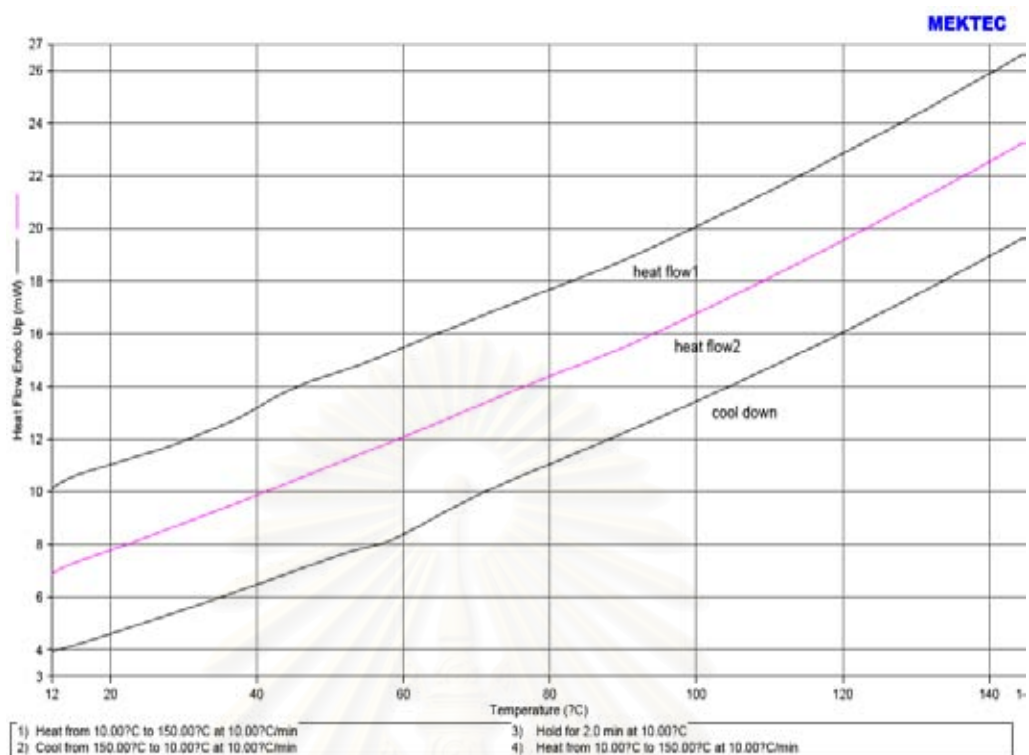


Figure B-7 DSC curve of ethylene/1-hexene copolymer produce with SiO₂ (SP)

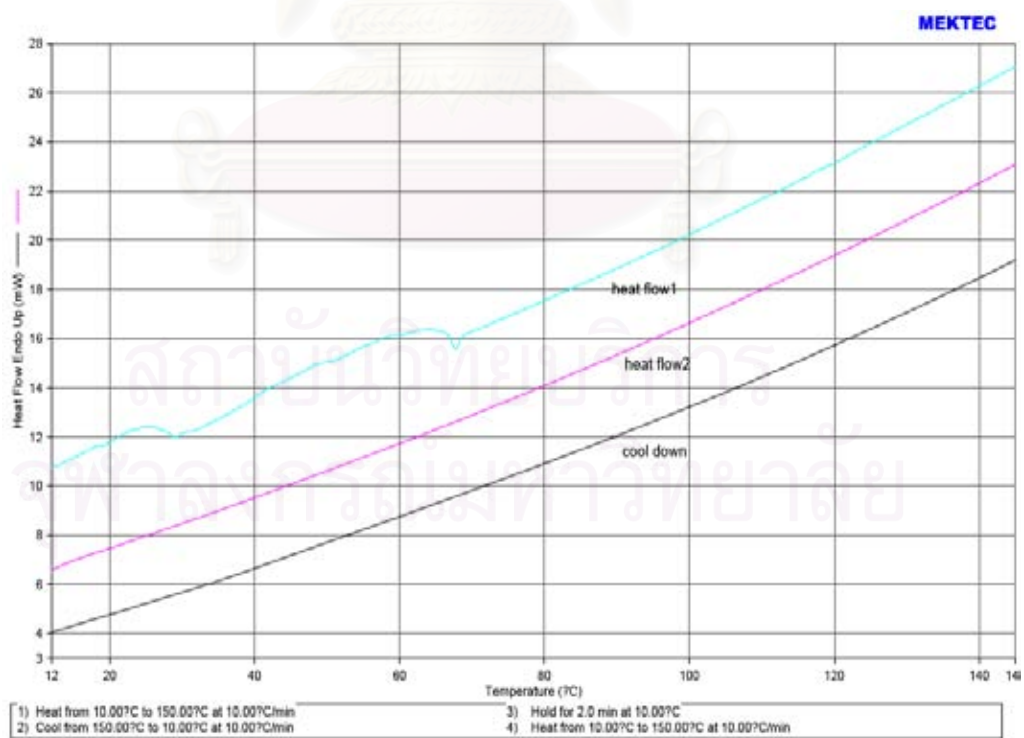


Figure B-8 DSC curve of ethylene/1-octene copolymer produce with SiO₂ (SP)

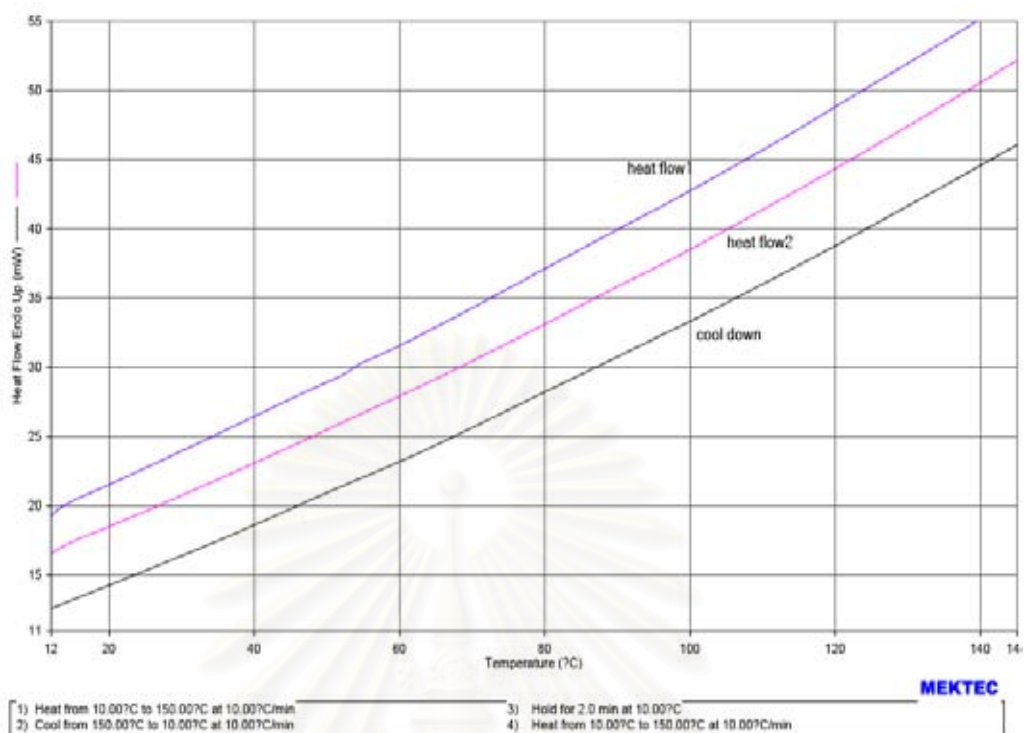


Figure B-9 DSC curve of ethylene/1-decene copolymer produce with SiO₂ (SP)

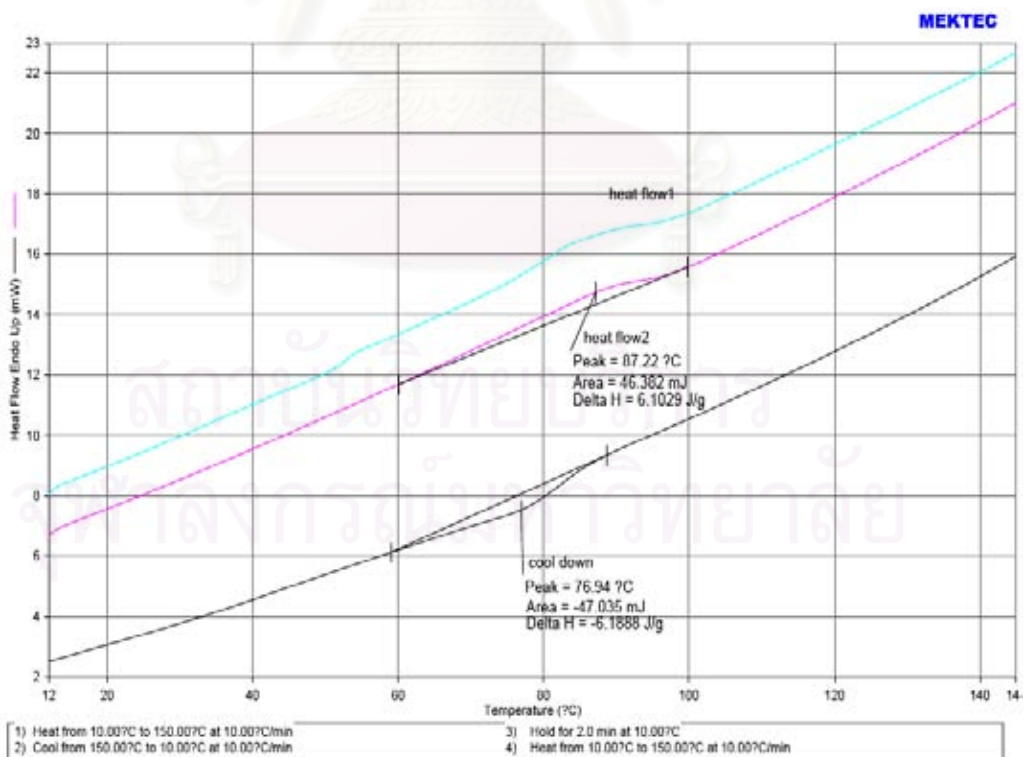


Figure B-10 DSC curve of ethylene/1-hexene copolymer produce with Si-Al (BP)

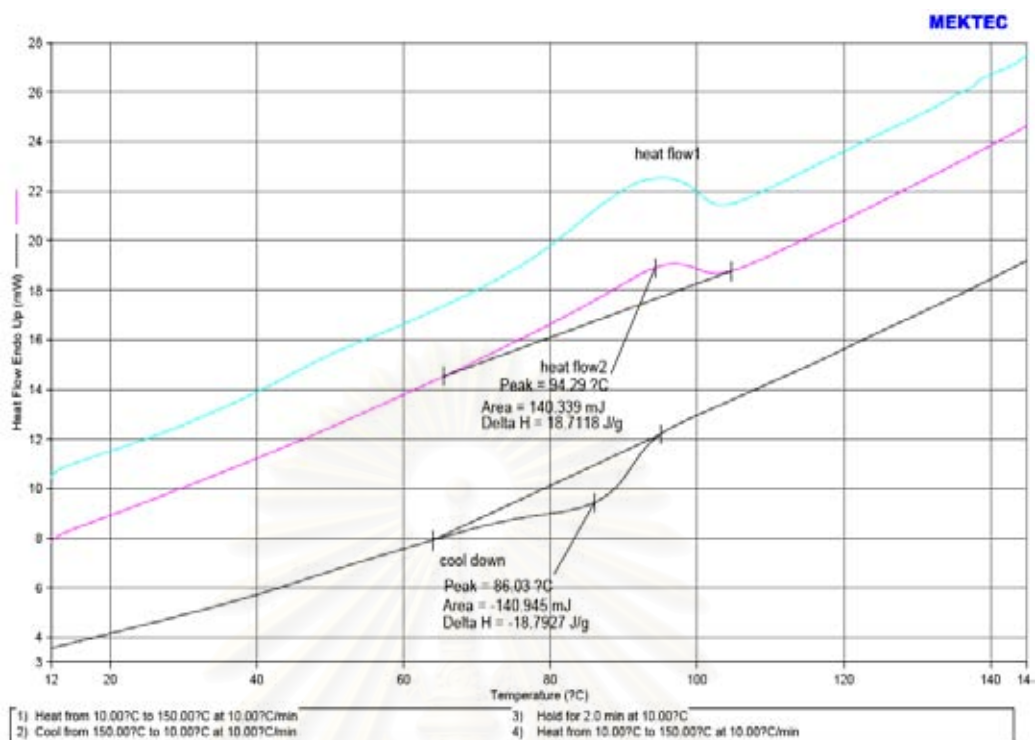


Figure B-11 DSC curve of ethylene/1-octene copolymer produce with Si-Al (BP)

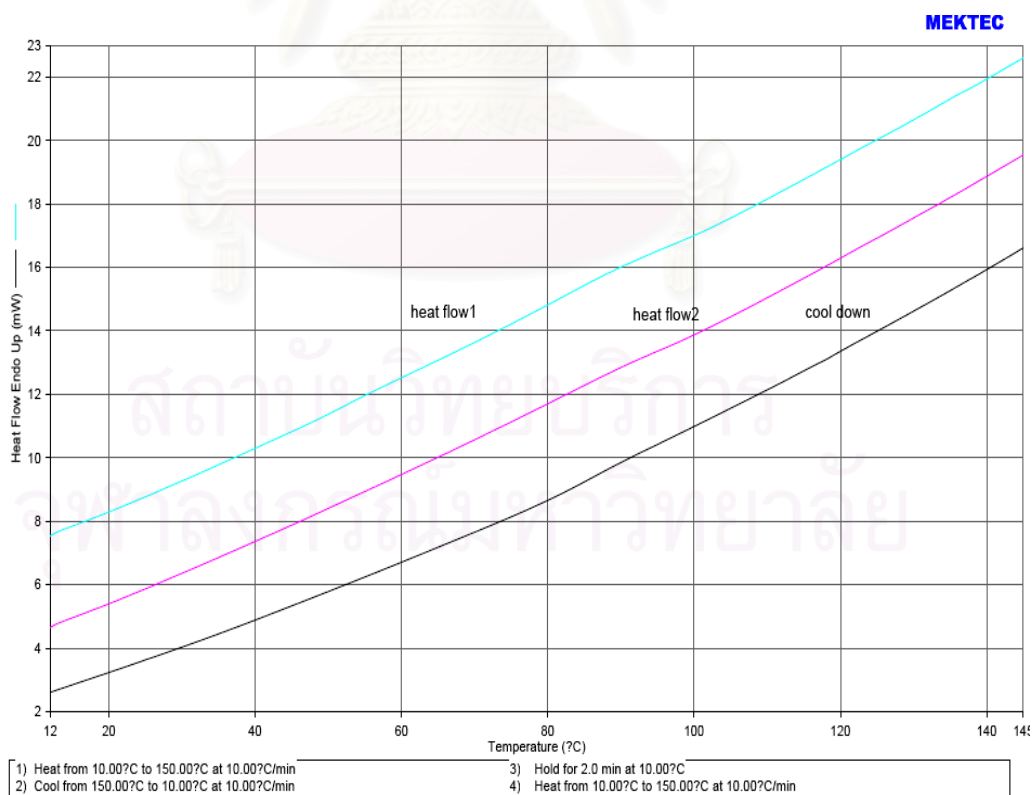


Figure B-12 DSC curve of ethylene/1-decene copolymer produce with Si-Al (BP)



APPENDIX C
(Energy dispersive x-ray spectroscopy)

สถาบันวิทยบริการ
จุฬาลงกรณ์มหาวิทยาลัย

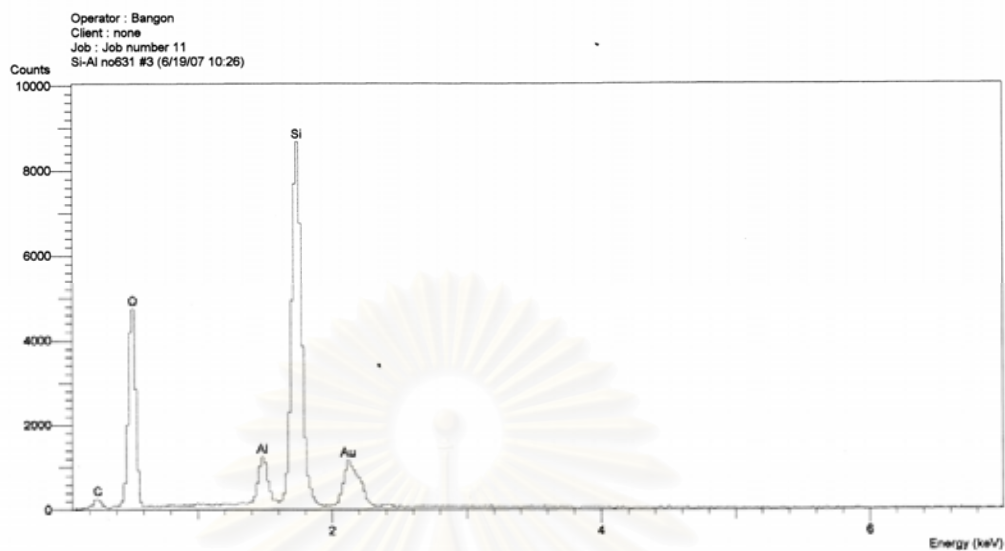


Figure C-1. EDX profiles of $[Al]_{Al_2O_3}$ on Si-Al (BP) supports

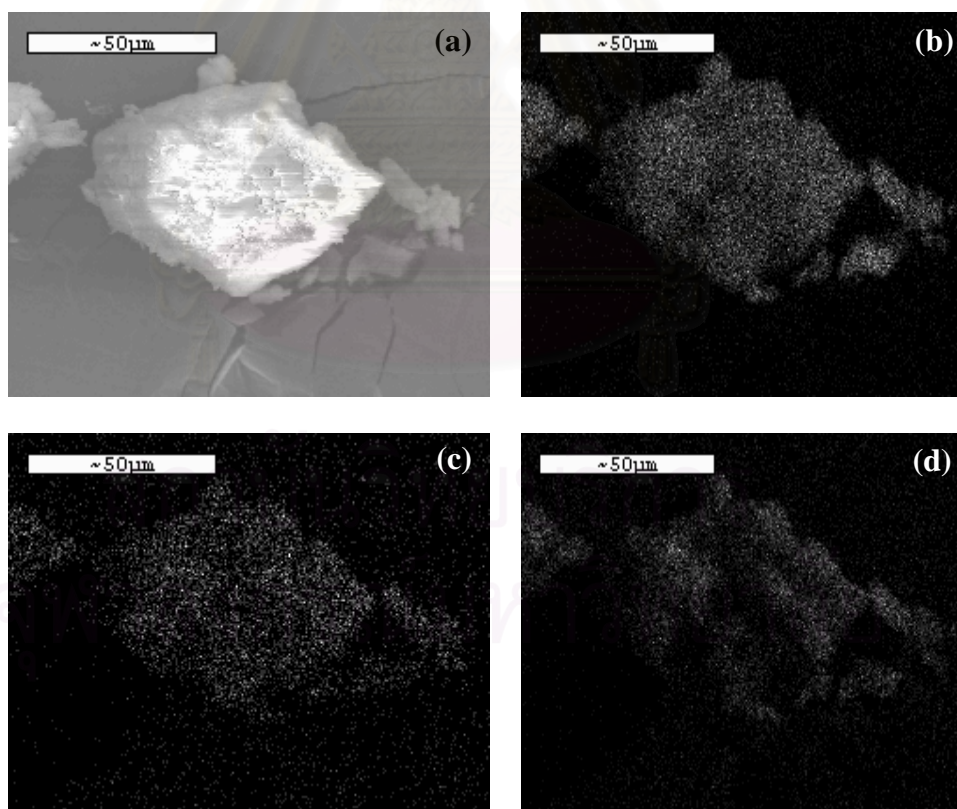


Figure C-2. EDX mapping of Si-Al (BP) scan no.3: (a) Si-Al (BP);
(b) Si-mapping of Si-Al (BP); (c) Al-Mapping of Si-Al (BP);
(d) O-Mapping of Si-Al (BP).

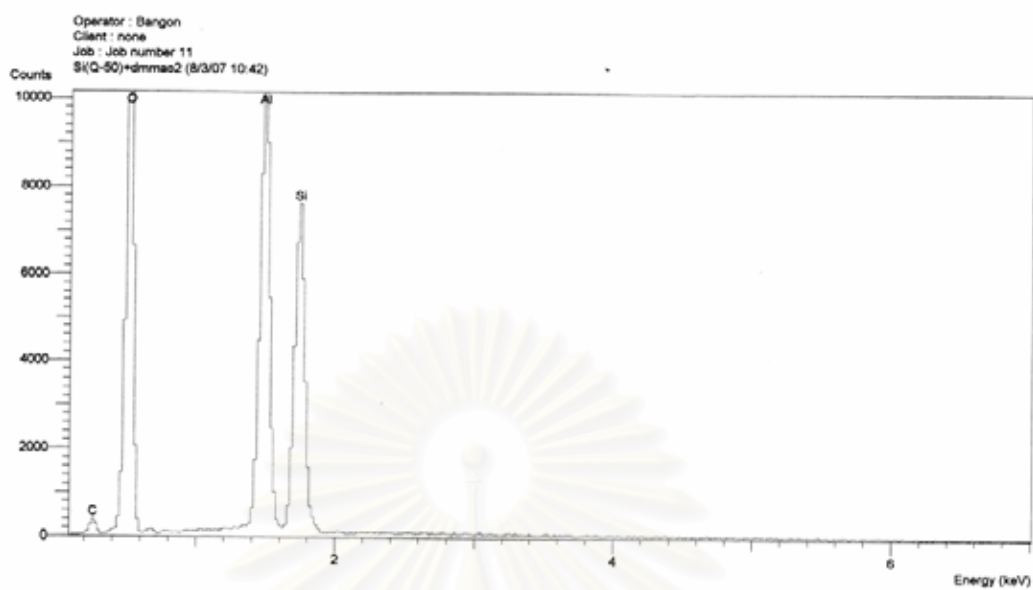


Figure C-3. EDX profiles of [Al]_{dMMAO} on SiO₂ (LP) supports

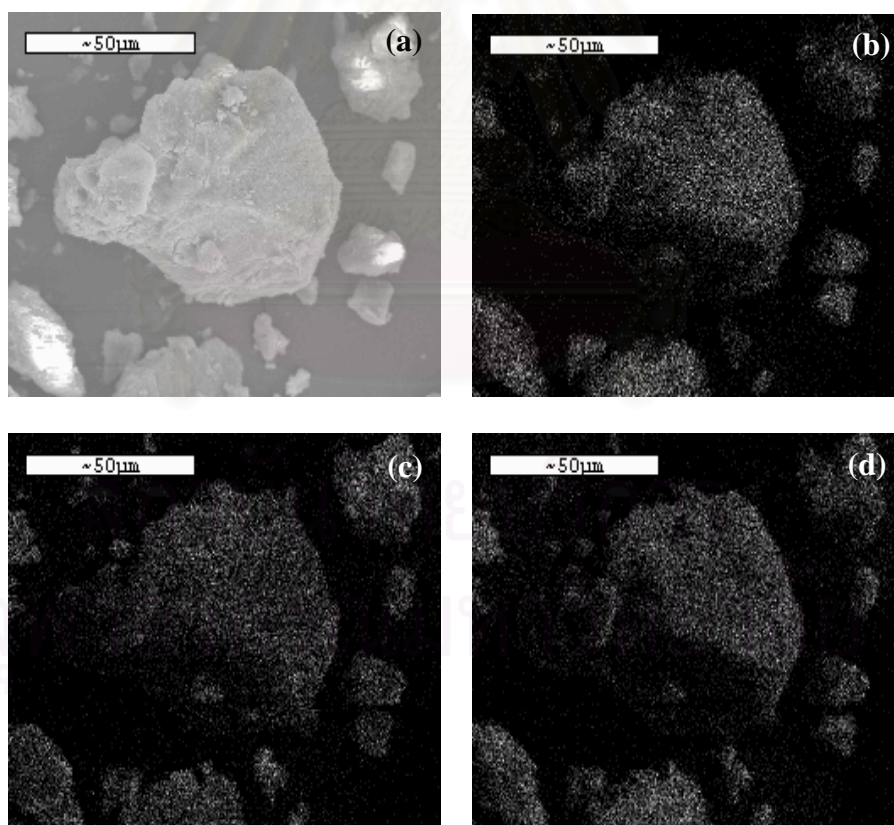


Figure C-4. EDX mapping of dMMAO/SiO₂ (LP) scan no.3: (a) SiO₂ (LP); (b) Si-mapping of SiO₂ (LP); (c) Al-Mapping of SiO₂ (LP); (d) O-Mapping of SiO₂ (LP)

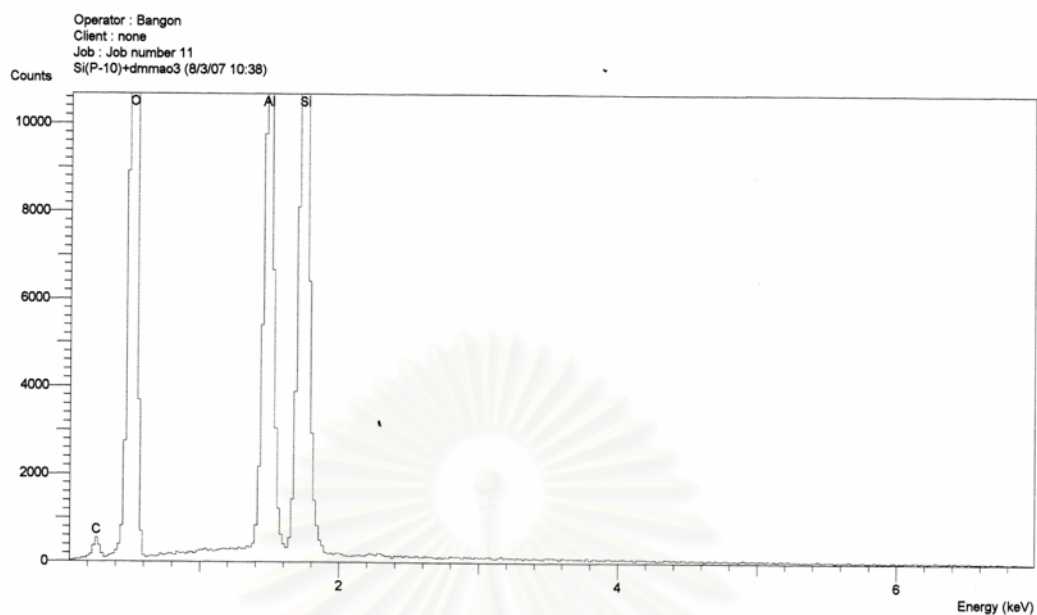


Figure C-5. EDX profiles of $[Al]_{dMMAO}$ on SiO_2 (SP) supports

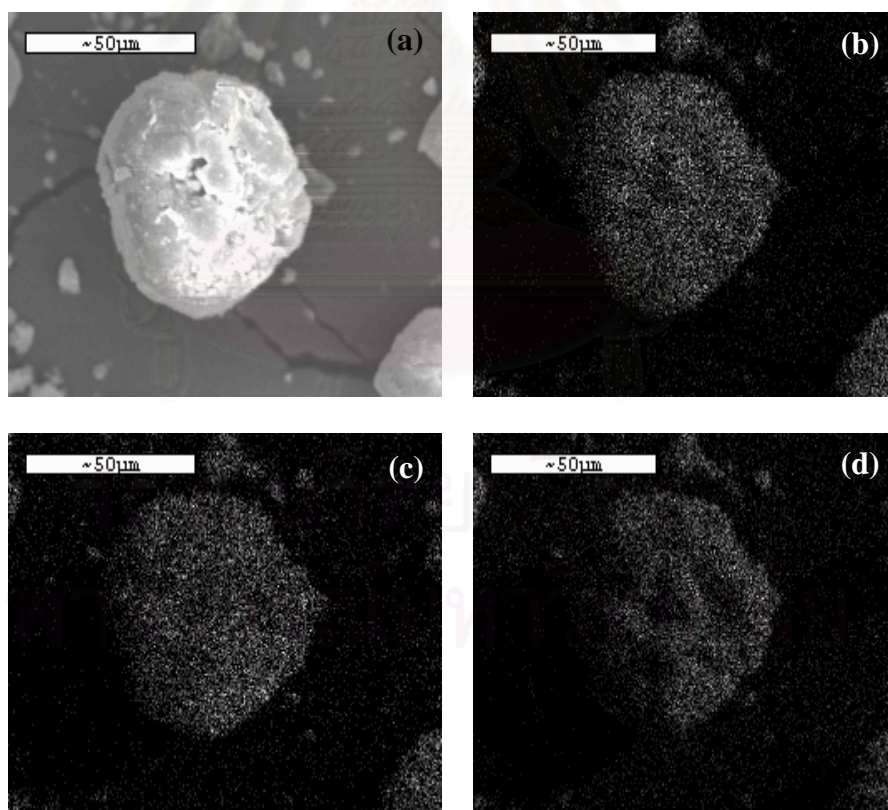


Figure C-6. EDX mapping of $dMMAO/SiO_2$ (SP) scan no.3: (a) SiO_2 (P-10); (b) Si-mapping of SiO_2 (SP); (c) Al-Mapping of SiO_2 (SP); (d) O-Mapping of SiO_2 (SP)

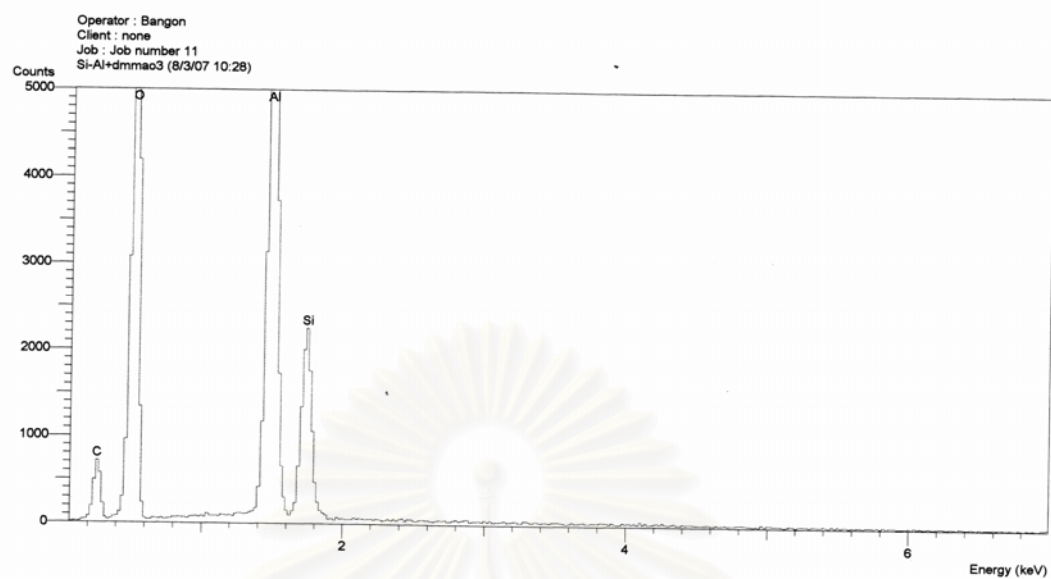


Figure C-7. EDX profiles of $[Al]_{dMMAO}$ on Si-Al (BP) supports

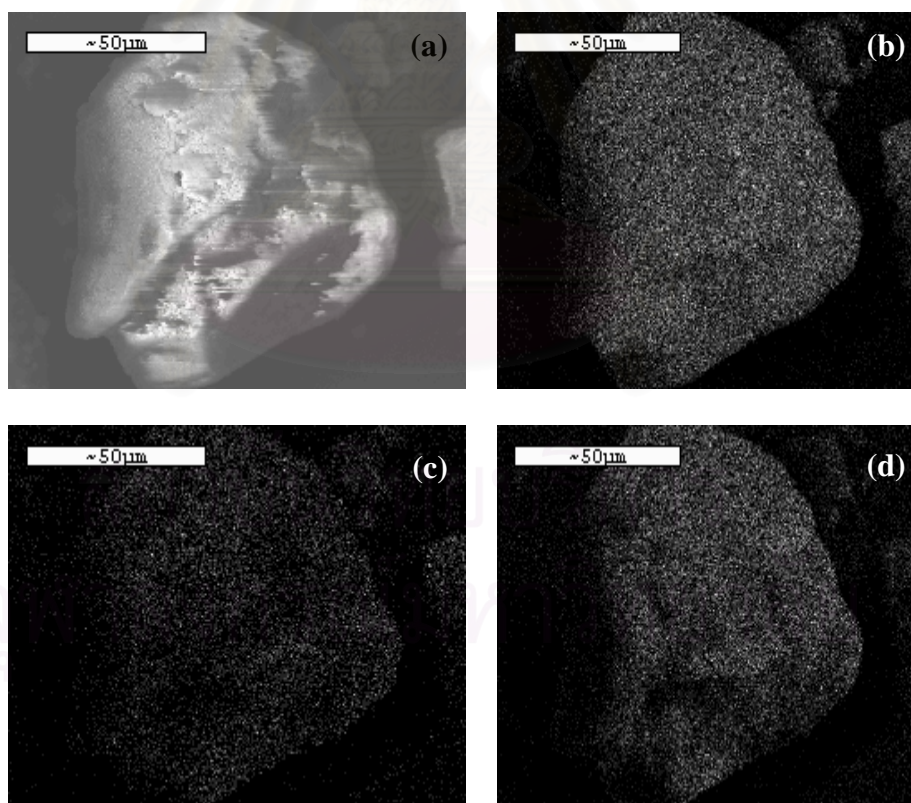


Figure C-8. EDX mapping of dMMAO/ Si-Al (BP) scan no.3: (a) Si-Al (BP); (b) Si-mapping of Si-Al (BP); (c) Al-Mapping of Si-Al (BP); (d) O-Mapping of Si-Al (BP).

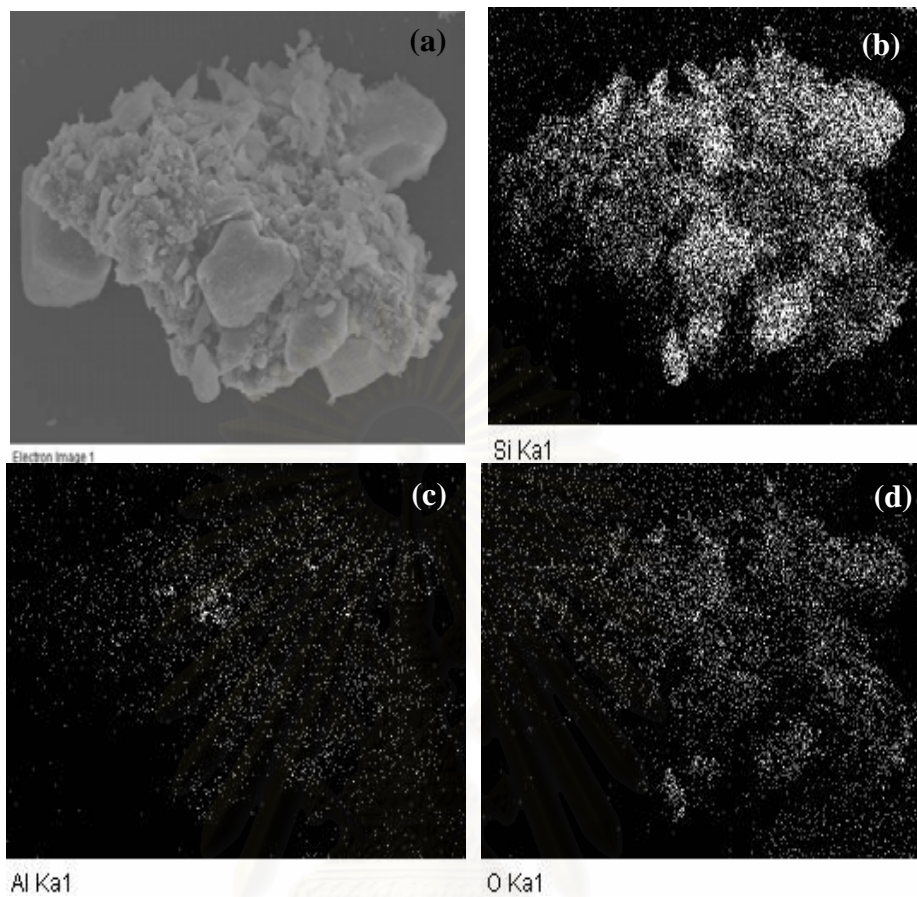


Figure C-9 EDX mapping of LLDPE(EH)/Si-Al (BP)
(a) LLDPE/Si-Al (BP); (b) Si-mapping of Si-Al (BP);
(c) Al-Mapping of Si-Al (BP); (d) O-Mapping of Si-Al (BP).
Ethylene/1-hexene copolymerization is denoted as EH

สถาบันวิทยบริการ
จุฬาลงกรณ์มหาวิทยาลัย

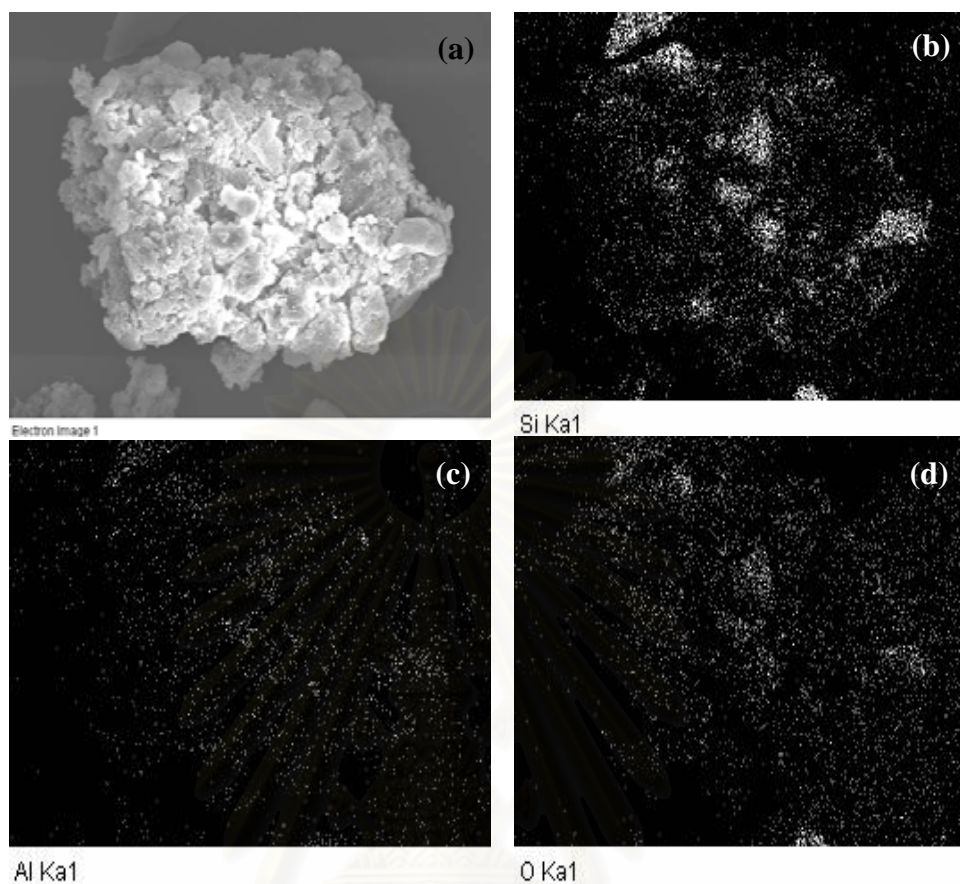


Figure C-10 EDX mapping of LLDPE(EO)/Si-Al (BP)
(a) LLDPE/Si-Al (BP); (b) Si-mapping of Si-Al (BP);
(c) Al-Mapping of Si-Al (BP); (d) O-Mapping of Si-Al (BP).
Ethylene/1-octene copolymerization is denoted as EO

สถาบันวิทยบริการ
จุฬาลงกรณ์มหาวิทยาลัย

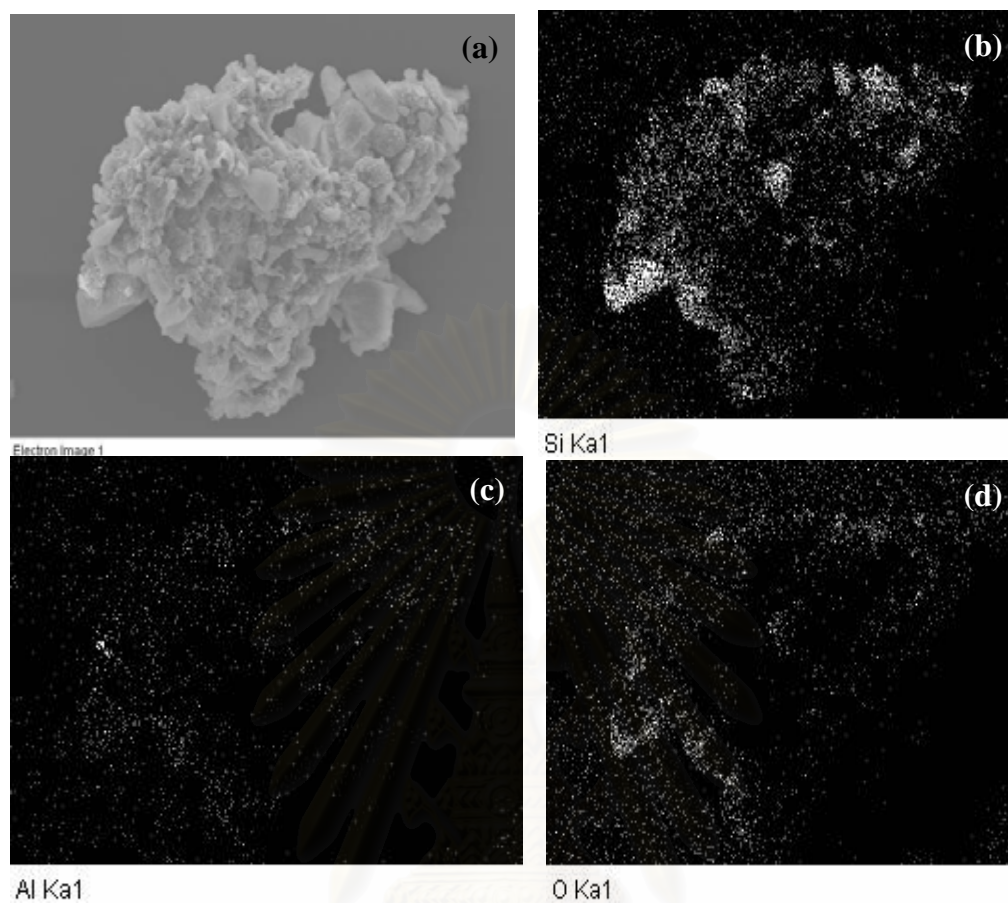


Figure C-11 EDX mapping of LLDPE(ED)/Si-Al (BP)
(a) LLDPE/Si-Al (BP); (b) Si-mapping of Si-Al (BP);
(c) Al-Mapping of Si-Al (BP); (d) O-Mapping of Si-Al (BP).
Ethylene/1-decene copolymerization is denoted as ED

สถาบันวิทยบริการ
จุฬาลงกรณ์มหาวิทยาลัย



APPENDIX D
(Calculation of polymer properties)

สถาบันวิทยบริการ
จุฬาลงกรณ์มหาวิทยาลัย

D-1 Calculation of polymer microstructure

Polymer microstructure and also triad distribution of monomer can be calculated according to the Galland G.B. [90]. in the list of reference. The detail of calculation for ethylene/ α -olefin copolymer was interpreted as follow.

1-Hexene

The integral area of ^{13}C -NMR spectrum in the specify range are listed.

| | | | |
|-------|---|-------------|-----|
| T_A | = | 39.5 - 42 | ppm |
| T_B | = | 38.1 | ppm |
| T_C | = | 33 - 36 | ppm |
| T_D | = | 28.5 - 31 | ppm |
| T_E | = | 26.5 - 27.5 | ppm |
| T_F | = | 24 - 25 | ppm |
| T_G | = | 23.4 | ppm |
| T_H | = | 14.1 | ppm |

Triad distribution was calculated as the followed formula.

$$\begin{aligned}
 k[\text{HHH}] &= 2T_A - T_C + T_G + 2T_F + T_E \\
 k[\text{EHH}] &= 2T_C - 2T_G - 4T_F - 2T_E - 2T_A \\
 k[\text{EHE}] &= T_B \\
 k[\text{EEE}] &= 0.5T_D - 0.5T_G - 0.25T_E \\
 k[\text{HEH}] &= T_F \\
 k[\text{HEE}] &= T_E
 \end{aligned}$$

1-Octene

The integral area of ^{13}C -NMR spectrum in the specify range are listed.

| | | | |
|-------|---|-------------|-----|
| T_A | = | 39.5 - 42 | ppm |
| T_B | = | 38.1 | ppm |
| T_C | = | 36.4 | ppm |
| T_D | = | 33 - 36 | ppm |
| T_E | = | 32.2 | ppm |
| T_F | = | 28.5 - 31 | ppm |
| T_G | = | 25.5 - 27.5 | ppm |
| T_H | = | 24 - 25 | ppm |
| T_I | = | 22 - 23 | ppm |
| T_J | = | 14 - 15 | ppm |

Triad distribution was calculated as the followed formula.

| | | |
|-----------------|---|------------------------------|
| $k[\text{OOO}]$ | = | $T_A - 0.5T_C$ |
| $k[\text{EOO}]$ | = | T_C |
| $k[\text{EOE}]$ | = | T_B |
| $k[\text{EEE}]$ | = | $0.5T_F - 0.25T_E - 0.25T_G$ |
| $k[\text{OEO}]$ | = | T_H |
| $k[\text{OEE}]$ | = | $T_G - T_E$ |

สถาบันวิทยบริการ
จุฬาลงกรณ์มหาวิทยาลัย

1-Decene

The integral area of ^{13}C -NMR spectrum in the specify range are listed.

| | | | |
|-------|---|-------------|-----|
| T_A | = | 39.5 - 42 | ppm |
| T_B | = | 38.1 | ppm |
| T_C | = | 36.4 | ppm |
| T_D | = | 33 - 36 | ppm |
| T_E | = | 32.2 | ppm |
| T_F | = | 28.5 - 31 | ppm |
| T_G | = | 25.5 - 27.5 | ppm |
| T_H | = | 24 - 25 | ppm |
| T_I | = | 22 - 23 | ppm |
| T_J | = | 14 - 15 | ppm |

Triad distribution was calculated as the followed formula.

| | | |
|-----------------|---|----------------------------------|
| $k[\text{DDD}]$ | = | $T_A - 0.5T_C$ |
| $k[\text{EDD}]$ | = | T_C |
| $k[\text{EDE}]$ | = | T_B |
| $k[\text{EEE}]$ | = | $0.5T_F - 0.5T_E - 0.5T_G - T_I$ |
| $k[\text{DED}]$ | = | T_H |
| $k[\text{DEE}]$ | = | $T_G - T_I$ |

สถาบันวิทยบริการ
จุฬาลงกรณ์มหาวิทยาลัย

Table D-1 Reactivity ratios of ethylene and α -olefin monomers

| system | comonomer | $r_E r_C$ |
|-----------------------|-----------|-----------|
| homogeneous | 1-hexene | 1.15 |
| | 1-octene | 0 |
| | 1-decene | 0 |
| SiO ₂ (LP) | 1-hexene | 1.6 |
| | 1-octene | 0 |
| | 1-decene | 0 |
| SiO ₂ (SP) | 1-hexene | 2.43 |
| | 1-octene | 0 |
| | 1-decene | 0 |
| Si-Al (BP) | 1-hexene | 0 |
| | 1-octene | 0 |
| | 1-decene | 0 |

All copolymer was calculated for the relative comonomer reactivity (r_E for ethylene and r_C for the comonomer) and monomer insertion by using the general formula below.

$$r_E = 2[EE]/([EC]X) \qquad r_C = 2[CC]X/[EC]$$

where

$$r_E = \text{ethylene reactivity ratio}$$

$$r_C = \text{comonomer } (\alpha \text{-olefin) reactivity ratio}$$

$$[EE] = [EEE] + 0.5[CEE]$$

$$[EC] = [CEC] + 0.5[CCE] + [ECE] + 0.5[ECC]$$

$$[CC] = [CCC] + 0.5[ECC]$$

$$X = [E]/[C] \text{ in the feed} = \text{concentration of ethylene (mol/L) / concentration of comonomer (mol/L) in the feed.}$$

$$\%E = [EEE] + [EEC] + [CEC]$$

$$\%C = [CCC] + [CCE] + [ECE]$$

D.2 Calculation of crystallinity for ethylene/ α -olefin copolymer

The crystallinities of copolymers were determined by differential scanning calorimeter. %crystallinity of copolymers is calculated from equation [91].

$$\chi(\%) = \frac{\Delta H_m}{\Delta H_{m_0}} \times 100$$

Where $\chi(\%)$ = % crystallinity

ΔH_m = the heat of fusion of sample (J/g)

ΔH_{m_0} = the heat of fusion of perfectly crystalline polyethylene
(286 J/g) [90]



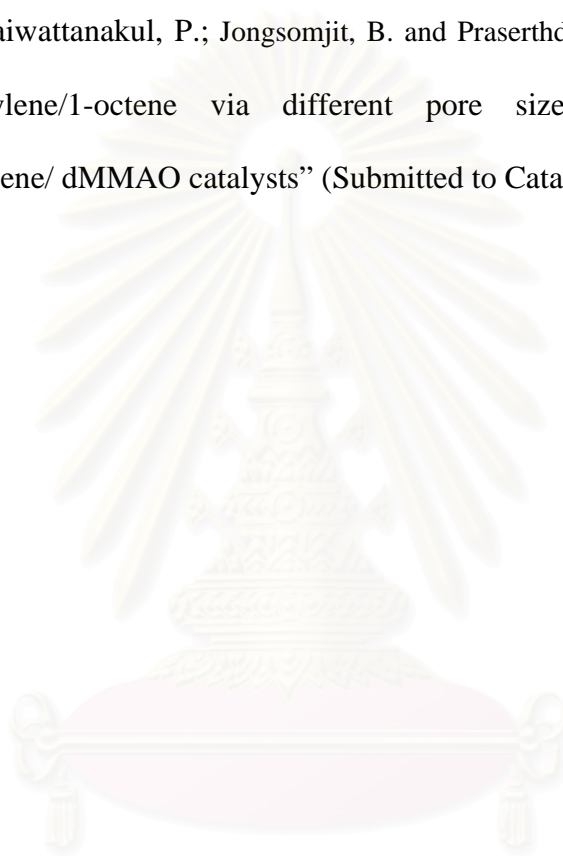
สถาบันวิทยบริการ
จุฬาลงกรณ์มหาวิทยาลัย



APPENDIX E
(LIST OF PUBLICATION)

สถาบันวิทยบริการ
จุฬาลงกรณ์มหาวิทยาลัย

1. Wongwaiwattanakul, P.; Jongsomjit, B. and Praserthdam, P. “Effect of bimodal silica-alumina-supported metallocene catalyst for ethylene/1-octene copolymerization” (The Proceeding of 17th Thailand Chemical Engineering and Applied Chemistry Conference, TIChe 2007, Chiang Mai)
2. Wongwaiwattanakul, P.; Jongsomjit, B. and Praserthdam, P. “Copolymerization of ethylene/1-octene via different pore sized silica-based-supported zirconocene/ dMMAO catalysts” (Submitted to Catalysis Communications)



สถาบันวิทยบริการ
จุฬาลงกรณ์มหาวิทยาลัย

VITA

Mr.Pongsathorn Wongwaiwattanakul was born on April 4, 1984 in Songkla, Thailand. He received the Bachelor's Degree of Chemical Engineering from the Department of Chemical Engineering, Faculty of Engineering, Prince of Songkla University in March 2006, he continued his Master's study at Chulalongkorn University in June, 2006.



สถาบันวิทยบริการ
จุฬาลงกรณ์มหาวิทยาลัย